2016

MEASURING AND MODELING OF THERMODYNAMIC SOLUBILITY OF BIOACTIVE PHYTOCHEMICALS COMPOUNDS IN SUPERCRITICAL CARBON DIOXIDE: NOBILETIN + CO2 AND MENADIONE + CO2
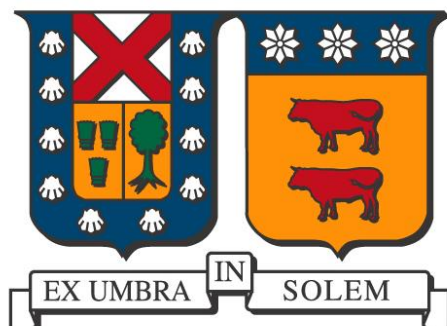
CABRERA PALACIOS, ADOLFO LUIS

UNIVERSIDAD TÉCNICA FEDERICO SANTA MARÍA

DEPARTAMENTO DE INGENIERÍA QUÍMICA Y AMBIENTAL

Measuring and modeling of thermodynamic solubility of bioactive phytochemicals compounds in supercritical carbon dioxide: nobiletin + CO₂ and menadione + CO₂

Adolfo Luis Cabrera Palacios

Thesis to qualify for the title of

CIVIL CHEMICAL ENGINEER

and the degree of

MASTER IN CHEMICAL ENGINEERING SCIENCES

Tutor professor: Juan C. de la Fuente, Ph. D.

Co-referent professor (internal): Gonzalo Núñez, Ph. D.

Co-referent professor (external): Flavia Zacconi, Ph. D.

November – 2016

I dedicate this work to our Lord Jesus Christ, and to my mother Patricia, my father Félix and my brothers for their love and support and for advising, comforting and cheering me during my whole life. I also want to thank and acknowledge the people who offered me their support during this thesis, specially to my advisors: Juan de la Fuente, Flavia Zacconi and Gonzalo Nuñez; my colleagues: Andrea Reveco and Ana Gonzalez who taught me a lot; and to my university friends: Pablo Lopez and Rafael Villablanca for their support and sympathy during the development of the thesis.

Abstract in spanish

Se realizaron mediciones de isotermas de solubilidad de 2-(3,4-Dimethoxyphenyl)-5,6,7,8-tetramethoxychromen-4-one (nobiletina) y 2-methyl-1,4-naphthoquinone (menadiona) en dióxido de carbono supercrítico a temperaturas de (313, 323 y 333) K y presiones de (9 a 32) MPa usando una metodología analítica con recirculación, con determinación directa de la composición molar de la fase rica en dióxido de carbono usando cromatografía líquida de alto rendimiento. Los resultados indican que el rango de la solubilidad de nobiletina medida fue de $107 \cdot 10^{-6}$ mol · mol^{-1} a 333 K y 18.35 MPa a $182 \cdot 10^{-6}$ mol · mol^{-1} a 333 K y 31.40 MPa. Similarmente, la solubilidad de menadiona medida varió de $630 \cdot 10^{-6}$ mol · mol^{-1} a 333 K y 9.72 MPa a $1057 \cdot 10^{-6}$ mol · mol^{-1} a 333 K y 13.43 MPa. La validación de los datos de solubilidad experimentales se realizó usando tres enfoques, a saber, estimación de la incertidumbre combinada expandida para cada punto de solubilidad a partir de valores de parámetros experimentales ($\leq 23 \cdot 10^{-6}$ mol · mol^{-1} y $\leq 111 \cdot 10^{-6}$ mol · mol^{-1} para nobiletina y menadiona, respectivamente); consistencia termodinámica, verificada utilizando un test adaptado de herramientas basadas en la ecuación de Gibbs-Duhem y datos de solubilidad obtenidos de modelación; y auto-consistencia, demostrada mediante la correlación de los datos de solubilidad con un modelo semi-empírico como una función de la temperatura, presión y densidad de CO_2 puro.

Abstract

Isothermal solubility of 2-(3,4-Dimethoxyphenyl)-5,6,7,8-tetramethoxychromen-4-one (nobiletin) and 2-methyl-1,4-naphthoquinone (menadione) in supercritical carbon dioxide at temperatures of (313, 323 and 333) K and pressures from (9 to 32) MPa was measured using an analytic-recirculation methodology, with direct determination of the molar composition of the carbon dioxide-rich phase by using high performance liquid chromatography. Results indicated that the range of the measured nobiletin solubility was between $107 \cdot 10^{-6}$ mol $\cdot$ mol^{-1} at 333 K and 18.35 MPa to $182 \cdot 10^{-6}$ mol $\cdot$ mol^{-1} at 333 K and 31.40 MPa. Similarly, the measured menadione solubility ranged from $630 \cdot 10^{-6}$ mol $\cdot$ mol^{-1} at 333 K and 9.72 MPa to $1057 \cdot 10^{-6}$ mol $\cdot$ mol^{-1} at 333 K and 13.43 MPa. The validation of the experimental solubility data was carried out using three approaches: estimation of combined expanded uncertainty for each solubility data point from experimental parameters values ($\leq 23 \cdot 10^{-6}$ mol $\cdot$ mol^{-1} and $\leq 111 \cdot 10^{-6}$ mol $\cdot$ mol^{-1} for nobiletin and menadione, respectively); thermodynamic consistency, verified utilizing a test adapted from tools based on Gibbs–Duhem equation and solubility modeling results; and self-consistency, proved by correlating the solubility data with a semi-empirical model as a function of temperature, pressure and pure CO_2 density.

Contents

List of Figures

List of Tables

Symbols and abbreviations

T	temperature	K
p	pressure	bar
y_i	experimental solubility of component i	$\text{mol}\cdot\text{mol}^{-1}$
MW_i	molecular weight of compound i	$\text{kg}\cdot\text{mol}^{-1}$
p_2^{Subl}	sublimation pressure of the pure solid solute (i=2)	bar
V_2^S	pure solid solute molar volume (i=2)	$\text{m}^3\cdot\text{mol}^{-1}$
a	attraction parameter in the PR-EoS	$\text{J}\cdot\text{m}^3\cdot\text{mol}^{-2}$
b	size parameter in the PR-EoS (van der Waals co-volume)	$\text{m}^3\cdot\text{kmol}^{-1}$
k_{ij}	interaction parameter characteristic of each binary pair	-
H	enthalpy	$\text{J}\cdot\text{mol}^{-1}$
A	Helmholtz free energy	$\text{J}\cdot\text{mol}^{-1}$
G	Gibbs free energy	$\text{J}\cdot\text{mol}^{-1}$
R	universal gas constant	$=8.314 / \text{J}\cdot\text{K}^{-1}\cdot\text{mol}^{-1}$
Z	compressibility factor	-
ΔA_j	area deviation of data point j	-
A_i	chromatographic peak area of solute i of sample taken from the cell loop in units of absorbance	AU
A_{Si}	chromatographic peak area of solute i of sample taken from stock solution in units of absorbance	AU
V_{IV}	internal volume of the loop of the equilibrium cell	µL
V_S	internal volume of the loop of the injector	µL
C_{Si}	solute i concentration of the stock solution	$\text{mol}\cdot\text{m}^{-3}$

u	standard uncertainty	-
u_{Comb}	combined uncertainty	-
U_{Comb}	combined expanded uncertainty	-

Greek Letters

$\delta(y_i)_j$	relative differences between calculated (y_i^{Calc}) and measured (y_i) solubility	$mol \cdot mol^{-1}$
$\delta(y_i)$	relative root mean square deviation of the solubility of compound i	$mol \cdot mol^{-1}$
ρ	density	$kg \cdot m^{-3}$
υ	specific volume	$m^3 \cdot kg^{-1}$
α_{ij}	non-randomness parameter between species i and j of NRTL model	-
τ_{ij}	interaction energy parameters between species i and j of NRTL model	-
ϕ	fugacity coefficient	-
$\bar{\phi}_i^F$	fugacity coefficient of component i in the fluid mixture	-
ϕ_i^S	fugacity coefficient of component i in the pure solid	-

Superscripts

Calc	calculated
E	excess property
F	fluid
S	solid

Subscripts

| i,j | molecular species |
| m | mixture |

∞	infinite pressure state
0	low pressure state
c	critical property
r	reduced property
tp	triple point property

Acronyms

PMF	polymethoxyflavone
SC	supercritical
SCF	supercritical fluid
SCFE	supercritical fluid extraction
SLE	solid-liquid equilibrium
HPLC	high performance liquid chromatography
SCL	sub-cooled liquid
G-D	Gibbs-Duhem equation
AAD	average absolute deviation
EoS	equation of state
PR	Peng-Robinson EoS
WS	Wong-Sandler mixing rules
NRTL	non-random two liquid activity coefficient model

Introduction

There is an increasing demand from the public, governments and health and environmental agencies to produce contaminant-free foods and drugs for human consumption using processes that are safe, energetically efficient and with little impact to the environment. Motivated by these facts, this thesis work seeks to contribute with relevant data for the design of processes involving the recovery of biological interest substances from reaction mixtures or natural substrates using an unconventional solvent and an environmentally friendly process.

Chemical compounds extracted from leaves, flowers, fruits, seeds and other vegetal matrices, known as phytochemicals, are of a high added value for pharmaceutical and food industry due to their beneficial biological activity for human health (bioactivity). 2-(3,4-Dimethoxyphenyl)-5,6,7,8-tetramethoxychromen-4-one or nobiletin is a flavonoid that belongs to the polymethoxyflavones (PMFs) and is one of the major components identified in citrus fruits, specifically abundant with large percentage content in citrus peels [1]. It has anti-carcinogenic effects and it is an effective anti-inflammatory, anti-diabetic [1], anti-viral and anti-microbial agent [2]. 2-methyl-1,4-naphthoquinone or menadione, is the precursor to various types of Vitamin K [3] and it is mainly used as a micronutrient for livestock and pet foods [4]. Moreover, it is used in the treatment of hypoprothrombinemia which is associated with a lack of Vitamin K resulting in a tendency to prolonged bleeding [5–7].

For the recovery of bioactive phytochemical compounds from plant material or from reaction mixtures there is a broad spectrum of solid–liquid extraction (SLE) techniques. Classically, SLE techniques can be divided into traditional and recent methods. Traditional methods include Soxhlet extraction, maceration, percolation, turbo-extraction (high speed mixing) and sonication. These techniques have been used for many decades; however, they are very often time-consuming and require relatively large quantities of organic solvents, such as *n*-hexane and chloroform which are hazardous for human health. Traditional methods such as distillation have drawback of requiring high thermal loads which can deteriorate

thermolabile compounds present in plant material (thermolabile refers to a substance which is subject to destruction/decomposition or change in response to heat).

.

For the recovery of the selected phytochemical compounds, the use of a non-conventional solvent for the extraction process is proposed in this work, specifically, an inert gas present in the atmosphere, carbon dioxide (CO_2) at supercritical (SC) conditions, i.e., at a temperature (T) and pressure (p) over the substance critical values (for CO_2: $T_c = 304.1$ K, $p_c = 7.38$ MPa). SC-CO_2 is a fluid capable of solvating phytochemicals compounds from vegetal substrates which can be recovered at a decompression stage obtaining a contaminant free product in a process known as Supercritical Fluid (SCF) Extraction (SCFE), which is a fast and efficient unconventional extraction method developed for extracting analytes from solid matrixes. The use of SCFE allows selectively isolating high purity bioactive compounds from biological substrates and avoiding deleterious chemical reactions that are related to the use of conventional solvents. The only drawback of SCFE is the higher investment costs if compared to traditional atmospheric pressure extraction techniques. However, the base process scheme (extraction plus separation) is relatively cheap and very simple to be scaled up to industrial scale [8].

For the economic feasibility study and scale-up of processes that use SC-CO_2 it is required to have information of the equilibrium between phases, *i.e.*, thermodynamic solubility (y_i) of solute i in CO_2-rich phase at system T and p. Additionally, for the design, simulation and optimization of the extraction processes, a thermodynamic model is needed to represent the solubility as a function of temperature, pressure and other parameters adjusted from validated experimental data of model binary systems. Together with thermodynamic information, kinetic studies are also necessary, but will not be covered in this work.

The objective of this thesis is to contribute with experimental validated information and models to represent the thermodynamic solubility (mole fraction) of binary systems: nobiletin + CO_2 and menadione + CO_2 at near room temperature. The specific objectives are: (1) to verify the operation and to incorporate improvements (if needed) to the experimental equipment for measuring fluid (F) + solid (S) phase equilibria (FSE) available in the

Laboratorio de Termodinámica de Procesos (LTP) in the *Departamento de Ingeniería Química y Ambiental* (DIQA) in *Universidad Técnica Federico Santa María* (UTFSM); (2) to provide with experimental solubility data (new and that available in the literature) of binary systems, nobiletin + CO_2 and menadione + CO_2, with respect to operation pressure ($p < 32$ MPa) and temperature (313 K, 323 K and 333 K); (3) to establish the worthiness of the experimental information of objective (2) using a procedure that considers: (3.1) estimation of uncertainties, (3.2) evaluation of the thermodynamic consistency and (3.3) evaluation of self-consistency; and (4) to select model(s) available in the literature for the correlation/estimation of the solubility of solutes in SC-CO_2 at high pressure and to adjust the required parameters in the model(s) to the experimental information validated in objective (3).

This work is divided in 6 chapters. In **Chapter 1**, nobiletin and its family of compounds (flavonoids) characteristics are described with emphasis on the biological activities that makes nobiletin beneficial for human health. Similarly, **Chapter 2** describes menadione and its family of compounds (naphthoquinones). **Chapter 3** describes SCFs solvent properties and SCFE process focused on the recovery of natural substrates, its advantages over conventional separation technologies and SCFE processes with CO_2 as extraction solvent. **Chapter 4** describes phase equilibrium of solid + fluid mixtures, particularly, the solubility behavior of solids in a SCF, the different methods for measuring high pressure equilibrium with emphasis on FSE, how to validate experimental solubility data and procedures for modeling FSE. In **Chapter 5** is presented the experimental methodology used in this work for measuring solubility data of binary mixtures containing a solid solute in SC-CO_2. Lastly, **Chapter 6** presents the results and discussion which are followed by the conclusions and ongoing work.

1. First studied solute: nobiletin

This chapter provides information about nobiletin and flavonoid compounds. **Section 1.1** introduces the structure, classification and general biological functions of flavonoids, with a special emphasis on polymethoxyflavones, particularly, nobiletin. **Section 1.2** presents some of the most important biological activities and recommended dietary intake of PMFs to understand their importance for human health. Finally, **Section 1.3** presents two different ways of obtaining polymethoxyflavones, from natural sources and from chemical reactions, to provide some insight on the advantage of extraction or chemical synthesis processes for the isolation of these substances.

1.1 Structure and biological functions

The natural compound that is described in this section, nobiletin, can be classified as a polyphenol per its structure. Polyphenols are one of the most numerous and widely distributed groups of substances in the plant kingdom. They are produced as the result of the secondary metabolism of plants and are frequently found attached to sugars (glycosides, i.e., any molecule in which a sugar group is bonded through its anomeric carbon to another group via a glycosidic bond), thus tending to be water-soluble. Occasionally, polyphenols also occur in plants as aglycones (organic compounds combined with the sugar portion of a glycoside). Polyphenols arise biogenetically from two main synthetic pathways: the shikimate pathway (a metabolic route used by bacteria, fungi, algae, parasites and plants for the biosynthesis of aromatic amino acids) and the acetate pathway (a metabolic route for the biosynthesis of phenols, prostaglandins, fatty acids and macrolide antibiotics) [9]. More than 8000 polyphenolic structures are currently known; their common feature is an aromatic ring bearing at least one hydroxyl substituent [10]. Polyphenols can be divided into at least 10 different classes based upon their chemical structure [9].

Flavonoids are the largest class of polyphenols that comprise a diverse group of plant metabolites with over 10,000 compounds that have been identified until now. However, only very few of them have been investigated in detail [11]. They have a common structure

(**Figure 1.1**), consisting of two aromatic rings linked through three carbon atoms. All naturally occurring flavonoids possess three hydroxyl groups, two of which are on the ring A at positions five and seven, and one is located on the ring B, position three (3', **Figure 1.1**). The flavonoid subclasses, based on types of chemical structure, include: flavonols, flavones, flavanones, flavanols, anthocyanins and isoflavones [12] (**Table 1.1**). They have several important functions in plants, such as providing protection against harmful ultraviolet (UV) radiation or plant pigmentation. In addition, they have antioxidant, antiviral and antibacterial properties [12]. They also regulate gene expression and modulate enzymatic action [11]. Biochemical actions of flavonoids depend on the presence and position of various substituent groups, that affect metabolism of each compound.
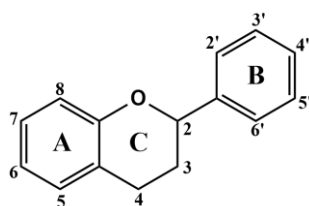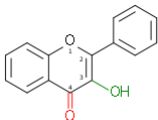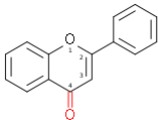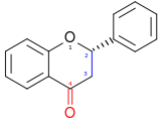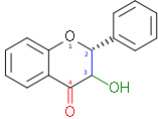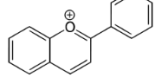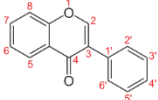
Figure 1.1. Basic flavonoid structure [13].

Polymethoxyflavone is a general term for flavones (**Figure 1.2**) bearing two or more methoxy groups (-OCH$_3$) on their basic benzoc-pyrone (15-carbon, C6–C3–C6) skeleton with a carbonyl group at the C4 position.
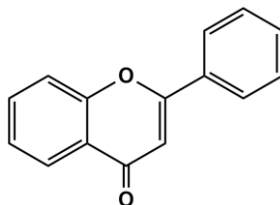
Figure 1.2. Flavone structure.

Table 1.1. Subclasses of flavonoids [12]**.**

Subclass	Examples of compounds	Common Structure
Flavonols	Quercetin, kaempferol, myricetin	
Flavones	Luteolin, apigenin, tangeretin, **nobiletin**	
Flavanones	Naringenin, hesperetin	
Flavanols	Catechin, epicatechin, epigallocatechin, glausan-3-epicatechin, proanthocyanidins	
Anthocyanins	Cyanidin, delphinidin, pelargonidin, malvidin	
Isoflavones	Genistein, daidzein	

PMFs exist almost exclusively in citrus plants and are one of the major constituents of citrus peels (**Figure 1.3** shows some common citrus PMFs). Current annual worldwide citrus production is estimated at over 105 million tonnes, with more than half of this being oranges [2]. For example, total citrus production of the United States (US) was 10.6 million metric tonnes in 2004–2005 (National Agricultural Statistics Service). Around 34% of these products were used for juice production, yielding approximately 44% (4–5 billion lbs. in the US) of peels as by-products. In some regions of the world, citrus peels like orange or tangeretin peels have been a traditional medicine for relieving stomach upset, cough, skin inflammation, muscle pain, and ringworm infections, as well as for lowering blood pressure [2]. PMFs have been of particular interest due to their documented broad spectrum of

biological activity, including anti-inflammatory [14–16], anti-carcinogenic [15–18], and anti-atherogenic properties [19,20].

	Scutellarein	Sinensetin	Tangeretin	Hexamethoxyflavone	**Nobiletin**	Heptamethoxyflavone
R_1	H	H	H	OCH_3	H	OCH_3
R_2	H	H	OCH_3	H	OCH_3	OCH_3
R_3	H	OCH_3	H	OCH_3	OCH_3	OCH_3
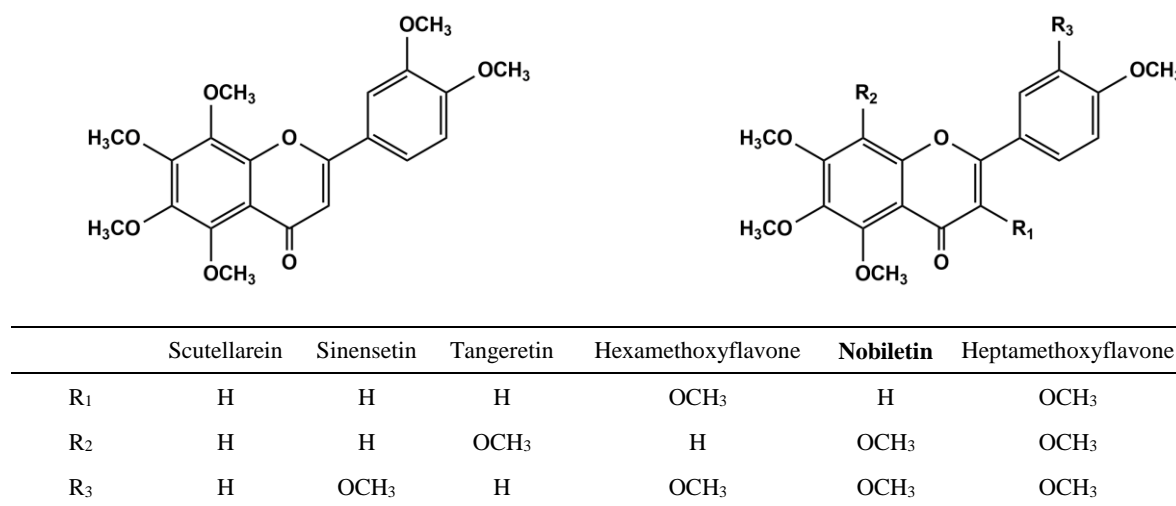
Figure 1.3. Nobiletin (left) and other citrus polymethoxylated flavones (right) [21].

2-(3,4-Dimethoxyphenyl)-5,6,7,8-tetramethoxychromen-4-one or nobiletin [CAS: 478-01-3] (**Figure 1.3**), a PMF, is one of the major components identified in citrus fruits, specifically abundant with large percentage content in citrus peels of sweet oranges and mandarin, and it may act in protecting from pathogenic attack taking into account its antiviral and antimicrobial capacity [2]. Nobiletin has shown many potential health promoting benefits, considering the cumulative evidences that indicate its biological activity, which gives to nobiletin pharmacological properties, including, anti-inflammatory (the most significant), anti-carcinogenic, anti-atherogenic and anti-diabetic [22].

1.2 Biological activities and dietary intake

Recent research data have provided additional supporting evidence that shows that citrus flavonoids, especially polymethoxyflavones, are directly associated with the inhibition of enzymes involved in the inflammation process [2]. Nobiletin has a potential anti-inflammatory effect with fewer side effects than commercial anti-inflammatory steroidal drugs [15,23]. The anti-inflammatory activities of nobiletin are likely linked to the prevention

of plaque formation during atherosclerosis These findings indicate that nobiletin could be a novel anti-inflammatory and/or immunomodulatory potential drug. Moreover, nobiletin can inhibit the proliferation of human prostate, skin, breast and colon carcinoma cell lines [14,24,25].and it has also shown to have anti-proliferative and apoptotic effects on a gastric cancer cell line. In an evaluation of 42 flavonoids, nobiletin showed the strongest anti-proliferative activity against six human cancer cell lines [26].

Although potentially beneficial for human health, the determination of dietary intake of polyphenols, including flavonoids, is challenging because the formation of flavonoids in plants is influenced by numerous factors including light, plant genetics, environmental conditions, germination, degree of ripeness, and processing and storage, as well as species variety [9], which make it difficult to estimate the flavonoid content in foodstuffs and confounds the ability to infer epidemiologic relationships regarding health and disease. **Table 1.2** provides an estimation of the daily dietary flavonoid intake by different countries.

Table 1.2. Estimated daily dietary flavonoids intakes by different countries [27].

Flavonoid	Country	[mg/day]	Main dietary sources
Flavonols / Flavones	Netherlands	23	Tea (48%), onions (29%), apples (7%)
	United States	20-24	Tea (26%), onions (24%), apples (8%)
	United Kingdom	26	Tea (82%), onions (10%)
	Finland	4	Apples and onions
	Spain	5	Tea (26%), onions (23%), apples (8%)
	Japan	16	Onions (46%), molokheya (10%), apples (7%), green tea (5%)
Catechins	Netherlands	50	Tea (83%), chocolate (6%), apples and pears (6%)
	United States	25	Tea (59%), apples and pears (26%)
Flavanones	Finland	20	Orange and grapefruit

1.3 Nobiletin and other flavonoids sources

Nobiletin and other flavonoids can be isolated from natural substrates in which they are present by extraction and purification processes (**Chapter 3**). Among natural substrates that provide large amounts of flavonoids are: citrus fruits, blueberries, blackberries, onions, peppers, a variety of teas, and also oregano and parsley [12]. **Table 1.3** provides flavone content in chosen foodstuffs. So far, about 30 PMFs have been isolated and identified from different tissues of the citrus plants [28]. Nobiletin can be isolated from citrus peels or obtained via chemical synthesis (see synthetic routes of different citrus PMFs in ref. [29]).

Table 1.3. Content of flavones in chosen foodstuffs (mg/100g foodstuff) [12].

Vegetable	Flavones [μg/100g]
Kohlrabi	1.3
Red grapes	1.3
Lemons	1.9
Chicory	2.85
Celeriac	3.90
Green pepper	4.71
Artichokes	9.69
Fresh parsley	216.15
Dried oregano	1046.46
Dried parsley	4523.25

2. Second studied solute: menadione

This chapter provides information about vitamin K family, particularly, menadione. **Section 2.1** introduces the structure, classification and general biological functions of K vitamins, with a special emphasis on menadione. **Section 2.2** presents some of the most important biological activities and recommended dietary intake of vitamin K to understand their importance for human health. Finally, **Section 2.3** presents two different ways of obtaining vitamin K, from natural sources and from chemical reactions, to provide some insight on the advantage of extraction or chemical synthesis processes for the isolation of these substances.

2.1 Structure and biological functions

The natural compound that will be described in this section, menadione, can be classified as a quinone per its structure, specifically, a naphthoquinone. Quinones are widely-distributed aromatic compounds present throughout nature that can be found in several families of plants, fungi, algae and bacteria. They are classified into benzoquinones, anthraquinones and naphthoquinones according to their main chemical core [30]. Naphthoquinones are compounds present as secondary metabolites of plants and microorganisms that confer activity in various biological oxidative processes and represent a chemical defense used by many plants [31]. They are highly reactive organic compounds, used as natural or synthetic dyes whose colors range from yellow to red. Naphthoquinones are structurally related to naphthalene (**Figure 2.1a**) and are characterized by their two carbonyl groups in the 1,4 position, and as such, are named 1,4-naphthoquinones (**Figure 2.1b**).

a   b
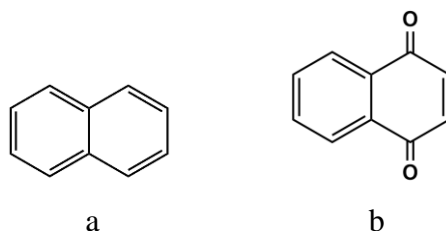
Figure 2.1. Chemical structure of naphthalene (a) and 1,4-naphthoquinone (b) [32].

Naturally occurring 1,4-naphthoquinones are widely distributed in nature, especially in several families of higher plants besides also being present in algae, fungi, some animals and as products of metabolism in some bacteria [30,33].

2-methyl-1,4-naphthoquinone, or menadione [CAS: 58-27-5] (**Figure 2.2a**), also called vitamin K_3 [7] and all derivatives that qualitatively exhibit the biological activity of 2-methyl-3-phytyl-1,4-naphthoquinone, or phylloquinone [CAS: 84-80-0] (Vitamin K_1) (**Figure 2.2c**), are called K Vitamins. These vitamins function as a cofactor for the γ-carboxylation of specific glutamic acid residues of the precursor protein of prothrombin, converting the protein to biologically active prothrombin [34], which is a coagulation (clotting) factor that is needed for the normal clotting of blood. The K vitamins found in nature are phylloquinone (with a 2´E,7´R,11´R configuration [32]) and 2-methyl-3-polyprenyl-1,4-naphthoquinone, o*r* Menaquinone-*n* [CAS: 863-61-6] (Vitamin K_2) (**Figure 2.2b**), abbreviated MK-*n*, for *n* being the number of prenyl residues, which is found in nature with side chains of 4 – 13 prenyl residues and usually exhibits the all-*trans* configuration. In a study performed in rats, it was found that menadione is released from phylloquinone in the intestine and converted to menaquinone-4 in tissues after being reduced; thus, menadione is a catabolic product of phylloquinone and circulating precursor of tissue menaquinone-4 [3]. In the organism, menadione is distributed over many tissues, but very rapidly eliminated. Only a small part of menadione is converted to menaquinone-4.

       a   b   c
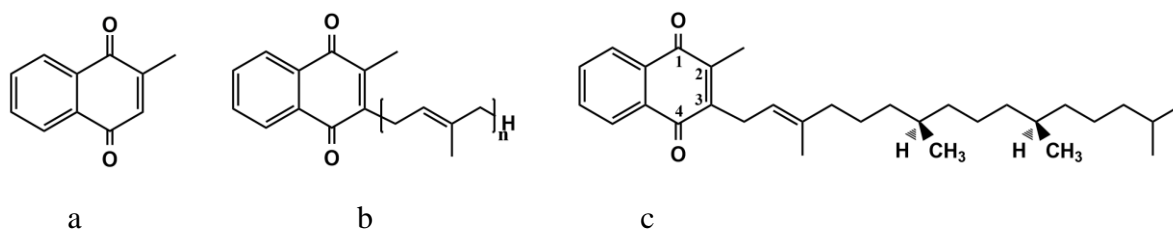
Figure 2.2. Vitamin K family structures: menadione (a), menaquinone-n (b) and phylloquinone (c) [32].

2.2 Biological activities and dietary intake

The biological function of all forms of vitamin K is to act as a cofactor for the posttranslational carboxylation of certain protein-bound glutamate residues, which are converted into gamma-carboxy glutamate (Gla). These Gla residues form calcium-binding sites which are essential for the activity of the proteins in which they are found [35]. Vitamin K activity is exhibited by 2-methyl-l,4-naphthoquinones substituted at position 3 (see **Figure 2.2**) with a phytyl group (phylloquinone) or a muItiprenyl side chain (the menaquinone series) [36].

Menadione and other naturally occurring quinones have shown antineoplastic activity (i.e., that inhibits or prevents the growth and spread of tumors or malignant cells) with IC_{50} (half maximal inhibitory concentration) values of 0.04–25 µM essayed in various cancer cell lines [37]. This quantitative measure indicates how much of a drug or other substance is needed to inhibit a given biological process (or component of a process, i.e. an enzyme, cell, cell receptor or microorganism) by half.

The daily dietary intake of vitamin K is mainly (90%) in the form of phylloquinone (green vegetables and plant margarines). The daily vitamin K requirement of a healthy human is generally estimated at $1 - 2$ µg/kg of body weight [32].

2.3 Menadione and other vitamin K sources

Menadione can be chemically synthesized from the oxidation of 2-methylnaphtalene or 2-methyl-1-naphtol using conventional organic solvents and SC-CO_2 [38–41]. The use of SC-CO_2 as the solvent medium in the synthesis allows to obtain a solvent free reaction product. A common process for the production of menadione is the oxidation of 2-methylnaphthalene with, e.g., CrO_3 or H_2O_2 in acetic acid or $Na_2Cr_2O_7$ in sulfuric acid [32]. Since menadione is an intermediate compound of fast elimination, it cannot be isolated from natural substrates. The other vitamin K can be obtained from leafy vegetables (phylloquinone) [42] and fermentation products such as cheese (menaquinone-n) [43].

3. Supercritical fluid extraction

One of the motivations for measuring solubility data of a solute in SC-CO_2 is to determine the optimal conditions for its recovery from a natural substrate using SCFE. This chapter, describes the SCF state, the SCFE process and the convenience of using CO_2 in SCFE instead of other solvents.

3.1 Supercritical fluid solvents and supercritical fluid extraction processes

A substance is called to be in the state of supercritical fluid when both variables, temperature and pressure, exceed the critical point values (for CO_2: T_c = 304.1 K, p_c = 7.38 MPa) as illustrated in **Figure 3.1**.
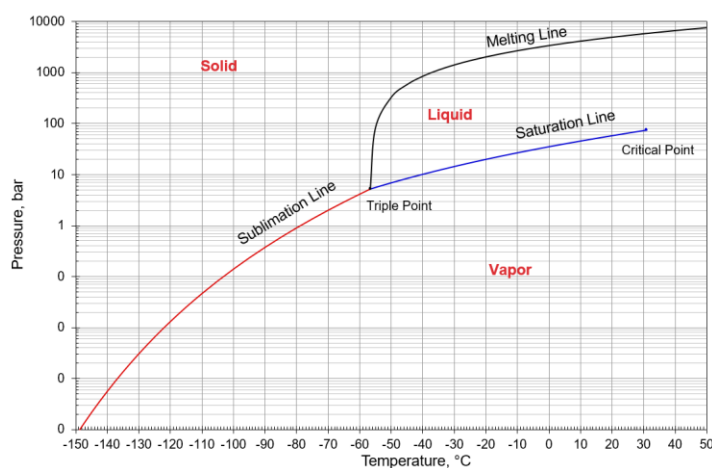
Figure 3.1. Carbon dioxide pressure–temperature phase diagram.

When a substance reaches its critical point, the densities of the vapor phase and the liquid phase become equal, thus forming a single fluid. Along a near-critical isotherm (between T_c and 1.2 T_c) [44], the density, transport properties (such as viscosity and diffusivity), and other physical properties (such as dielectric constant and solvent strength), can be varied in a continuum from gas-like to liquid-like with relatively small changes around the critical pressure. Specifically, these fluids display twin advantageous properties of having high

density (liquid-like), offering high solvency, as well as high compressibility (gas-like), offering large variability of solvency by small changes in temperature and density, as illustrated in **Figure 3.2,** and consequently, high selectivity of separation (offering high purity). Also, the SCF state has very favorable transport properties, such as high diffusivity and low viscosity as compared in **Table 3.1**.
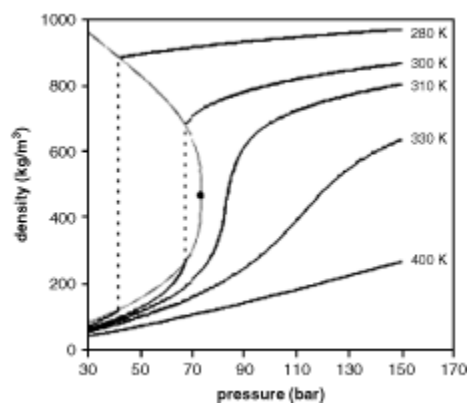
Figure 3.2. Carbon dioxide density variation with pressure and temperature [45].

Table 3.1. Comparison of density, viscosity and diffusivity for typical liquid, gas and supercritical fluid [45].

	Density / $kg \cdot m^{-3}$	Viscosity / cp	Diffusivity / $mm^2 \cdot s^{-1}$
Gas	1	0.01	1-10
SCF	100-1000	0.05-0.1	0.01-0.1
Liquid	1000	0.5-1.0	0.001

SCFE has emerged in the last thirty years as a highly promising environmentally benign technology to produce natural extracts with high potency of active ingredients – such as flavors, fragrances, spice oils and oleoresins, natural colors, nutraceuticals or herbal medicines – for the food, cosmetics, and pharmaceutical industries. The SCFE technique ensures high consistency and reliability in the quality and safety of the bioactive heat-sensitive botanical products because it does not alter the delicate balance of bioactivity of natural molecules. SCFE is a two-step process involving extraction and separation by varying the solvating power of the solvent at different conditions. The feed, generally ground solid, is charged into the extractor.

Figure 3.3 shows a schematic SCFE process using SC-CO_2 for the recovery of an oil extract: SC-CO_2 is fed to the extractor through a high-pressure liquid CO_2 pump, usually between 100–400 bar and 40 to 60 °C (as indicated by Melo et al. [46] after comparing 543 publications on SCFE from vegetable raw materials from 2000 to 2013). The extract-laden CO_2 is sent to a separator (60–120 bar) via a pressure reduction valve. At reduced temperature and pressure conditions, the extract precipitates out in the separator due to reduction in its solvent power. Alternatively, it is possible to reduce the solvent power of the extractant in the separator, not only by reducing the pressure, but also by increasing the temperature or adding a third substance, depending on the nature of the feed and process economics. For example, for coffee decaffeination, either hot water is pumped to the separator or the extract-laden CO_2 is passed through a bed of activated charcoal to remove caffeine from the CO_2 stream. The extract-free CO_2 stream leaving the separator is then recycled to the extractor. In the case of liquid feed, the extractor is modified into a column through which feed and SC-CO_2 are fed either co-currently or concurrently.
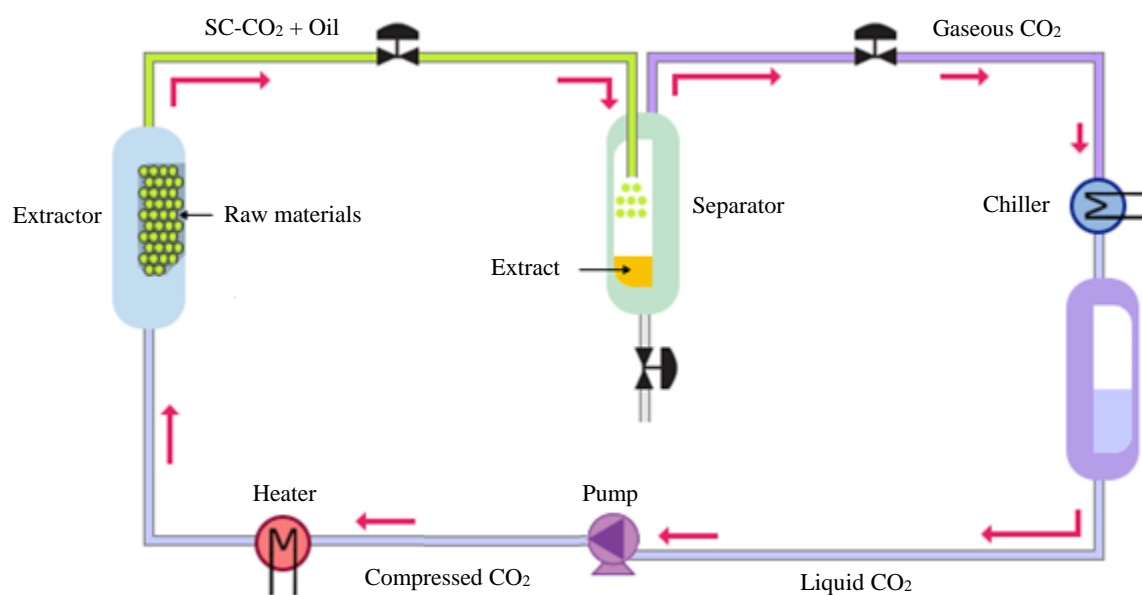
Figure 3.3. Supercritical Fluid Extraction process using carbon dioxide for the recovery of an oil extract.

3.2 Supercritical fluid extraction processes with carbon dioxide

Several solvents are used in SCFE. In fact, any solvent can be used as a supercritical solvent; however, the technical viability (critical properties), toxicity, cost, and solvation power determine the best-suited solvent for an application. Nowadays, among the various substances possible as a SCF solvent (**Table 3.2**), SC-CO_2 at near-ambient temperatures is one of the most desirable SCF solvent for extraction of natural products as it is non-toxic, inexpensive, non-flammable, non-corrosive and non-polluting. Its near-ambient critical temperature (31.1 °C) makes it ideally suitable for thermally labile natural products. It is generally regarded as safe (GRAS) by U.S Food and Drug Administration (FDA) and European Food Safety Authority (EFSA) [47] and yields contamination-free, tailor-made extracts having superior organoleptic profile and enhanced shelf life (i.e., the length of time that a substance may be stored without becoming unfit for use, consumption, or sale). Also, various advantages, i.e., the generation of minimum wastes, its usability as a solvent medium, easy separation of solutes for the recycling of solvent and unique thermo-physical and transport properties of SC-CO_2, have given impetus to the development of several alternative SC-CO_2-based processes.

Table 3.2. Critical properties of various solvents [48].

Solvent	MW / g·mol^{-1}	T_c / K	p_c / MPa	ρ_c / kg·m^{-3}
Carbon dioxide (CO_2)	44.01	304.1	7.38	469
Water (H_2O)	18.02	647.3	22.12	348
Methane (CH_4)	16.04	190.4	4.60	162
Ethane (C_2H_6)	30.07	305.3	4.87	203
Propane (C_3H_8)	44.09	369.8	4.25	217
Ethylene (C_2H_4)	28.05	282.4	5.04	215
Propylene (C_3H_6)	42.08	364.9	4.60	232
Methanol (CH_3OH)	32.04	512.6	8.09	272
Ethanol (C_2H_5OH)	46.07	513.9	6.14	276
Acetone (C_3H_6O)	58.08	508.1	4.70	278

Since CO_2 is a gas at low pressures, there is no solvent residue in the extracts obtained with SC-CO_2 and they are very close in smell and taste to those in nature. In addition, the energy required for attaining supercritical state (for p_c = 73.8 bar) is more than compensated by the negligible energy required for solvent recovery from the extract, resulting in less energy requirements than in traditional steam distillation (SD) or solvent extraction (SE). For example, a comparison of different extraction methods for the extraction of oleoresin from dried onion showed that the yield after SC-CO_2 extraction was 22 times higher than that after SD. During this century, SC-CO_2 may very well qualify as the most preferred considering the current environmental concerns, regulations, and cost effectiveness that are driving the proactive stance of the industrial sector in the development of environmentally friendly processes.

SC-CO_2 has successfully been used in many application at industrial scale since the 1980s, including the extraction of caffeine from coffee and tea, extraction of hops, natural products like essential oils, flavors, fragrances, food ingredients, nutraceuticals, pharmaceutical and cosmetic active principles [49], and more. SC-CO_2 has successfully been used for the extraction of nobiletin (and other flavonoids) and fat-soluble vitamins closely related to the menadione. For example, Lee et al. (2010) [50] used SC-CO_2 to extract PMFs from Citrus *depressa* Hayata; their results showed that the optimal temperature and pressure for selective SCFE of nobiletin with SC-CO_2 were 80 °C and 30 MPa, respectively, and the nobiletin yield of SCFE was 7% greater as compared with conventional SE method. Schneidermann *et al.* (1988) extracted vitamin K_1 from commercial soy protein-based and milk-based powdered infant formulas by using SCFE with CO_2 at 55 MPa and 60 °C for quantification. They achieved a recovery greater than 94%.

4. Solid + fluid phase equilibria at high pressures

Obtaining experimental solubility data of a solid solute in a SCF is a necessary step to determine the process conditions at which a certain solute in a mixture has a preference over other solutes to be in a greater concentration in the supercritical phase, and is the first step in the design and optimization of a SCFE process at a pilot or industrial scale.

In this chapter, it is established the solubility behavior of a solid solute in a SCF solvent (phenomenology of the systems studied), followed by a description of the different experimental methods for measuring thermodynamic phase equilibrium properties, particularly for solid + fluid binary systems at high pressure and the basic criterions for selecting a suitable experimental method for a system. Consecutively, three methods for validating p-T-y_i data of solid + fluid binary systems are described. Lastly, the fundamental thermodynamic equations, procedures and criterions for modeling multicomponent fluid phase equilibria are given.

4.1 Solubility behavior of solids in a supercritical fluid

Phase equilibrium information is critical in designing and assessing separation processes under supercritical conditions. Solute solubility in SC-CO_2 (and any other SCF solvent) depends markedly on the operational conditions of pressure and temperature. This is illustrated in **Figure 4.1** for the changes in solubility in SC-CO_2 of two simple phenolic compounds such as benzoic acid (a and b) and salicylic acid (c and d) as a function of system pressure, for different temperatures (a and c), and as a function of system temperature, for different pressures (b and d). In both cases, the molar fraction of the solute in a saturated SC-CO_2 phase (y_2) increases monotonously with CO_2 pressure because, under supercritical conditions, density increases with pressure with the result of a reduction in intermolecular distance between CO_2 molecules, thus contributing to enhanced solute–solvent interactions (i.e., solvation). The effect of system temperature on solute solubility is more complex than the effect of system pressure. Indeed, there are two main effects on the solubility in SC-CO_2

when T increases isobarically [51]: the density and solvent power of CO_2 decrease, and the vapor pressure and volatility of the solute increase.
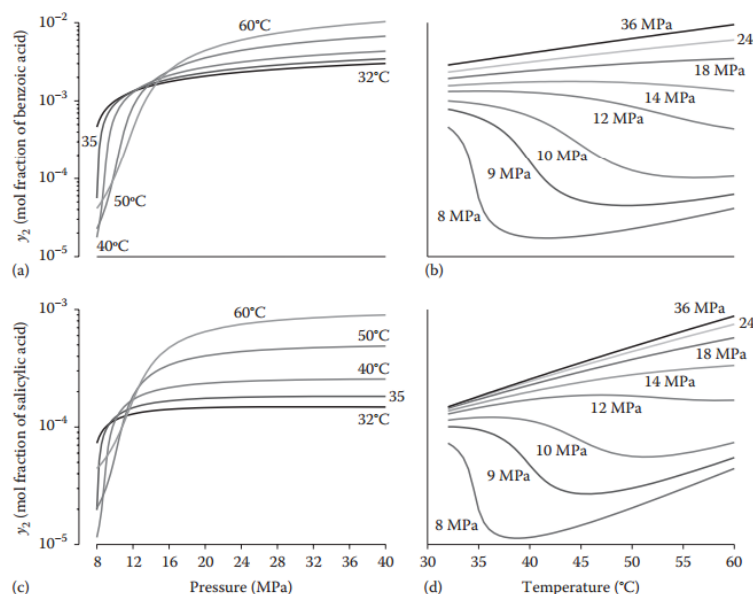
Figure 4.1. Solubility of (a, b) benzoic acid and (c, d) salicylic acid in supercritical CO_2 as a function of (a, c) system pressure (lines indicate solubility isotherms at noted temperatures) or (b, d) system temperature (lines indicate solubility isobars at noted pressures) [52].

These two effects have opposite consequences in solubility that decreases when solvent power decreases and increases when solute volatility increases. Depending on which of these two effects dominates, solubility decreases, remains constant, or increases as T increases isobarically. Density effects dominate near the critical point, where CO_2 is highly compressible and experiences large changes in density thus from moderate changes in T. On the other hand, vapor pressure effects dominate away from the critical point, where CO_2 is less compressible and density changes moderately thus from large changes in T. There is an intermediate pressure, the so-called crossover pressure [53], where the density and vapor pressure effects are similar, and the solubility remains constant when temperature changes. For benzoic acid, the crossover pressure between 50 °C and 60 °C is ca. 16 MPa, and the crossover pressure decreases as the temperature decreases (**Figure 4.1a**). Thus, at ca. 10 MPa, the solubility of benzoic acid decreases as the temperature increases.

The solubility of solids in a SCF will also depend strongly on the type of solvent. The fluids used as solvents can be classified in compounds of high T_c, such as long chain alkanes and polar compounds like water or methanol, and compounds of low T_c, usually condensable gases like CO_2 and propane. The main differences in this classification correspond to the selectivity and solvent power. Compounds of high T_c operate at high temperatures (from 500 to 700 K), have a very good solvent power and are capable of solubilizing compounds of high molecular weight. However, they have low selectivity in multicomponent mixtures and are not suited to work with thermolabile compounds. On the other hand, low T_c compounds have affinity for compounds with low molecular weight and low polarity. For solutes of importance in the pharmaceutical and food industry, which are frequently natural compounds, it is necessary to use a low temperature in solubility measurements and extraction processes to avoid a possible chemical degradation of the solutes. This can be used to justify the utilization of a low T_c solvent, such as CO_2, instead of a high T_c solvent, as a SCF for the isolation and purification of phytochemical compounds like menadione and nobiletin. Lastly, the solubility of a solute in a SCF can be modified by adding another compound to the SCF, called an entrainer, which acts as a co-solvent or an anti-solvent, in a small amount, usually below 5% mol·mol^{-1}. By doing so, the solid solubility is altered by a change in polarity.

4.2 Measuring high pressure solid + fluid phase equilibrium

There exists a wide variety of methods and techniques available for experimental studies of phase equilibria at high pressures. To decide which method is suitable for a specific case it is necessary to consider the properties of the components and the phenomena that will be investigated. A complete review on the different techniques, classified per the error sources of the different methods, with their main advantages and limitations was made recently (2012) by R. Dohrn and collaborators [65] and only a brief description is given in what follows.

There are basically two main types of methods for measuring fluid phase equilibria at high pressures: the analytical methods and the synthetic methods. This classification is based on whether the compositions of the equilibrium phases are determined (analytically) or the

mixture has been prepared (synthesized) with precisely known composition [54]. The characteristic error sources of all analytical methods are related to the precise determination (analysis) of the compositions of the coexisting phases, either by sampling or by composition determination under equilibrium pressure. The main challenges of all synthetic methods are the precise preparation of the investigated mixture, detection of a phase transition, and determination of additional properties needed for the evaluation of the raw data. In general, the analytic methods are recommended for systems in which the number of phases present and its nature (at the studied conditions of temperature and pressure) are known, while synthetic methods are recommended for exploratory analysis of phase behavior in terms of the number and type of the phases present in equilibrium. A summary of the different methods for measuring high pressure fluid phase equilibria is depicted in **Figure 4.2.**
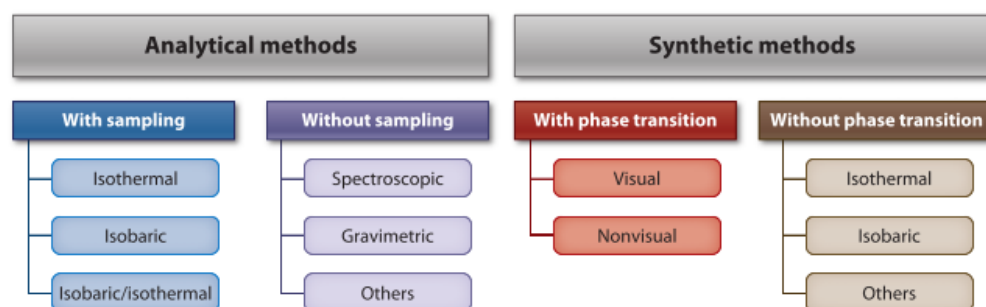
Figure 4.2. Classification of experimental methods for phase equilibria at high pressures [54].

Per the objectives of the present thesis, an analytical-isothermal method will be used for measuring thermodynamic solubility at different pressures at constant temperature. The reason for using an analytical method instead of a synthetic method is that there is evidence, from previous information, of the number and nature of the phases present, solid + fluid, for solids solutes in SC-CO_2, specifically, compounds of the family of nobiletin (flavonoids) [55,56] and fat-soluble vitamins [57,58] at near room temperatures.

The analytical isothermal methods have three fundamental steps: a) preparation of the mixture, (b) system equilibration, and (c) sampling and analysis of the phase compositions.

The third step is the most critical. Sampling from a closed high-pressure vessel leads to a pressure drop and to a change in the total composition. Therefore, a new equilibration step is initiated that results in changed compositions of the equilibrated phases as well as a changed level of the phase boundaries in the cell. Both must be carefully considered if more than one sample is taken.

There are several technical options to avoid negative feedback of sampling on the state in the equilibrium cell [59]. Using a large equilibrium cell or taking small samples through capillaries or special valves reduces the pressure drop. Alternatively, the pressure in the equilibrium cell can be kept constant during sampling by reducing the cell volume using a piston or a bellows, by blocking off the content of the cell from the sample before withdrawing it, or by adding one or more components to the equilibrium cell during sampling. When special valves are used, such as high performance liquid chromatography (HPLC) multiport valves or systems such as the rapid on-line sample injector (ROLSI^{TM}) valves [60], the equilibrium cell can be directly coupled to analytical equipment, usually using chromatographic methods such as HPLC, supercritical-fluid chromatography (SFC), or gas chromatography (GC). This direct coupling can prevent contact of the sample with potentially reactive substances or gases in the atmosphere. Furthermore, the extremely low dead volumes, low sample volumes, and immediate flushing with a (preheated) inert fluid counteract the incomplete removal of the sample from the valve. Finally, sampling from a recirculation line [61] can prevent errors related to the pressure drop during sampling, such as differential vaporization. Many of these solutions have been implemented in the solubility measurement methodology used in this work as it will be described in **Chapter 5**.

4.3 Validation of experimental data

The reliability and accuracy of physicochemical property data has an impact on the modeling, design and optimization of processes [62], and also affects the estimation of costs on a project. Consequently, it is relevant in any research involving measurements of physicochemical data, in particular properties of high pressure phase equilibria in chemical thermodynamics, to include estimation of uncertainties in order to assess the accuracy of the

data reported [63]. In this investigation, three methodologies are used for validating the experimental data, namely, estimation of uncertainties of measurement, evaluation of the thermodynamic consistency and self-consistency of the data which are described in what follows.

4.3.1   Estimation of uncertainties of measurement

Uncertainty is the quantitative parameter used to estimate the dispersion or closeness of the value measured from the true (but unknowable) value [64]. Uncertainties of properties can be estimated using two approaches [65]: (A) by a probability distribution from a defined large number of repetitions, or (B) by propagation of uncertainties using the available information, combined with common scientific sense based on previous experience. For thermodynamic properties of phase equilibria (e.g., sets of compositions of phases, temperature and pressure), approach (A) most of the time is inappropriate, considering the dimension of the effort and cost associated, and is limited to verify the repeatability (a type of precision equal to one minus the standard deviation) of a few measures [62]. Consequently, approach (B) is preferred for thermodynamic properties of phase equilibrium data. For properties like equilibrium temperature and pressure the standard uncertainty (u) is calculated with one standard deviation (68.27% of level of confidence for a normal distribution). Generally, the standard deviation may be estimated from the type of experimental apparatus, methodology and other sources of information from literature, among others [65].

In this work, the uncertainty for each mole fraction can be assessed with the combined uncertainty (u_{comb}), an arrangement that quantifies the propagation of the individual standard uncertainties of each variable or constraint, appropriately combined and weighted, which defines the mole fraction (inherent error). For a property f that is calculated as a function of n variables x_i as in **Equation (4.1)**, the inherent error Δf is calculated with **Equation (4.2)** where dx_i corresponds to the uncertainty of variable x_i. The combined expanded

uncertainty, U_{comb}, **Equation (4.3)**, is defined as the product of the combined uncertainty with a number (k, coverage factor) greater or equal to one (e.g., 1.645 for 90% of level of confidence for a normal distribution). Note that the definition of all elements for the combined uncertainty in approach (B) is in most of the cases unrealizable, and therefore uncertainties declared for a given set of experimental values are estimations of the real dispersion. The level of confidence or confidence interval (CI) of the experimental results $f_{\% CI}$ [65], **Equation (4.4)**, is evaluated with U_{comb}.

$$f = f(x_1, x_2, ..., x_n) \tag{4.1}$$

$$u_{comb}(f) = \Delta f = \sum_{i=1}^{n} \left| \frac{\delta f}{\delta x_i} \right| \cdot dx_i \tag{4.2}$$

$$U_{comb}(f) = k \cdot u_{comb}(f) \tag{4.3}$$

$$f_{\% CI} = f \pm U_{comb}(f) \tag{4.4}$$

The estimation of uncertainties for the solubilities of nobiletin and menadione in SC-CO$_2$ are performed using both approaches A and B and are explained as it follows: Approach (A). From three to five consecutive measures of solubility of either solute in SC-CO$_2$ at similar temperature and pressure are completed for every condition. Results indicate that the repeatability is above 95%, which is adequate to verify the precision of the experimental apparatus and methodology used. Approach (B). The standard (u) and combined expanded $\left(U_{comb} \right)$ uncertainties are estimated using the available information for the apparatus, experimental methodology and measured values (see **Table 6.2** for details).

4.3.2   Thermodynamic consistency test

Thermodynamic consistency tests are supplementary tools to evaluate the reliability of a data set (e.g., temperature, pressure and phase compositions at equilibrium), based on the over determination of experimental properties measured, according to the phase rule, along

with the use of the Gibbs–Duhem (G-D) equation to generate values of any one of these properties and to compare them with the laboratory results [66]. Particularly, for experimental solubility of a solid solute dissolved in SC-CO$_2$, i.e., temperature, pressure and solute mole fraction in CO$_2$-rich phase at equilibrium, Valderrama and Zavaleta [67] described a simple methodology for evaluating the thermodynamic consistency that combines the G-D equation with an appropriate calculation of the compressibility factor $\left(Z^F \right)$ and fugacity coefficients of the solute $\left(\overline{\phi}_2^F \right)$ and CO$_2$ $\left(\overline{\phi}_1^F \right)$ in the supercritical fluid phase using an equation of state (EoS) (**Section 4.4** describes how these properties are calculated at thermodynamic equilibrium). The G-D equation for a binary homogeneous gas mixture at constant temperature can be written as:

$$\left[\frac{Z^F - 1}{p} \right] dp = y_1 d \left(\ln \overline{\phi}_1^F \right) + y_2 d \left(\ln \overline{\phi}_2^F \right) \tag{4.5}$$

The test proposed by Valderrama and Zavaleta [67] states that for a data set to be considered consistent, the left side of **Equation (4.5)** should be equal to the right side within acceptable deviations (explained in the next paragraph). **Equation (4.5)** can be conveniently expressed in an integral form and be further arranged to obtain an equation to assess the thermodynamic consistency of an individual data point (j) by using the information of the next data point (j+1). This equation is called the area deviation (ΔA_j) and is calculated as follows:

$$\Delta A_j = \frac{\int_j^{j+1} \left(p \cdot y_2 \right)^{-1} dp - \left\{ \int_j^{j+1} \overline{\phi}_2^F \cdot \left(Z^F - 1 \right)^{-1} d\overline{\phi}_2^F + \int_j^{j+1} \left(1 - y_2 \right) \cdot \left[y_2 \cdot \left(Z^F - 1 \right) \cdot \overline{\phi}_1^F \right]^{-1} d\overline{\phi}_1^F \right\}}{\int_j^{j+1} \left(p \cdot y_2 \right)^{-1} dp} \tag{4.6}$$

According to Valderrama and Zavaleta [67] there are two stages in the test that have to be completed. The first stage is to verify that the EoS with the mixing and combining rules selected to model the FSE for each isotherm properly represent y_i, i.e., with the optimized

fitting parameters the square root of the sum of relative differences between calculated (y_i^{Calc}) and measured (y_i) solubility ($\delta(y_i)_j = \left(y_i^{Calc} - y_i\right)_j / y_{ij}$) squared and divided by the number (N) of data points ($\delta(y_i) = \sqrt{\sum_{j=1}^{N} \delta(y_i)_j^2 / N}$, relative root mean square deviation) [65] is within ±20%. To try a different model (TDM) is recommended if this condition is unfulfilled.

The second stage is to analyze the values of all ΔA_j calculated with **Equation (4.6)** and to check that all of them are within ±20% to declare the experimental data set -thermodynamically consistent- (TC). In case that only the 75% of the calculated values of ΔA_j verify the condition of ±20%, the data set is defined as -not fully consistent- (NFC). If less than 75% of the calculated values of ΔA_j verify the condition of ±20%, the data set is considered -thermodynamically inconsistent- (TI).

4.3.3 Self-consistency test

Some issues about the consistency test are mainly related to the performance of the equation of state and the lack of information for the solid solute such as, critical parameters, acentric factor, molar volume, and sublimation pressure required for calculations with an EoS [68,69]. The semi-empirical model proposed by Mendez-Santiago and Teja (MS-T) [70] is used to correlate the solid solute solubility as a function of temperature, pressure and pure CO_2 density, removing the restriction aforementioned, data of solute properties and performance of equations of state. The adjustable parameters included in the model are temperature independent, therefore, an appropriate representation of solute solubility, temperature and pressure versus CO_2 density could result in a collapse of all the experimental data on one straight line for a range approximately from half to twice of the CO_2 critical density for a wide range of temperatures, representing a self-consistency test for an experimental solubility data set [68,69,71]. This kind of uncertainty assessment could be

referred to as precision, because it can be classified as the measure of the deviation from a fitted curve (representing the expected physicochemical relation among properties) for an experimental data set [65].

The self-consistency of the experimental solubility data reported in this work is evaluated with the MS-T model [70], according to **Equation (4.7)**, with three adjustable parameters, A_i, B_i and C_i. Using multivariable linear regression of the experimental data, the best-fit parameters A_i, B_i and C_i are assessed. The density of the CO_2-rich phase in **Equation (4.7)** is replaced with the density of the pure CO_2, because of the low solubility of the solid solutes. According to Mendez-Santiago and Teja, the fact that (after fitting the experimental data to the model) all solubility isotherms collapse to a single line makes this model a powerful tool to determine the self-consistency of experimental data. This technique is used in this work to identify questionable data sets or data points in our analysis.

$$T\left[\ln\left(p\cdot y_i\right)-C_i\right]=A_i+B_i\cdot\rho_1 \tag{4.7}$$

4.4 Modeling solid + fluid phase equilibria

4.4.1 Procedures and criterions for modeling solid + fluid phase equilibria

The state of thermodynamic equilibrium of a two-phase system, fluid + solid, of n components, is established when the temperature, pressure and molar Gibbs free-energy of every component i $\left(G_i\right)$ of both phases are equal:

$$T^F = T^S \qquad p^F = p^S \qquad G_i^S = G_i^F \qquad \left(i=1,...,n\right) \tag{4.8}$$

The equality of temperatures, pressures and Gibbs free-energies indicates an equal flux of heat, momentum and moles between one phase and the other, respectively. For a system at constant temperature and pressure (as the systems studied in this work) the state of

equilibrium is attained when the total Gibbs free energy of the system reaches a global minimum. With the purpose of determining the state of equilibrium of a system using only macroscopic measurable properties, G. N. Lewis (USA, 1875-1942) replaced the Gibbs free energy equilibrium condition for the concept of a modified partial pressure, called fugacity $\left(\overline{f_i} \right)$, **Equation (4.9)**, which is calculated as the product of the partial pressure of component i in the mixture $\left(p_i \right)$ and the fugacity coefficient $\left(\overline{\phi_i} \right)$ as in **Equation (4.10)**.

$$d\overline{G_i} = RTd \ln \overline{f_i} \tag{4.9}$$

$$\overline{f_i} = \overline{\phi_i} \cdot p_i \tag{4.10}$$

Therefore, the third equilibrium condition of **Equation (4.8)** is replaced by the equality of fugacities of each component i in both phases as in **Equation (4.11)**.

$$\overline{f}_i^F = \overline{f}_i^S \tag{4.11}$$

There are two approaches for solving **Equation (4.11)**, the isofugacity and the *G* minimization approaches. Based on the conditions of the system, one of these approaches needs to be selected for solving the FSE. For a binary mixture with only two phases, as verified visually for the systems studied in this work, there is only one minimum in the Gibbs free energy, consequently, the simpler method is selected for solving the FSE, that is, the isofugacity method. The equality of fugacities of component i between the fluid and solid phases is represented using a $\phi - \phi$ approach, in which the fugacity of component i in both phases is calculated directly from **Equation (4.10)**. The fugacity of component i in the fluid phase is calculated as:

$$\overline{f}_i^F = y_i \cdot p \cdot \overline{\phi}_i^F \tag{4.12}$$

The fugacity of solute i in the solid phase can be calculated with two different approaches, namely, the McHugh [72] and Kikic [73] approaches. The McHugh approach is selected for calculating the fugacity of nobiletin in the solid phase, while the Kikic approach is used for menadione. The reason for using a different model for calculating the solubility of each solute

in SC-CO_2 is for learning only, since both equations give similar results by using different parameters. Assuming that the solid phase is a pure solute [68], from the equality of fugacities, **Equation (4.11)**, y_i is calculated according to **Equation (4.13)** for the case of nobiletin, and **Equation (4.14)** for menadione.

$$y_2 = \frac{p_2^{\text{Subl}} \cdot \exp\left[\dfrac{\tilde{V}_2^{S}}{RT} \cdot \left(p - p_2^{\text{Subl}}\right)\right]}{p\bar{\phi}_2^{F}} \tag{4.13}$$

In **Equation (4.13)**, p_2^{Subl} is the sublimation pressure of the pure solid solute at the equilibrium temperature, V_2^{S} is the pure solid solute molar volume, and R is the universal gas constant.

$$y_2 = \frac{\phi_2^{S}}{\bar{\phi}_2^{F}} \tag{4.14}$$

In **Equation (4.14)**, ϕ_2^{S} is the fugacity coefficient of the pure solute, which is obtained using **Equation (4.15)**.

$$\ln \phi_2^{S} = \ln \phi_2^{\text{SCL}} + \frac{\Delta H_{\text{tp}}}{R} \cdot \left(\frac{1}{T_{tp}} - \frac{1}{T}\right) \tag{4.15}$$

Equation (4.15) relates the fugacity coefficient of the solid solute to the fugacity coefficient of the sub-cooled liquid (SCL) at equilibrium temperature and pressure. The only data which are required for calculating the fugacity coefficient of the pure solid phase, are the heat of fusion at the triple point $\left(\Delta H_{tp}\right)$, the triple point temperature $\left(T_{tp}\right)$ and the fugacity coefficient of the pure solute in the sub-cooled liquid phase $\left(\phi_2^{\text{SCL}}\right)$ at T and p.

Finally, $\bar{\phi}_i^{F}$ is calculated with **Equation (4.16)**, where V is the molar volume of the mixture and n_i are the moles of component i in the mixture.

$$\ln \overline{\phi}_i^F = \frac{\ln f_i}{y_i \cdot p} = \frac{1}{RT} \int_{V=\infty}^{V=\frac{Z^F RT}{p}} \left[\frac{RT}{V} - n \left(\frac{\delta p}{\delta n_i} \right)_{T,V,n_{j \neq i}} \right] dV - \ln Z^F \qquad (4.16)$$

To solve **Equation (4.16)**, it is necessary to use an EoS with proper mixing and combining rules that will be given in the following section.

4.4.2 Equations of state

Phase equilibrium of a fluid phase can be modeled using an equation of state, i.e., a thermodynamic relation between the volumetric properties of the system, namely, temperature, pressure and volume. Since equations of state describe mathematically the physicochemical behavior of a fluid, they can be used to obtain fundamental properties for the design of separation processes, such as, vapor pressures, densities, critical properties, fugacities, among others. To extend the applicability of an EoS from a system of one component to a mixture it is necessary to introduce the so-called mixing rules, which introduce a composition dependence to the parameters of the EoS.

In this work, the Peng–Robinson (PR) EoS [74] with the Wong–Sandler (WS) mixing rules [75] is used to calculate the fugacity coefficients of the solid solute and the solvent in the fluid phase [76]. For a single component, the PR-EoS is described in **Equations 4.17-21**.

$$p = \frac{RT}{V-b} + \frac{a}{V(V+b) + b(V-b)} \qquad (4.17)$$

$$a = 0.457235 \left(\frac{R^2 T_c^2}{p_c} \right) \alpha(T_r) \qquad (4.18)$$

$$b = 0.077796 \left(\frac{RT_c}{p_c} \right) \qquad (4.19)$$

$$\alpha(T_r) = \left[1 + F \left(1 - T_r^{0.5} \right) \right]^2 \qquad (4.20)$$

41

$$F = 0.37646 + 1.54226\omega - 0.26992\omega^2 \tag{4.21}$$

For mixtures, the WS mixing rules for parameters a and b (a_m and b_m) are as follows:

$$a_m = b_m \left(\sum y_i \left[\frac{a_i}{b_i} \right] + \frac{A_\infty^E(\mathbf{y})}{\Omega} \right) \tag{4.22}$$

$$b_m = \frac{\sum\sum y_i y_j \left(b - \frac{a}{RT} \right)_{ij}}{1 - \sum \frac{y_i a_i}{b_i RT} - \frac{A_\infty^E(\mathbf{y})}{\Omega RT}} \qquad \left(b - \frac{a}{RT} \right)_{ij} = \frac{1}{2} \left[b_i + b_j \right] - \frac{\sqrt{a_i a_j}}{RT} \left(1 - k_{ij} \right) \tag{4.23}$$

$$\Omega = 0.34657 \tag{4.24}$$

$$A_\infty^E(\mathbf{y}) \approx A_0^E(\mathbf{y}) \approx G_0^E(\mathbf{y}) \tag{4.25}$$

The excess Gibbs free energy $G_0^E(\mathbf{y})$ is calculated with the Non Random Two Liquid (NRTL) [77] activity coefficient model as follows:

$$\frac{G_0^E(x)}{RT} = y_1 y_2 \left(\frac{\tau_{21} G_{21}}{y_1 + G_{21} y_2} + \frac{\tau_{12} G_{12}}{y_2 + G_{12} y_1} \right) \tag{4.26}$$

$$\frac{G_{12}}{RT} = \exp\left[-\alpha_{12} \tau_{12} \right] \qquad \frac{G_{21}}{RT} = \exp\left[-\alpha_{12} \tau_{21} \right] \tag{4.27}$$

In **Equation (4.27)**, parameters τ_{12} and τ_{21} are temperature dependent and α_{12} is a non-randomness parameter. The model parameters, (k_{12}, α_{12}, τ_{12}, τ_{21} and p_2^{Subl}) for nobiletin and (k_{13}, α_{13}, τ_{13} and τ_{31}) for menadione, are calculated using an algorithm which minimizes the average absolute deviation (*AAD*) of the solubility which is calculated as:

$$AAD = \frac{1}{N} \sum_{j=1}^{N} \delta(y_i)_j \tag{4.28}$$

5. Materials and methods

This chapter describes the materials, experimental equipment and methodology used in this work for measuring the thermodynamic solubility of nobiletin and menadione in SC-CO_2.

5.1 Materials

For the determination of the solubilities in SC-CO_2 of the solutes studied in this work, the following chemicals were used: nobiletin (0.97 mass fraction purity or w/w) was from CHEMOS GmbH (Regenstauf, Germany), menadione (0.98 w/w) was from Sigma-Aldrich (Saint Louis, Missouri, USA), and low pressure (5.7 MPa) carbon dioxide (0.9999 w/w) was from AGA-Chile S.A. (Santiago, Chile). In **Table 5.1** were summarized the specifications of the chemical samples used in this work.

Table 5.1. Specification of chemical samples.

Chemical name	Source	Initial mass fraction purity / $kg \cdot kg^{-1}$	Purification method	Final mass fraction purity / $kg \cdot kg^{-1}$	Analysis Method
Carbon dioxide	AGA-Chile S.A.	0.9999	None	0.9999	None
Nobiletin	CHEMOS GmbH	0.97	None	0.97	None
Menadione	Sigma-Aldrich	0.98	None	0.98	None
Acetonitrile	Tedia	0.999	None	0.999	GC[a]
Methanol	Merck KGaA	0.999	None	0.999	GC[a]
Water	Merck KGaA	0.99999	None	0.99999	GC[a]

[a]Gas Chromatography

5.2 Experimental equipment

The experimental equipment used for measuring solubility of the solutes in SC-CO_2 (see **Figure 5.1**) consists of a stirred, 50 cm^3 (Thar-Tech, Pittsburgh, PA) view-cell placed in a temperature-controlled air bath, a syringe pump (Teledyne ISCO 260D, Lincoln, NE) used to load CO_2 into the system and adjust system pressure, and a gear pump (GAH-T23, Eurotechnica, Bargteheide, Germany) to recirculate the CO_2-rich phase and aid system equilibration. The equilibration system is coupled to a HPLC, for detecting the mole fraction of the solute in the fluid phase, that consists of an L-7100 pump, L-7350 oven, and L-7455 photodiode array detector (Hitachi LaChrom, Tokyo, Japan). The closed loop is contained in an acrylic box (the air bath in **Figure 5.1**) to maintain the temperature of the system constant.
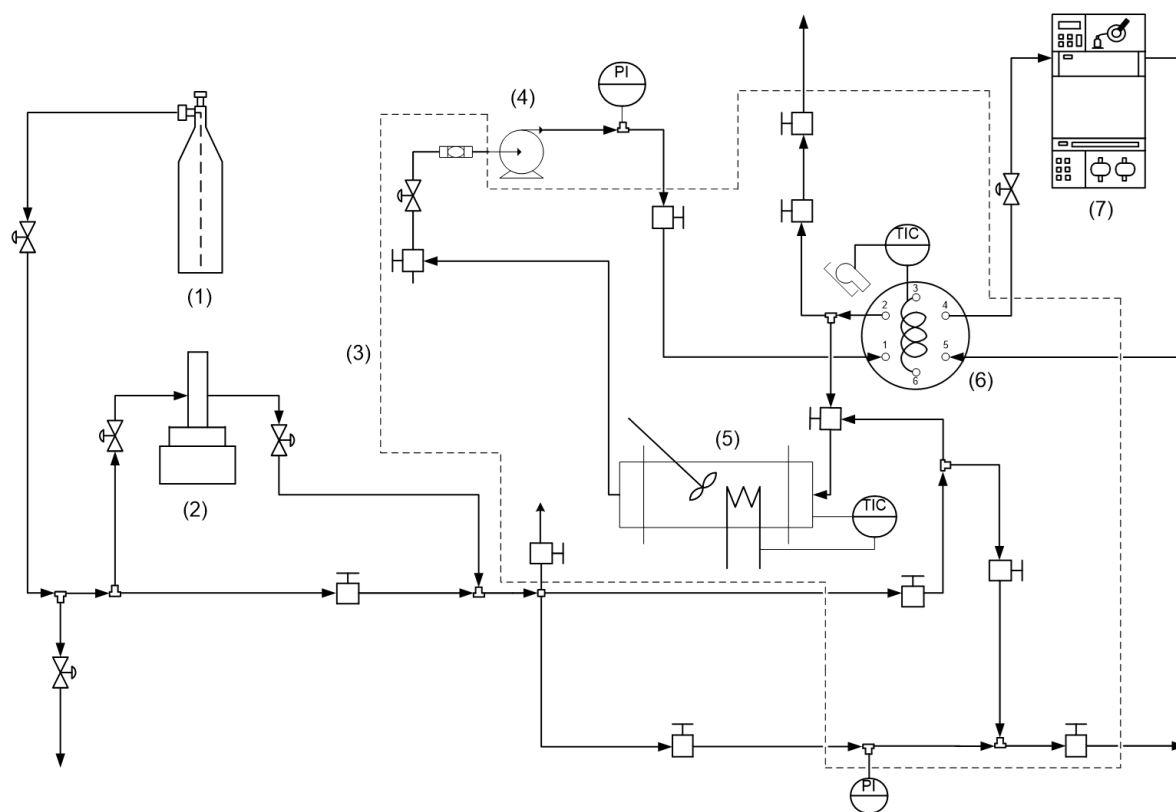
Figure 5.1. Experimental analytic system. (1) CO_2, (2) syringe pump, (3) air bath (dotted line), (4) recirculation pump, (5) equilibrium cell, (6) six-way high pressure valve, and (7) high performance liquid chromatograph.

To feed samples of the CO_2-rich phase to the HPLC coupled to the equilibration system, to determine the solubility, a six-way high pressure sampling valve (Rheodyne 7010, Rohnert Park, CA) is used. The sample is taken from a 20 µL sample loop (inside (6) in **Figure 5.1**). The cell, the recirculation pump and the sampling valve form a closed loop and, because of the recirculation flow, it can be considered that the sample loop has the same temperature, pressure and composition than the fluid mixture in the cell. The equipment and methodology used in this work is a modification of the analytic setup of de la Fuente et al. (2006) [78] and it was first described in the undergraduate thesis in chemical engineering of Roberto Canales at UTFSM [79] which is available online at https://catalogo.usm.cl. The experimental equipment and procedure was validated [80] by measuring solubility isotherms of β-carotene in SC-CO_2 and comparing the results with those of literature and it was found that the new setup improved equilibration time from twelve to eight hours and standard errors of solubility measurements from an average of 37% to 24% (for carotenoid pigments) thanks to the incorporation of a recirculation pump A complete description of the equipment and the methodology used in this work can be found in reference [79] and only a brief description of the methodology is given in the next section.

5.3 Experimental methodology

5.3.1   Starting up the experiment

To measure the solubility of either solute (menadione or nobiletin) in SC-CO_2 a dynamic-analytical methodology [63] was used. It consists in the following: first, the equilibrium cell is loaded with the solute (usually 0.2 to 2.0 grams, depending on the solubility) with a sufficient amount to ensure complete saturation in the supercritical phase, then the residual air is removed by displacement with CO_2 from a gas cylinder, released with a vacuum pump (Welch Vacuum, Skokie, IL) and, after that, CO_2 is loaded into the equilibrium cell using the high-pressure syringe pump. With both components loaded in the equilibrium cell, the stirring system, i.e., the magnetic bar, and the recirculation of the CO_2-rich phase, are activated to reach the equilibrium conditions. By using the two sapphire

windows of the view-cell, it is verified, for every condition of T and p, the presence of two phases, fluid and solid. The solubility isotherm is completed by adding CO_2 to the cell to increase the pressure and attaining new equilibrium conditions up to reaching the required final pressure [81]. Additional isotherms are obtained repeating this procedure using another initial temperature.

5.3.2   Sampling and analysis of carbon dioxide rich phase

Prior to sampling the CO_2-rich phase from the cell and determine how much of the solute dissolved in the CO_2, it is necessary to obtain the chromatographic response of a stock solution of a known concentration of the solute of interest to compare it with the one that will be obtained from a sample taken from the cell. This is done by injecting an aliquot of the stock solution directly to the HPLC by using a syringe. This is repeated at least three times to obtain an average value with a repeatability of 95%. This procedure is done every day to check the correct performance of the HPLC. The solute content of aliquots sampled from the cell, was determined using a slightly modified version of the isocratic HPLC method of Robert et al. [82]. For the HPLC analysis of nobiletin [83], the mobile phase used 1 cm^3·min^{-1} of a 40:60 v/v (volume fraction) mixture of HPLC-grade acetonitrile from Tedia (Fairfield, OH) and HPLC-grade water from Merck KGaA (Darmstadt, Germany), and a reverse-phase, 4.6-mm (inner diameter) wide, 25-cm long, C18 column (Waters symmetry column, Waters, Milford, MA) packed with 5-μm (diameter) particles of stationary phase. The solute was detected at a wavelength of 470 nm. Stock solutions containing C_S = 0.044 mg·cm^{-3} of nobiletin in acetonitrile were prepared and injected for calibration. Similarly, for the HPLC analysis of menadione [84], the mobile phase used 1 cm^3·min^{-1} of a 70:30 v/v mixture of HPLC-grade acetonitrile from Tedia (Fairfield, OH) and HPLC-grade water from Merck KGaA (Darmstadt, Germany), and a reverse-phase, 2.0-mm (inner diameter) wide, 25-cm long RP-18 HPLC column from Merck KGaA (Darmstadt, Germany) packed with 5-μm (diameter) adsorbent beads. The solute was detected at a wavelength of 300 nm. Stock solutions containing C_S = 0.1 mg·cm^{-3} of menadione in methanol were prepared and injected for calibration.

After equilibration of temperature, pressure and composition, which is considered to take place after eight hours [80], as verified in this work, a sample (aliquot) is taken from the cell using the six-way valve. This is done with the recirculation pump turned off. The aliquot taken from the cell is sufficiently small to not alter the equilibrium significantly and continue measuring at the same condition of temperature and pressure (replicas). At least five replicas are taken at each condition with a repeatability of 95%. After the injection, the sample loop gets loaded with the mobile phase of the HPLC, and it should be cleaned before making another measurement, otherwise, the mixture in the cell would get contaminated. This cleansing is accomplished by closing the four valves that form the closed loop and then injecting SC-CO_2 to the sample loop with the syringe pump.

5.3.3   Solubility quantification

Values of y_i are calculated using **Equation (5.1)** [81] based on the chromatographic response (units of absorbance), peak area A_i, of V_{IV} = 20 µL-aliquot (Rheodyne, Rohnert Park, CA), from the loop of the equilibrium cell, as compared to the chromatographic response (peak area A_{Si}) of a V_S = 20 µL-aliquot (Rheodyne, Rohnert Park, CA), from the loop of the HPLC injector, of a stock solution of known concentration (C_{Si}) of the solute used for calibration purposes, and properties of CO_2, molar mass (MW_1) and specific volume at test conditions (v_1) calculated as a function of system temperature and pressure using NIST [85] database. From **Equation (5.1)** it is assumed that the density of the fluid mixture is the same as the density of pure CO_2, which is a very good approximation when the solute present in the SC-CO_2 is in a mole fraction below $1 \cdot 10^{-3}$ mol·mol^{-1}.

$$y_i = \left(\frac{A_i / V_{IV}}{A_{Si} / V_S} \right) \cdot C_{Si} \cdot v_1 \cdot MW_1 \qquad (5.1)$$

6. Results and discussion

This chapter presents the experimental solubility data obtained in this work for the binary fluid + solid systems: CO_2 + nobiletin and CO_2 + menadione, that was validated with the estimation of uncertainties and the evaluation of the thermodynamic consistency and self-consistency of the data. First, the experimental results for both systems, with their corresponding uncertainties are presented, followed by the thermodynamic consistency and self-consistency test results.

6.1 Nobiletin in supercritical carbon dioxide

Isothermal solubility for the system (CO_2 + solid nobiletin) at temperatures of (313, 323 and 333) K as a function of pressure are reported in **Table 6.1** and represented graphically in **Figure 6.1** [63] (**Appendix A**).

Table 6.1 Experimental molar fraction of nobiletin (2) (solubility, y_2) in supercritical CO_2 (1)-rich phase as a function of system pressure (p) or density of pure CO_2 (ρ_1) at temperatures (T) of (313, 323, and 333) K.

T / K	p / MPa	ρ_1 / kg·m^{-3}	Nobiletin (2)	
			$y_2 \cdot 10^6$ / mol·mol^{-1}	$U_{comb}(y_2) \cdot 10^6$ / mol·mol^{-1}
313	17.97	819.0	114	14
	21.93	856.7	126	16
	28.22	899.1	141	18
323	18.09	758.6	109	14
	21.79	804.4	138	18
	27.87	855.7	154	20
	31.03	876.8	164	21
333	18.35	694.1	107	14
	21.95	751.6	152	19
	27.92	813.4	179	23
	32.40	839.6	182	23

u(T) = 0.1 K, u(p) = 0.001 MPa. Combined expanded uncertainties for molar fraction of nobiletin, $U_{Comb}(y_2)$, were estimated with a 0.90 level of confidence.
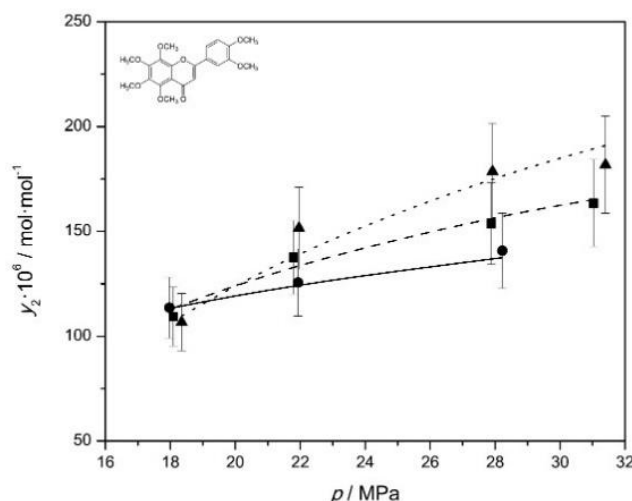
Figure 6.1. Molar fraction of nobiletin (2) (solubility, y_2) in supercritical CO_2 (1)-rich phase as a function of system pressure (p) at temperatures of at 313 K ($\bullet$, ———); 323 K ($\blacksquare$, — —) and 333 K ($\blacktriangle$, – –). Error bars represent the uncertainties informed in **Table 6.1**. Lines represent correlation of Mendez-Santiago and Teja [86].

The standard and combined expanded uncertainties were estimated using the available information for the apparatus, experimental methodology and measured values. Results are included in **Table 6.1** for temperature, pressure and each individual value of the mole fraction. **Table 6.2** details the methodology used to estimate the uncertainties for all variables and properties measured in this work for nobiletin in SC-CO_2 (the methodology for menadione is equivalent). The values of the $U_{comb}(y_2)$ in **Table 6.1** differ from the ones published [63], because the estimation of the uncertainties of the volumes of the sample loops ($u(V_{IV})$ and $u(V_S)$ in **Table 6.2**) were equal to 2 µL (information provided by the manufacturer), while in this work the volumes were measured with an uncertainty of 0.2 µL with the method of Devoe et al. [87].

Results for nobiletin indicate that solubility started from $y_2 = 107 \cdot 10^{-6}$ mol·mol^{-1} at $T = 333$ K and $p = 18.35$ MPa and increased up to $y_2 = 182 \cdot 10^{-6}$ mol·mol^{-1} at $T = 333$ K and $p = 31.40$ MPa (the highest pressure measured). At constant temperature, the solubility showed an increase with pressure, driven by the increment in the CO_2 density and its positive effect over the solvent power.

Table 6.2. Estimation of the combined expanded uncertainty for molar fraction of nobiletin (2) (solubility, y_2) in supercritical CO_2 (1)-rich phase, $U_{Comb}(y_2)$, based on the contributions of properties and variables measured and calculated [81].

Property, Variable	Type of uncertainty (Level of confidence / %)	Uncertainty	Contribution to $U_{comb}(y_2)$ / %
Temperature $(313 \leq T \leq 333)$ K	Standard	$u(T) = 0.1$ K	-
Pressure $(17.97 \leq p \leq 31.40)$ MPa	Standard	$u(p) = 0.01$ MPa	-
Chromatographic area for sample of nobiletin dissolved in CO_2 $(5778650 \leq A_2 \leq 11390338)$ AU[(1)]	Standard	$u(A_2) = 3500$ AU	1
Chromatographic area for the stock solution $(344727 \leq A_{S2} \leq 375559)$ AU	Standard	$u(A_{S2}) = 3500$ AU	12
Volume of sampler loop of the equilibrium cell $(V_{IV} = 20 \ \mu L)$	Standard	$u(V_{IV}) = 2 \ \mu L$	13
Volume loop of the HPLC injector $(V_S = 20 \ \mu L)$	Standard	$u(V_S) = 2 \ \mu L$	13
Concentration of stock solution $C_{S2} = \dfrac{m_2}{V_{VF} \cdot MW_2}$ $C_{S2} = 0.10935 \cdot 10^{-6} \ mol \cdot cm^{-3}$	Combined (68.27)	$\dfrac{u_{Comb}(C_{S2})}{C_{S2}} = \dfrac{u(m_2)}{m_2} + \dfrac{u(V_{VF})}{V_{VF}}$	60
Mass of nobiletin dissolved in acetonitrile $m_2 = 22$ mg	Standard	$u(m_2) = 0.0001$ g	-
Volume of flask to dissolve nobiletin in acetonitrile $V_{VF} = 50 \ cm^3$	Standard	$u(V_{VF}) = 0.08 \ cm^3$	-
Specific volume of CO_2 $v_1 = f(T, p)$ $(4.89 \leq v_1 \leq 6.34) \ x10^{-5} \ m^3 \cdot mol^{-1}$	Combined (68.27)	$\dfrac{u_{Comb}(v_1)}{v_1} = \left\lvert \dfrac{1}{v_1} \dfrac{\partial v_1}{\partial T} \right\rvert \cdot u(T) + \left\lvert \dfrac{1}{v_1} \dfrac{\partial v_1}{\partial p} \right\rvert \cdot u(p)$	1
Volumetric expansibility of CO_2 $\alpha_1 = \left\lvert \dfrac{1}{v_1} \dfrac{\partial v_1}{\partial T} \right\rvert$ $(0.00446 \leq \alpha_1 \leq 0.1019) \ K^{-1}$	-	NIST	-
Isothermal compressibility of CO_2 $\beta_1 = \left. \dfrac{1}{v_1} \dfrac{\partial v_1}{\partial p} \right\rvert$ $(0.00065 \leq \beta_1 \leq 0.00283) \ MPa^{-1}$	-	NIST	-
Molar fraction of nobiletin in CO_2-rich phase $y_2 = \left(\dfrac{A_2 / V_{IV}}{A_{S2} / V_S} \right) \cdot C_{S2} \cdot v_1 \cdot MW_2$ $(107 \leq y_2 \leq 182) \cdot 10^{-6} \ mol \cdot mol^{-1}$	Combined expanded (90)	$\dfrac{U_{Comb}(y_2)}{1.645 \cdot y_2} = \dfrac{\Delta A_2}{A_2} + \dfrac{\Delta A_{S2}}{A_{S2}} + \dfrac{\Delta V_{IV}}{V_{IV}} + \dfrac{\Delta V_S}{V_S} + \dfrac{\Delta C_{S2}}{C_{S2}} + \dfrac{\Delta v_1}{v_1}$	-

[(1)] Area units.

An enhancement in the solubility values of nobiletin with the temperature at isobaric condition was observed, indicating that increasing the solute vapor pressure overwhelmed the reduction in CO_2 density. As seen in **Figure 6.1**, an inversion in the isothermal response was detected for solubility data at the lowest value of pressure measured, the behavior shifted around 18 MPa (temperature crossover), from a negative effect of temperature on solubility (the increasing in the solute vapor pressure with the temperature cannot balance the decreasing in the CO_2 density) to a positive effect. In addition to solubility data of nobiletin reported in this contribution, there is no information in literature about solubility of nobiletin or any other PMFs in SC-CO_2. As a reference, the solubility of flavone (the backbone of the nobiletin molecule) in SC-CO_2 at $T = (308.2$ and $318.2)$ K [56] is approximately 3.7 times higher when is compared with the solubility of nobiletin at $T = 313.2$ K and pressure range

from (17.97 to 28.22) MPa. The lower values in solubility of nobiletin are due to the presence of the six methoxy groups that contribute to increase its molar mass and polarity relative to flavone, which affect negatively over the solvent power of the SC-CO_2 [51].

6.2 Menadione in supercritical carbon dioxide

Isothermal solubility for the system (CO_2 + solid menadione) at temperatures of (313, 323 and 333) K as a function of pressure are reported in **Table 6.3** and represented graphically in **Figure 6.2** [88] (**Appendix B**) along with solubility data published by Knez and Skerget (2001) [57] and Johannsen and Brunner (1997) [58].

Table 6.3. Experimental molar fraction of menadione (3) (solubility, y_3) in supercritical CO_2 (1)-rich phase as a function of system pressure (p) or density of pure CO_2 (ρ_1) at temperatures (T) of (313, 323, and 333) K.

T / K	p / MPa	ρ_1 / kg·m^{-3}	Menadione (3)	
			$y_3 \cdot 10^6$ / mol·mol^{-1}	$U_{comb}(y_3) \cdot 10^6$ / mol·mol^{-1}
313	10.32	650.0	833	78
	14.13	765.7	888	79
	17.61	815.1	874	77
	19.58	835.8	924	82
	22.41	860.5	893	79
	25.72	884.3	882	78
	30.67	913.5	887	78
323	9.87	368.7	792	80
	15.36	785.8	928	83
	20.38	788.9	908	81
	21.90	805.5	1091	94
	26.41	845.4	910	80
333	9.72	273.5	630	57
	13.15	514.9	934	111
	13.43	531.2	1057	95
	17.17	668.8	982	84
	20.53	732.0	914	103
	24.24	778.6	937	79

u(T) = 0.1 K, u(p) = 0.001 MPa. Combined expanded uncertainties for molar fraction of menadione, $U_{Comb}(y_3)$, were estimated with a 0.90 level of confidence.
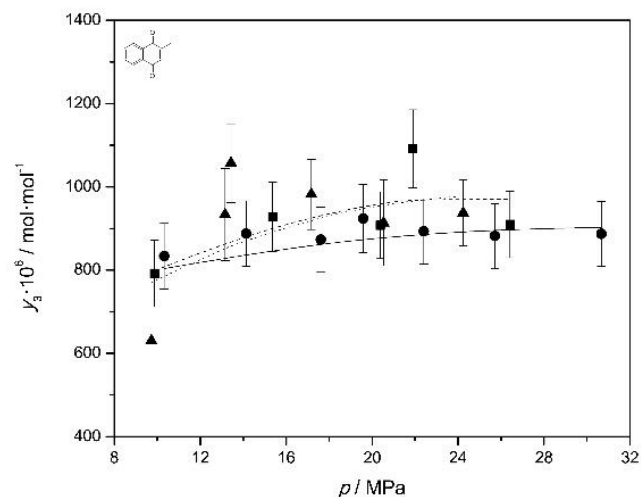
a
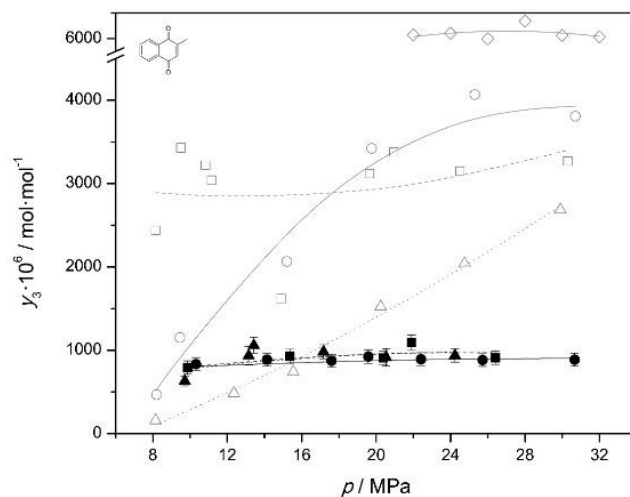
b

Figure 6.2. Molar fraction of menadione (3) (solubility, y_3) in supercritical CO_2 (1)-rich phase as a function of system pressure (p) at temperatures of at 313 K ($\bullet$, ——); 323 K ($\blacksquare$, — —) and 333 K ($\blacktriangle$, – –). Error bars represent the uncertainties informed in **Table 6.3**. Open symbols represent the solubility of menadione in supercritical CO_2 reported by Knez and Skerget [57] at 313 K ($\circ$, ——), 333 K ($\square$, — —) and 353 K ($\triangle$, – –), and those of Johannsen and Brunner [58] at 313 K ($\lozenge$, —). Lines represent the trend.

Results indicate that solubility started from $y_3 = 630 \cdot 10^{-6}$ mol·mol^{-1} at $T = 333$ K and $p = 9.72$ MPa and increased up to $y_3 = 1091 \cdot 10^{-6}$ mol·mol^{-1} at $T = 323$ K and $p = 21.89$ MPa. It can be seen from **Figure 6.2a** that, for the data measured in this work, at pressures higher

than 21.90 MPa at 323 K and 17.17 MPa at 333 K there was a fall in solubility, probably because of an obstruction on the recirculation loop from solute accumulation in the line that reduced drastically the recirculation flow. Consequently, true equilibrium condition was probably not reached for these points.

Comparing our results with those of literature, as it can be seen in **Figure 6.2b**, the solubility of menadione in SC-CO_2 measured in this work does not coincide with previous results of Johannsen and Brunner at 40 °C, nor those of Knez and Skerget at 40 or 60 °C. It is important to notice that literature data does not provide an estimation of inherent errors of measurements. Knez and Skerget found that the solubility of menadione in CO_2 was in the range $160 \cdot 10^{-6}$ mol/mol at 353 K and 8.5 MPa to $4070 \cdot 10^{-6}$ mol/mol at 313 K and 25.3 MPa. **Figure 6.2** shows that at constant pressure there is an increase in the solubility with decreasing temperature for isotherms 313 K and 353 K. At 333 K solubility takes an unusual course, with an average of $2963 \cdot 10^{-6}$ mol/mol and no clear dependence of the solubility to pressure or density, as it remains relatively constant, except at 14.9 MPa where it drops drastically. Johannsen and Brunner solubility measurements of menadione in SC-CO_2 at 313 K are in the range of $5990 \cdot 10^{-6}$ mol/mol at 26 MPa to $6680 \cdot 10^{-6}$ mol/mol at 28 MPa. These results are about 50 to 60 % higher than those of Knez and Skerget at 313 K.

Discrepancies between literature data for binary systems of pure minor lipids, such as β-carotene, tocopherols and fat soluble vitamins (like vitamin K) have been attributed to the purity of the samples and the limitations of the experimental techniques used, such as the lack of a high pressure window on the extraction cells used, lack of attainment of equilibrium and solute loss during depressurization or due to entrainment (the entrapment or carrying of one substance by another substance) [89]. An extensive report of variation of solubility behavior between different authors, experimental techniques used, causes of solute loss, etc., can be found on reference [90].

Table 6.4 provides a comparison between the techniques used, purity of solute, operating conditions, number of measurements and standard deviation, to determine the source of the discrepancies of the equilibrium data. The lack of recirculation of the CO_2 rich phase could explain the great differences between literature data and this work, because of an accumulation of the solute in the sample collector, which can be expected at low flow rates. On the contrary, micro recirculation, used in this work, minimizes solute accumulation on the sampler and the time required for reaching thermodynamic equilibrium. Also, as we have found during research of other solid solute + SC-CO_2 binary systems, when recirculation flow gets reduced (which can be seen through the cell windows) because of the accumulation of solute in the capillaries, chromatograms area peaks, for a same temperature and pressure condition, are considerably higher (up to 800%) compared to measurements in normal operating conditions. This could explain the higher values of solubilities reported in literature. This situation can be detected by doing replicas of each measurement, to avoid the report of doubtful data, as it was done in this work.

Table 6.4. Comparison between experimental methodologies used by different authors for measuring the solubility of menadione in supercritical carbon dioxide.

Author	Method	Recirculation	Phase Separation	Solute Purity	Relative Std. Dev.	Average N° of measurements
This work	analytic-dynamic	CO_2-rich phase	8 [h]	98%	<5%	5
Knez & Skerget [57]	static-analytic	no	1 [h]	98%	0.2-15.6 %	2
Johannsen & Brunner [58]	static-analytic	no	Unspecified	98%	<5%	5

6.3 Thermodynamic consistency test

In order to assess the thermodynamic consistency of the solubility data of this work, pure component properties of nobiletin and menadione were needed to be estimated, while CO_2 properties were taken from NIST database [85].

All pure component properties used in this work are summarized in **Table 6.5** along with the method used for their estimation. For the solid solutes, the Joback [91] group contribution method was used to estimate the pure solid molar volume, critical temperature and pressure, and saturation pressure at the reduced temperature of 0.7 (for calculating the acentric factor) [48] when literature data was not available. The sublimation pressure (for nobiletin) was included as a fifth optimization parameter [68], along with the four binary interaction coefficients (k_{12}, α_{12}, τ_{12}, τ_{21}), common to both solutes, included in the combination rules of PR + (WS + NRTL).

Table 6.5. Pure component properties for carbon dioxide (1), nobiletin (2) and menadione (3) from literature or estimated in this work.

Property	Value	Source (Estimation Method)	Reference
Carbon dioxide (1)			
Molecular weight (MW_1, Da)	44.01	-	-
Critical temperature ($T_{c,1}$, K)	304.2	NIST	[85]
Critical pressure ($p_{c,1}$, MPa)	7.38	NIST	[85]
Acentric factor (ω_1)	0.2252	NIST	[85]
Nobiletin (2)			
Molecular weight (MW_2, Da)	402.40	-	-
Critical temperature ($T_{c,2}$, K)	1256	Joback	[48,91]
Critical pressure ($p_{c,2}$, MPa)	1.54	Joback	[48,91]
Acentric factor (ω_2)	1.1884	Definition	-
Molar volume ($V_2^S \cdot 10^6$, m^3/mol)	1067.5	Joback, assumed equal to critical volume	[48,91]
Menadione (3)			
Molecular weight (MW_3, Da)	172.18	-	-
Critical temperature ($T_{c,3}$, K)	639.58	Literature	[57]
Critical pressure ($p_{c,3}$, MPa)	46.53	Optimized from data	-
Acentric factor (ω_3)	0.6226	Optimized from data	-
Triple point temperature (T_{tp}, K)	379.3	Joback, assumed equal to fusion temperature	[48]
Heat of fusion at triple point (ΔH_{tp}, J·mol^{-1})	21488	Joback, assumed equal to fusion temperature	[48]

Table 6.6 contains results for the first stage, with values for the selected optimization parameters and the corresponding $\delta(y_i)$ calculated for each isotherm. Deviations between modeled and measured data sets of nobiletin and menadione were $\delta(y_i) < 12\%$, verifying the test condition that it should be lower than 20%, and therefore was confirmed that the combination PR + (WS + NRTL) was appropriate to represent the FSE.

Table 6.6. Results for the first stage of the consistency test for solid + fluid equilibria of CO_2 (1) + Nobiletin (2) and CO_2 (1) + Menadione (3): Optimal values of parameters for the Peng-Robinson equation of state (p_2^{Subl}, for nobiletin only) with Wong-Sandler mixing rule (k_{1i}) and Non-Random Two Liquid model (α_{1i}, τ_{1i}, τ_{i1}) for the correlation of the solubility of solute i (y_i).

Nobiletin

T / K	k_{12}	α_{12}	τ_{12}	τ_{21}	p_2^{Subl} / MPa	$\delta(y_i)$ / %
313	0.876	0.074	22.97	10.19	$2.9 \cdot 10^{-16}$	6.62
323	0.867	0.085	21.12	10.57	$2.7 \cdot 10^{-16}$	7.01
333	0.856	0.075	19.43	11.09	$3.1 \cdot 10^{-16}$	11.9

Menadione

T / K	k_{13}	α_{13}	τ_{13}	τ_{31}	$\delta(y_i)$ / %
313	-0.5155	0.0924	5.9078	1.5356	3.20
323	-0.5042	0.0953	7.2113	1.6122	6.55
333	0.0579	0.1264	5.1901	3.0692	11.0

For the second stage, the PR + (WS + NRTL) was used to calculate the fugacity coefficients of both components in the fluid phase to apply of the consistency test. Individual calculations of area deviations (j) were assessed with **Equation (4.6)** and are listed as absolute values ($|\Delta A|_j$) in **Table 6.7**. In addition, for each data point (j) in **Table 6.7,** the absolute value for the relative deviation between solute solubility calculated from PR + (WS + NRTL) and the experimental measured value, $\delta(y_i)_j$, are included. Results listed indicate that at $T = (313, 323$ and $333)$ K, the $|\Delta A|_j$ values were $< (18.9, 17.2,$ and $17.0)$ % for nobiletin and $< (5.2, 8.0,$ and $14.0)$ % for menadione, therefore all measured isotherms are thermodynamically consistent, per the criteria established for the test.

Table 6.7. Results for the second stage of the consistency test for solid + fluid equilibria of CO_2 (1) + Nobiletin (2) and CO_2 (1) + Menadione (3) using Peng-Robinson equation of state with Wong-Sandler mixing rule and Non Random Two Liquid model: Assessed values of the absolute relative deviation ($\left|\delta(y_i)_j\right|$) and area deviation ($\left|\Delta A\right|_j$) for individual solute solubility data points (y_i) according to **Equation (4.6)**.

Nobiletin

| j | T / K = 313 K | | | T / K = 323 K | | | T / K = 333 K | | |
	p / MPa	$\left\|\delta(y_2)_j\right\|$ / %	$\left\|\Delta A\right\|_j$ / %	p / MPa	$\left\|\delta(y_2)_j\right\|$ /%	$\left\|\Delta A\right\|_j$ / %	p / MPa	$\left\|\delta(y_2)_j\right\|$ /%	$\left\|\Delta A\right\|_j$ / %
1	17.97	0.33	18.9	18.09	0.32	17.2	18.35	0.31	17.0
2	21.93	11.5	14.3	21.79	9.05	13.6	21.95	14.8	16.6
3	28.22	0.14		27.87	0.10	13.5	27.92	0.22	9.22
4				31.03	10.7		31.40	18.6	

Menadione

| j | T / K = 313 K | | | T / K = 323 K | | | T / K = 333 K | | |
	p / MPa	$\left\|\delta(y_3)_j\right\|$ / %	$\left\|\Delta A\right\|_j$ / %	p / MPa	$\left\|\delta(y_3)_j\right\|$ /%	$\left\|\Delta A\right\|_j$ / %	p / MPa	$\left\|\delta(y_3)_j\right\|$ /%	$\left\|\Delta A\right\|_j$ / %
1	10.32	10.1	0.66	9.87	0.13	7.99	9.72	21.6	13.96
2	14.13	0.06	5.16	15.36	6.58	5.72	13.15	6.16	6.11
3	17.61	4.61	4.90	20.38	0.01	6.56	13.43	16.2	4.30
4	19.58	1.09	3.08	21.89	19.6	-	17.17	0.10	-
5	22.41	1.09	3.89						
6	25.72	0.00	0.84						
7	30.67	5.32	-						

Table 6.8 summarizes the thermodynamic consistency test results, including literature data of menadione solubility. Calculations for correlating the solubility with the PR + (WS + NRTL) model and for evaluation of the thermodynamic consistency of the equilibrium data were performed using MATLAB^{TM} algorithms based on the codes developed by Martin et al. (2011) [92] which are available online.

Table 6.8. Consistency Test Results for solute + supercritical CO_2 equilibrium.

Nobiletin

T/K	ND	$\delta(y_i)$	Max $\left|\Delta A\right|_j$ / %	Result	Reference
313	3	6.62	18.9	TC	
323	4	7.01	10.7	TC	This work
333	4	11.9	18.6	TC	

Menadione

T/K	ND	$\delta(y_i)$	Max $\left|\Delta A\right|_j$ / %	Result	Reference
313	7	3.20	5.16	TC	
323	4	6.55	7.99	TC	This work
333	4	11.0	14.0	TC	
313	6	10.7	14.70	TC	
333	9	>20	-	TDM	[57]
353	6	>20	-	TDM	
313	6	>20	-	TDM	[58]

6.4 Self-consistency test

Using multivariable linear regression of the three isothermal solubility data sets of nobiletin and menadione in SC-CO_2 informed in **Tables 6.1** and **6.3**, the best-fit parameters of MS-T model in **Equation (4.7)** were estimated for assessing the self-consistency or precision of the solubility data. Results of the optimization are presented also in **Equations (6.1)** and **(6.2)**. The root mean square deviations were $\delta(y_2) = 3.2$ % and $\delta(y_3) = 18.6$ %. The projection $T\left[\ln\left(p \cdot y_i^{Calc}\right) - C_i\right]$ versus $\Gamma_1(T, p)$ (**Figure 6.3**), confirms that most of the experimental data falls on a single straight line, behavior observed by Mendez-Santiago and Teja [70], a graphical verification of the self-consistency for both experimental data sets.

$$y_2^{\text{Calc}} = \frac{1}{p} \cdot \exp\left[\frac{-6872.0 + 2.4962 \cdot \rho_1}{T} + 23.0331\right] \qquad \textbf{(6.1)}$$

$$y_3^{\text{Calc}} = \frac{1}{p} \cdot \exp\left[\frac{-4835.4 + 1.0139 \cdot \rho_1}{T} + 22.4218\right] \qquad \textbf{(6.2)}$$
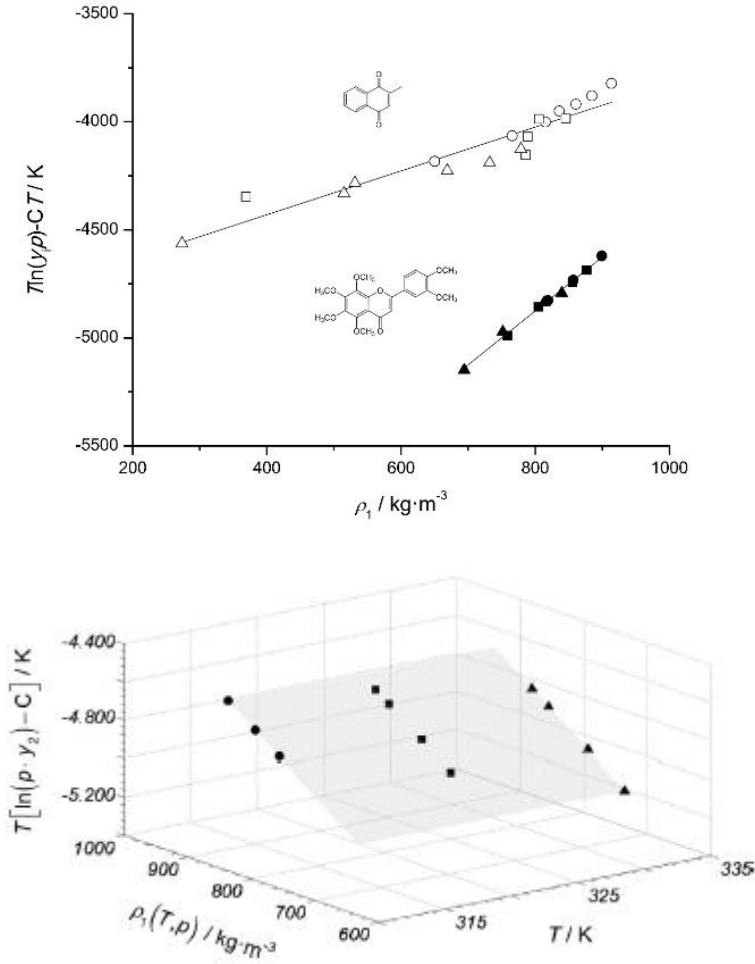
Figure 6.3. Representation of solute molar fraction (solubility, y_i) in supercritical CO_2 (1)-rich phase, CO_2 density (ρ_1) and temperature (T) in a two-dimensional arrangement (upper) and three-dimensional arrangement (lower), $T \cdot \left[\ln\left(p \cdot y_i\right) - C_i\right]$ versus $r_1\left(T, p\right)$ and $T \cdot \left[\ln\left(p \cdot y_i\right) - C_i\right]$ versus $r_1\left(T, p\right)$ versus T, respectively. Symbols represent experimental results measured in this work (**Tables 6.12** and **6.3**). Nobiletin (2) at 313 K (●); 323 K (■) and 333 K (▲); Menadione (3) at 313 K (○); 323 K (□) and 333 K (△). Straight lines represent the Mendez-Santiago and Teja correlation with constants according **Equations (6.1)** and **(6.2)**. Nobiletin: A_2 = -6872.0 K; B_2 = 2.4962 K·m³·kg⁻¹ and C_2 = 23.0331, with $\delta(y_2) \leq 3.2$ %; Menadione: A_3 = -4835.4 K; B_3 = 1.0139 K·m³·kg⁻¹ and C_3 = 22.4218, with $\delta(y_3) \leq 18.6$ % .

Conclusions

The isothermal solubility of two solid compounds, 2-(3,4-Dimethoxyphenyl)-5,6,7,8-tetramethoxychromen-4-one (nobiletin) and 2-methyl-1,4-naphthoquinone (menadione) dissolved in supercritical carbon dioxide at $T = (313, 323$ and $333)$ K and pressures lower than 31.40 MPa was obtained by a direct analytic recirculation methodology. The six solubility data sets (three for each compound) were validated using a procedure that allowed the estimation of the combined expanded uncertainty for each value of the experimental solute mole fraction in the CO_2-rich phase value, to verify for every isothermal data sets their thermodynamic consistency (reliability of data), and to evaluate the self-consistency (a kind of precision) of the measured solubility. The validation procedure for the solubility data of the solute + CO_2 systems indicated that the combined expanded uncertainty of the solubility was $\leq 23 \cdot 10^{-6}$ mol·mol^{-1} for nobiletin and $\leq 111 \cdot 10^{-6}$ mol·mol^{-1} for menadione; that every isotherm for both systems was thermodynamically consistent $\left(\Delta A_j < 20\% \right)$; and that the self-consistency of nobiletin and menadione is SC-CO_2, assessed with the MS-T equation, were $\delta\left(y_2 \right) = 3.2$ % and $\delta\left(y_3 \right) = 18.6$ %.

The solubility behavior of the studied systems corresponded, in general, with the tendencies expected (**Section 4.1**) for solid solutes in SC-CO_2 in the *p-T* region where only the solid and fluid phases are present; particularly, a monotonous increase in the molar fraction of the solute in the saturated SC-CO_2 phase was observed with increasing pressure (density effect) for all nobiletin data and the 40 °C isotherm of menadione. The temperature effect, on the other hand, was clearly observed for nobiletin with the presence of a crossover around 18 MPa; as for menadione, due to dispersion in the results, it was not possible to clearly determine the location of the crossover since many data points deviate significantly from the trend. Consequently, additional measurements are recommended for the 50 °C and 60 °C isotherms as their solute solubility trend lines are practically equal. Lastly, comparison with literature data (available only for menadione) showed great differences between authors, however, the data measured in this work has more value than literature data due to the validation procedure and the more reliable experimental methodology.

Ongoing Work

A continuation of this work will be to systematically evaluate the relationship between the solute structure and solubility in CO_2, starting from menadione and continue with different new derivatives, synthesized by performing structural changes to the basic chemical structure of menadione (core molecule). The changes included in this future study will consider side chain variations, e.g., length and grade of chain branching, number of rings, position and type of substituents in the molecules considering the possible change in the solubility in supercritical CO_2 due to these variations of the core molecule.

The data generated with this study will be correlated with computational approaches, such as molecular simulations, to develop a semi-empirical model for the prediction of the solubility using molecular descriptor obtained from molecular simulations. This information could explain and identify the molecular and electronic characteristics that define the solubility levels of the derivatives in SC-CO_2.

References

[1]   S. Li, C.Y. Lo, C.T. Ho, Hydroxylated polymethoxyflavones and methylated flavonoids in sweet orange (Citrus sinensis) peel, J. Agric. Food Chem. 54 (2006) 4176–4185. doi:10.1021/jf060234n.

[2]   S. Li, M.H. Pan, C.Y. Lo, D. Tan, Y. Wang, F. Shahidi, C.T. Ho, Chemistry and health effects of polymethoxyflavones and hydroxylated polymethoxyflavones, J. Funct. Foods. 1 (2009) 2–12. doi:10.1016/j.jff.2008.09.003.

[3]   Y. Hirota, N. Tsugawa, K. Nakagawa, Y. Suhara, K. Tanaka, Y. Uchino, A. Takeuchi, N. Sawada, M. Kamao, A. Wada, T. Okitsu, T. Okano, Menadione (vitamin K3) is a catabolic product of oral phylloquinone (vitamin K1) in the intestine and a circulating precursor of tissue menaquinone-4 (vitamin K2) in rats., J. Biol. Chem. 288 (2013) 33071–80. doi:10.1074/jbc.M113.477356.

[4]   A. Thompson, Ingredients: Where Pet Food Starts, Top. Companion Anim. Med. 23 (2008) 127–132. doi:10.1053/j.tcam.2008.04.004.

[5]   T. Kayashima, M. Mori, R. Mizutani, K. Nishio, K. Kuramochi, K. Tsubaki, H. Yoshida, Y. Mizushina, K. Matsubara, Synthesis and biological evaluation of vitamin K derivatives as angiogenesis inhibitor., Bioorg. Med. Chem. 18 (2010) 6305–9. doi:10.1016/j.bmc.2010.07.022.

[6]   D.J. Card, R. Gorska, J. Cutler, D.J. Harrington, Vitamin K metabolism: current knowledge and future research., Mol. Nutr. Food Res. 58 (2014) 1590–600. doi:10.1002/mnfr.201300683.

[7]   G.K. Scott, C. Atsriku, P. Kaminker, J. Held, B. Gibson, M.A. Baldwin, C.C. Benz, Vitamin K3 (menadione)-induced oncosis associated with keratin 8 phosphorylation and histone H3 arylation., Mol. Pharmacol. 68 (2005) 606–15. doi:10.1124/mol.105.013474.

[8]   E. Reverchon, I. De Marco, Supercritical fluid extraction and fractionation of natural matter, J. Supercrit. Fluids. 38 (2006) 146–166. doi:10.1016/j.supflu.2006.03.020.

[9]   L. Bravo, Polyphenols: Chemistry, Dietary Sources, Metabolism, and Nutritional Significance, Nutr. Rev. 56 (2009) 317–333. doi:10.1111/j.1753-4887.1998.tb01670.x.

[10]   K.D. Croft, The Chemistry and Biological Effects of Flavonoids and Phenolic Acidsa, Ann. N. Y. Acad. Sci. 854 (1998) 435–442. doi:10.1111/j.1749-6632.1998.tb09922.x.

[11]   S. Pollastri, M. Tattini, Flavonols: old compounds for old roles., Ann. Bot. 108 (2011) 1225–33. doi:10.1093/aob/mcr234.

[12]   A. Kozłowska, D. Szostak-Wegierek, Flavonoids--food sources and health benefits., Rocz. Państwowego Zakładu Hig. 65 (2014) 79–85. http://www.ncbi.nlm.nih.gov/pubmed/25272572.

[13]   S. Martens, A. Mithfer, Flavones and flavone synthases, Phytochemistry. 66 (2005) 2399–2407. doi:10.1016/j.phytochem.2005.07.013.

[14]   A. Murakami, Y. Nakamura, Y. Ohto, M. Yano, T. Koshiba, K. Koshimizu, H. Tokuda, H. Nishino, H. Ohigashi, Suppressive effects of citrus fruits on free radical generation and nobiletin, an anti-inflammatory polymethoxyflavonoid, BioFactors. 12 (2000) 187–192. doi:10.1002/biof.5520120130.

[15]   A. Murakami, T. Shigemori, H. Ohigashi, Zingiberaceous and citrus constituents, 1'-acetoxychavicol acetate, zerumbone, auraptene, and nobiletin, suppress lipopolysaccharide-induced cyclooxygenase-2 expression in RAW264.7 murine macrophages through different modes of action., J. Nutr. 135 (2005) 2987S–2992S. http://jn.nutrition.org/content/135/12/2987S.abstract (accessed February 29, 2016).

[16]   C.-S. Lai, S. Li, C.-Y. Chai, C.-Y. Lo, C.-T. Ho, Y.-J. Wang, M.-H. Pan, Inhibitory effect of citrus 5-hydroxy-3,6,7,8,3',4'-hexamethoxyflavone on 12-O-tetradecanoylphorbol 13-acetate-induced skin inflammation and tumor promotion in mice., Carcinogenesis. 28 (2007) 2581–8. doi:10.1093/carcin/bgm231.

[17]   A. Murakami, Y. Nakamura, K. Torikai, T. Tanaka, T. Koshiba, K. Koshimizu, S. Kuwahara, Y. Takahashi, K. Ogawa, M. Yano, H. Tokuda, H. Nishino, Y. Mimaki, Y. Sashida, S. Kitanaka, H. Ohigashi, Inhibitory effect of citrus nobiletin on phorbol ester-induced skin inflammation, oxidative stress, and tumor promotion in mice., Cancer Res. 60 (2000) 5059–66. http://europepmc.org/abstract/med/11016629 (accessed February 29, 2016).

[18]   M. Tang, K. Ogawa, M. Asamoto, N. Hokaiwado, A. Seeni, S. Suzuki, S. Takahashi, T. Tanaka, K. Ichikawa, T. Shirai, Protective effects of citrus nobiletin and auraptene in

transgenic rats developing adenocarcinoma of the prostate (TRAP) and human prostate carcinoma cells., Cancer Sci. 98 (2007) 471–7. doi:10.1111/j.1349-7006.2007.00417.x.

[19]   E.M. Kurowska, J.A. Manthey, Hypolipidemic effects and absorption of citrus polymethoxylated flavones in hamsters with diet-induced hypercholesterolemia., J. Agric. Food Chem. 52 (2004) 2879–86. doi:10.1021/jf035354z.

[20]   T. Saito, D. Abe, K. Sekiya, Nobiletin enhances differentiation and lipolysis of 3T3-L1 adipocytes., Biochem. Biophys. Res. Commun. 357 (2007) 371–6. doi:10.1016/j.bbrc.2007.03.169.

[21]   E. Tripoli, M. La Guardia, S. Giammanco, D. Di Majo, M. Giammanco, Food Chemistry Citrus flavonoids : Molecular structure , biological activity and nutritional properties : A review, 104 (2007) 466–479. doi:10.1016/j.foodchem.2006.11.054.

[22]   S. Li, H. Wang, L. Guo, H. Zhao, C.T. Ho, Chemistry and bioactivity of nobiletin and its metabolites, J. Funct. Foods. 6 (2014) 2–10. doi:10.1016/j.jff.2013.12.011.

[23]   N. Lin, T. Sato, Y. Takayama, Y. Mimaki, Y. Sashida, M. Yano, A. Ito, Novel anti-inflammatory actions of nobiletin, a citrus polymethoxy flavonoid, on human synovial fibroblasts and mouse macrophages, Biochem. Pharmacol. 65 (2003) 2065–2071. doi:10.1016/S0006-2952(03)00203-X.

[24]   A. Murakami, K. Koshimizu, H. Ohigashi, S. Kuwahara, W. Kuki, Y. Takahashi, K. Hosotani, S. Kawahara, Y. Matsuoka, Characteristic rat tissue accumulation of nobiletin, a chemopreventive polymethoxyflavonoid, in comparison with luteolin, Biofactors. 16 (2002) 73–82. http://content.iospress.com/articles/biofactors/bio00514 (accessed March 1, 2016).

[25]   K. Kawabata, A. Murakami, H. Ohigashi, Nobiletin, a Citrus Flavonoid, Down-Regulates Matrix Metalloproteinase-7 (matrilysin) Expression in HT-29 Human Colorectal Cancer Cells, Biosci. Biotechnol. Biochem. (2014). http://www.tandfonline.com/doi/abs/10.1271/bbb.69.307 (accessed March 1, 2016).

[26]   N. Yoshimizu, Y. Otani, Y. Saikawa, T. Kubota, M. Yoshida, T. Furukawa, K. Kumai, K. Kameyama, M. Fujii, M. Yano, T. Sato, A. Ito, M. Kitajima, Anti-tumour effects of nobiletin, a citrus flavonoid, on gastric cancer include: antiproliferative effects, induction of apoptosis and cell cycle deregulation., Aliment. Pharmacol. Ther. 20 Suppl 1 (2004) 95–101.

doi:10.1111/j.1365-2036.2004.02082.x.

[27] O.M. Andersen, K.R. Markham, Flavonoids. Chemistry, Biochemistry and Applications., 2006. doi:0-8493-2021-6.

[28] G.K. Jayaprakasha, P.S. Negi, S. Sikder, L.J. Mohanrao, K.K. Sakariah, Antibacterial Activity of Citrus reticulata Peel Extracts, Zeitschrift Für Naturforsch. C. 55 (2000) 1030–1034. doi:10.1515/znc-2000-11-1230.

[29] Q. Wang, Z. Wu, L. Liu, L. Zou, M. Luo, Synthesis of citrus bioactive polymethoxyflavonoids and flavonoid glucosides, Chin J Org Chem. (2010). http://sioc-journal.cn/Jwk_yjhx/EN/article/showWenXian.do?id=339373 (accessed August 2, 2016).

[30] Y. Kumagai, Y. Shinkai, T. Miura, A.K. Cho, The chemical biology of naphthoquinones and its environmental implications., Annu. Rev. Pharmacol. Toxicol. 52 (2012) 221–47. doi:10.1146/annurev-pharmtox-010611-134517.

[31] L.I. López-López, D.S. Nery-Flores, Y.S. Silva-Belmares, A. Sáenz-Galindo, NAPHTHOQUINONES: BIOLOGICAL PROPERTIES AND SYNTHESIS OF LAWSONE AND DERIVATIVES - A STRUCTURED REVIEW, Vitae. 21 (n.d.) 248–258. http://www.scielo.org.co/scielo.php?script=sci_arttext&pid=S0121-40042014000300010&lng=en&nrm=iso&tlng=en (accessed February 25, 2016).

[32] Ullmann's Encyclopedia of Industrial Chemistry, Wiley-VCH Verlag GmbH & Co. KGaA, Weinheim, Germany, 2000.

[33] L.I. López L., E. Leyva, R.F. García de la Cruz, Las naftoquinonas: más que pigmentos naturales, Rev. Mex. Ciencias Farm. 42 (n.d.) 6–17. http://www.scielo.org.mx/scielo.php?script=sci_arttext&pid=S1870-01952011000100002&lng=es&nrm=iso&tlng=es (accessed February 25, 2016).

[34] C.T. Esmon, J.A. Sadowski, J.W. Suttie, A new carboxylation reaction. The vitamin K-dependent incorporation of H-14-CO3- into prothrombin, J. Biol. Chem. 250 (1975) 4744–4748. http://www.jbc.org/content/250/12/4744.short (accessed April 8, 2016).

[35] K.L. Berkner, K.W. Runge, The physiology of vitamin K nutriture and vitamin K-dependent protein function in atherosclerosis., J. Thromb. Haemost. 2 (2004) 2118–32.

doi:10.1111/j.1538-7836.2004.00968.x.

[36]   J. Stenflo, J. Suttie, Vitamin K-dependent formation of γ-carboxyglutamic acid, Annu. Rev. Biochem.   (1977). http://www.annualreviews.org/doi/pdf/10.1146/annurev.bi.46.070177.001105 (accessed May 10, 2016).

[37]   L.M. Nutter, C. Ann-Lii, H. Hsiao-Ling, H. Ruey-Kun, E.O. Ngo, L. Tsang-Wu, Menadione: Spectrum of anticancer activity and effects on nucleotide metabolism in human neoplastic cell lines, Biochem. Pharmacol. 41 (1991) 1283–1292. doi:10.1016/0006-2952(91)90099-Q.

[38]   W. Adam, J. Lin, C.R. Saha-Möller, W.A. Herrmann, R.W. Fischer, J.D.G. Correia, Homogeneous Catalytic Oxidation of Arenes and a New Synthesis of Vitamin K3, Angew. Chemie Int. Ed. English. 33 (1995) 2475–2477. doi:10.1002/anie.199424751.

[39]   S. Narayanan, K.V.V.S.B.S.. Murthy, K.M. Reddy, N. Premchander, A novel and environmentally benign selective route for Vitamin K3 synthesis, Appl. Catal. A Gen. 228 (2002) 161–165. doi:10.1016/S0926-860X(01)00962-0.

[40]   G. Strukul, F. Somma, N. Ballarini, F. Cavani, A. Frattini, S. Guidetti, D. Morselli, The oxidation of 2-methyl-1-naphthol to menadione with H2O2, catalyzed by Nb-based heterogeneous systems, Appl. Catal. A Gen. 356 (2009) 162–166. doi:10.1016/j.apcata.2008.12.041.

[41]   E. Shimanskaya, V. Doluda, M. Sulman, V. Matveeva, E. Sulman, Catalytic syntheses of 2-methyl-1,4-naphthoquinone in conventional solvents and supercritical carbon dioxide, Chem. Eng. J. 238 (2014) 206–209. doi:10.1016/j.cej.2013.07.087.

[42]   M. Damon, N.Z. Zhang, D.B. Haytowitz, S.L. Booth, Phylloquinone (vitamin K1) content of vegetables, J. Food Compos. Anal. 18 (2005) 751–758. doi:10.1016/j.jfca.2004.07.004.

[43]   L.J. Schurgers, C. Vermeer, Determination of phylloquinone and menaquinones in food. Effect of food matrix on circulating vitamin K concentrations., Haemostasis. 30 (2001) 298–307. doi:54147.

[44]   B. Subramaniam, R.A. Rajewski, K. Snavely, Pharmaceutical Processing with Supercritical Carbon Dioxide, J. Pharm. Sci. 86 (1997) 885–890. doi:10.1021/js9700661.

[45]   M. Mukhopadhyay, Extraction and processing with supercritical fluids, J. Chem. Technol. Biotechnol. 84 (2009) 6–12. doi:10.1002/jctb.2072.

[46]   M.M.R. de Melo, A.J.D. Silvestre, C.M. Silva, Supercritical fluid extraction of vegetable matrices: Applications, trends and future perspectives of a convincing green technology, J. Supercrit. Fluids. 92 (2014) 115–176. doi:10.1016/j.supflu.2014.04.007.

[47]   M. Herrero, J.A. Mendiola, A. Cifuentes, E. Ibáñez, Supercritical fluid extraction: Recent advances and applications, J. Chromatogr. A. 1217 (2010) 2495–2511. doi:10.1016/j.chroma.2009.12.019.

[48]   B.E. Poling, J.M. Prausnitz, The Properties of Gases and Liquids, 2006.

[49]   M. Perrut, Supercritical Fluid Applications: Industrial Developments and Economic Issues Present Status of Industrial Applications of Supercritical Fluids 1-9, (n.d.). doi:10.1021/ie000211c.

[50]   Y.-H. Lee, A.L. Charles, H.-F. Kung, C.-T. Ho, T.-C. Huang, Extraction of nobiletin and tangeretin from Citrus depressa Hayata by supercritical carbon dioxide with ethanol as modifier, Ind. Crops Prod. 31 (2010) 59–64. doi:10.1016/j.indcrop.2009.09.003.

[51]   G. Brunner, Gas extraction: an introduction to fundamentals of supercritical fluids and the application to separation processes, (2013). https://books.google.es/books?hl=es&lr=&id=GIfnCAAAQBAJ&oi=fnd&pg=PA1&dq=Gas+Extraction.+An+Introduction+to+Fundamentals+of+Supercritical+Fluids+and+the+Application+to+Separation+Processes&ots=yvggdBdGou&sig=UfUlp5vntmoUpKKY53TnS16JSvc (accessed July 7, 2016).

[52]   J.C. Valenzuela, J.R. Vergara-Salinas, J.R. Perez-Correa, eds., Supercritical Fluid Extraction of Polyphenols, in: Adv. Technol. Prod. Food-Relevant Polyphenols, CRC Press, 2016: pp. 125–192. doi:10.1201/9781315371245-6.

[53]   N.R. Foster, G.S. Gurdial, J.S.L. Yun, K.K. Liong, K.D. Tilly, S.S.T. Ting, H. Singh, J.H. Lee, Significance of the Crossover Pressure in Solid-Supercritical Fluid Phase Equilibria, Ind. Eng. Chem. Res. 30 (1991) 1955–1964.

[54]   R. Dohrn, J.M.S. Fonseca, S. Peper, Experimental methods for phase equilibria at high

pressures., Annu. Rev. Chem. Biomol. Eng. 3 (2012) 343–67. doi:10.1146/annurev-chembioeng-062011-081008.

[55]   O. Ferreira, S.P. Pinho, Solubility of flavonoids in pure solvents, Ind. Eng. Chem. Res. 51 (2012) 6586–6590. doi:10.1021/ie300211e.

[56]   H. Uchiyama, K. Mishima, S. Oka, M. Ezawa, M. Ide, P.W. Park, Solubilities of Flavone and 3-Hydroxyflavone in Supercritical Carbon Dioxide, 1 (1997) 570–573.

[57]   Ž. Knez, M. Škerget, Phase equilibria of the vitamins D2, D3 and K3 in binary systems with CO2 and propane, J. Supercrit. Fluids. 20 (2001) 131–144. doi:10.1016/S0896-8446(01)00061-4.

[58]   M. Johannsen, G. Brunner, Solubilities of the Fat-Soluble Vitamins A, D, E, and K in Supercritical Carbon Dioxide, J. Chem. Eng. Data. 42 (1997) 106–111. doi:10.1021/je960219m.

[59]   S. Peper, R. Dohrn, Sampling from fluid mixtures under high pressure: Review, case study and evaluation, J. Supercrit. Fluids. 66 (2012) 2–15. doi:10.1016/j.supflu.2011.09.021.

[60]   P. Guilbot, A. Valtz, H. Legendre, D. Richon, D. Richon, Rapid on-line sampler-injector: a reliable tool for HT-HP sampling and on-line GC analysis, Analusis. 28 (2000) 426–431. doi:10.1051/analusis:2000128.

[61]   O. Pfohl, J. Timm, R. Dohrn, G. Brunner, Measurement and correlation of vapor-liquid-liquid equilibria in the glucose + acetone + water + carbon dioxide system, Fluid Phase Equilib. 124 (1996) 221–233. doi:10.1016/S0378-3812(96)03098-1.

[62]   Q. Dong, R.D. Chirico, X. Yan, X. Hong, M. Frenkel, Uncertainty Reporting for Experimental Thermodynamic Properties, (2005) 546–550.

[63]   A.L. Cabrera, A.R. Toledo, J.M. del Valle, J.C. de la Fuente, Measuring and validation for isothermal solubility data of solid 2-(3,4-Dimethoxyphenyl)-5,6,7,8-tetramethoxychromen-4-one (nobiletin) in supercritical carbon dioxide, J. Chem. Thermodyn. 91 (2015) 378–383. doi:10.1016/j.jct.2015.08.018.

[64]   Joint Committee For Guides In Metrology (JCGM), International vocabulary of metrology — Basic and general concepts and associated terms (VIM), VIM3 Int. Vocab. Metrol. 3 (2008)

104. doi:10.1016/0263-2241(85)90006-5.

[65]   R.D. Chirico, M. Frenkel, V. V Diky, K.N. Marsh, R.C. Wilhoit, ThermoMLsAn XML-Based Approach for Storage and Exchange of Experimental and Critically Evaluated Thermophysical and Thermochemical Property Data . 2 . Uncertainties, (2003) 1344–1359.

[66]   A. Muhlbauer, Phase Equilibria: Measurement & Computation, (1997). https://books.google.es/books?hl=es&lr=&id=pnimpqF4wsMC&oi=fnd&pg=PR13&dq=J.D .+Raal,+A.L.+M%C3%BChlbauer,+Phase+Equilibria+Measurement+and+Computation,+C RC+Press,+1997&ots=88vDVKXpg3&sig=Sh0eF54yhvr4gc8iH7tzUUpNyM8   (accessed June 30, 2016).

[67]   J.O. Valderrama, J. Zavaleta, Thermodynamic consistency test for high pressure gas–solid solubility data of binary mixtures using genetic algorithms, J. Supercrit. Fluids. 39 (2006) 20– 29. doi:10.1016/j.supflu.2006.02.003.

[68]   J.O. Valderrama, P. a. Robles, J.C. De La Fuente, Determining the sublimation pressure of capsaicin using high-pressure solubility data of capsaicin + CO2 mixtures, J. Chem. Eng. Data. 51 (2006) 1783–1787. doi:10.1021/je060188n.

[69]   M. Türk, M. Crone, T. Kraska, A comparison between models based on equations of state and density-based models for describing the solubility of solutes in CO2, J. Supercrit. Fluids. 55 (2010) 462–471. doi:10.1016/j.supflu.2010.08.011.

[70]   J. Méndez-Santiago, A.S. Teja, The solubility of solids in supercritical fluids, Fluid Phase Equilib. 158–160 (1999) 501–510. doi:10.1016/S0378-3812(99)00154-5.

[71]   C.A. Lee, M. Tang, Y.P. Chen, Measurement and correlation for the solubilities of cinnarizine, pentoxifylline, and piracetam in supercritical carbon dioxide, Fluid Phase Equilib. 367 (2014) 182–187. doi:10.1016/j.fluid.2014.01.041.

[72]   M.A. McHugh, J.J. Watkins, B.T. Doyle, V.J. Krukonis, High-pressure naphthalene-xenon phase behavior, Ind. Eng. Chem. Res. 27 (1988) 1025–1033. doi:10.1021/ie00078a023.

[73]   I.K. and, M. Lora, A. Bertucco, A Thermodynamic Analysis of Three-Phase Equilibria in Binary and Ternary Systems for Applications in Rapid Expansion of a Supercritical Solution (RESS), Particles from Gas-Saturated Solutions (PGSS), and Supercritical Antisolvent (SAS),

(1997). doi:10.1021/IE970376U.

[74]   D.-Y. Peng, D.B. Robinson, A New Two-Constant Equation of State, Ind. Eng. Chem. Fundam. 15 (1976) 59–64. doi:10.1021/i160057a011.

[75]   D.S.H. Wong, S.I. Sandler, A theoretically correct mixing rule for cubic equations of state, AIChE J. 38 (1992) 671–680. doi:10.1002/aic.690380505.

[76]   J.C. de la Fuente, J.O. Valderrama, S.B. Bottini, J.M. del Valle, Measurement and modeling of solubilities of capsaicin in high-pressure CO2, J. Supercrit. Fluids. 34 (2005) 195–201. doi:10.1016/j.supflu.2004.11.014.

[77]   H. Renon, J.M. Prausnitz, Local compositions in thermodynamic excess functions for liquid mixtures, AIChE J. 14 (1968) 135–144. doi:10.1002/aic.690140124.

[78]   J.C. de la Fuente, B. Oyarzún, N. Quezada, J.M. del Valle, Solubility of carotenoid pigments (lycopene and astaxanthin) in supercritical carbon dioxide, Fluid Phase Equilib. 247 (2006) 90–95. doi:10.1016/j.fluid.2006.05.031.

[79]   R.I. Canales Muñoz, J.C. de la(comisión de tesis) Fuente Badilla, Evaluación del efecto de cosolventes lìpidos sobre la solubilidad de pigmentos carotenoides en CO2 supercrítico, UTFSM, 2012.

[80]   K. a. Araus, J.M. del Valle, P.S. Robert, J.C. de la Fuente, Effect of triolein addition on the solubility of capsanthin in supercritical carbon dioxide, J. Chem. Thermodyn. 51 (2012) 190–194. doi:10.1016/j.jct.2012.02.030.

[81]   K.A. Araus, R.I. Canales, J.M. Del Valle, J.C. De La Fuente, Solubility of ??-carotene in ethanol- and triolein-modified CO 2, J. Chem. Thermodyn. 43 (2011) 1991–2001. doi:10.1016/j.jct.2011.07.013.

[82]   P. Robert, N. Romero, J. Ortiz, L. Masson, D. Barrera-Arellano, Effect of rosa mosqueta (Rosa rubiginosa) extract on the performance of chilean hazelnut oil (Gevuina avellana Mol.) at high temperature, J. Am. Oil Chem. Soc. 83 (2006) 691–695. doi:10.1007/s11746-006-5025-y.

[83]   S. V. Ting, R.L. Rouseff, M.H. Dougherty, J.A. Attaway, Determination of some methoxylated flavones in citrus juices by high performance liquid chromatography, J. Food Sci. 44 (1979) 69–71. doi:10.1111/j.1365-2621.1979.tb10006.x.

[84] O. Y.-P. Hu, C.-Y. Wu, W.-K. Chan, F. Y.-H. Wu, Determination of anticancer drug vitamin K3 in plasma by high-performance liquid chromatography, J. Chromatogr. B Biomed. Sci. Appl. 666 (1995) 299–305. doi:10.1016/0378-4347(94)00572-M.

[85] nist23, NIST, Fluid Thermodyn. Transp. Prop. Version 5.0. (http//www.nist.gov/srd/nist23.htm). (n.d.). http://www.nist.gov/srd/nist23.cfm (accessed September 3, 2015).

[86] J. Méndez-Santiago, A.S. Teja, The solubility of solids in supercritical fluids, Fluid Phase Equilib. 158–160 (1999) 501–510. doi:10.1016/S0378-3812(99)00154-5.

[87] H. Devoe, M.M. Miller, S. Wasikt, Generator Columns and High Pressure Liquid Chromatography for Determining Aqueous Solubilities and Octanol-Water Partition Coefficients of Hydrophobic Substances, J. Res. Natl. Bur. Stand. (1934). 86 (n.d.).

[88] A.G. Reveco-Chilla, A.L. Cabrera, J.C. de la Fuente, F.C. Zacconi, J.M. del Valle, L.M. Valenzuela, Solubility of menadione and dichlone in supercritical carbon dioxide, Fluid Phase Equilib. 423 (2015) 84–92. doi:http://dx.doi.org/10.1016/j.fluid.2016.04.001.

[89] Ö.G.-Ü. and, F. Temelli*, Correlating the Solubility Behavior of Fatty Acids, Mono-, Di-, and Triglycerides, and Fatty Acid Esters in Supercritical Carbon Dioxide, (2000).

[90] Ö. Güçlü-Üstündağ, F. Temelli, Correlating the solubility behavior of minor lipid components in supercritical carbon dioxide, J. Supercrit. Fluids. 31 (2004) 235–253. doi:10.1016/j.supflu.2003.12.007.

[91] K.G. Joback, R.C. Reid, Estimation of Pure-Component Properties From Group-Contributions, Chem. Eng. Commun. 57 (1987) 233–243. doi:10.1080/00986448708960487.

[92] Á. Martín, M.D. Bermejo, F.A. Mato, M.J. Cocero, Teaching advanced equations of state in applied thermodynamics courses using open source programs, Educ. Chem. Eng. 6 (2011) 114–121. doi:10.1016/j.ece.2011.08.003.

Appendixes

Appendix A. Published data of nobiletin solubility in SC-CO$_2$.

Appendix B. Published data of menadione solubility in SC-CO$_2$.

Appendix A. Published data of nobiletin solubility in SC-CO₂.

Measuring and validation for isothermal solubility data of solid 2-(3,4-Dimethoxyphenyl)-5,6,7,8-tetramethoxychromen-4-one (nobiletin) in supercritical carbon dioxide

Adolfo L. Cabrera [a], Alma R. Toledo [b], José M. del Valle [c], Juan C. de la Fuente [a,*]

[a] Laboratorio de Termodinámica de Procesos, Departamento de Ingeniería Química y Ambiental, Universidad Técnica Federico Santa María, Avda. España 1680, Valparaíso, Chile
[b] Centro de Investigación en Alimentación y Desarrollo, A.C., Carretera a La Victoria km. 0.6, Hermosillo, México
[c] Departamento de Ingeniería Química y Bioprocesos, Pontificia Universidad Católica de Chile, Avda. Vicuña Mackenna 4860, Santiago, Chile

ABSTRACT

Isothermal solubility of 2-(3,4-Dimethoxyphenyl)-5,6,7,8-tetramethoxychromen-4-one (nobiletin) in supercritical carbon dioxide at temperatures of (313, 323 and 333) K and pressures from (18 to 31) MPa was measured using an analytic-recirculation methodology, with direct determination of the molar composition of the carbon dioxide-rich phase by using high performance liquid chromatography. Results indicated that the range of the measured solubility of nobiletin was from $107 \cdot 10^{-6}$ mol · mol^{-1} at $T = 333$ K and 18.35 MPa to $182 \cdot 10^{-6}$ mol · mol^{-1} at $T = 333$ K and 31.40 MPa, with a temperature cross-over around 18 MPa. The validation of the experimental solubility data was carried out by using three approaches, namely, estimation of combined expanded uncertainty for each solubility data point from experimental parameters values ($\leqslant 77 \cdot 10^{-6}$ mol · mol^{-1}); thermodynamic consistency, verified utilizing a test adapted from tools based on Gibbs-Duhem equation and solubility modelling results; and, self-consistency, proved by correlating the solubility data with a semi-empirical model as a function of temperature, pressure and pure CO₂ density.

© 2015 Elsevier Ltd. All rights reserved.

1. Introduction

Flavonoids are polyphenolic compounds with a structure based on flavone (2-phenyl-4H-chromen-4-one), a backbone of 15 carbons arranged in a three rings skeleton, C_6—C_3—C_6 (figure 1A), with multiple substituent groups [1]. Nobiletin (2-(3,4-Dimethoxyphenyl)-5,6,7,8-tetramethoxychromen-4-one), illustrated in figure 1B, a flavonoid that belongs to the polymethoxyflavones (PMF), is one of the major components identified in citrus fruits, specifically abundant with large percentage content in citrus peels [2], and it may act in protecting from pathogenic attack taking into account its antiviral and antimicrobial capacity [3]. Nobiletin has shown many potential health promoting benefits, considering the cumulative evidences that indicate its biological activity, which gives to nobiletin pharmacological properties, including, anti-inflammatory (the most significant), anti-carcinogenic, anti-viral, anti-atherogenic and anti-diabetic [1].

Supercritical (SC) Fluid extraction (SCFE) is an environmentally friendly technology used to recover and/or purify high-value nonpolar and/or low-molecular-weight active principles (bioactive compounds, such as the PMF nobiletin) from biological matrices. The solvent used is a compressed inert gas above its corresponding critical temperature (T_c) and critical pressure (p_c), which confers a near-liquid density and a near-gas viscosity and self-diffusivity. Carbon dioxide (CO₂) ($T_c = 304.1$ K, $p_c = 7.38$ MPa) at supercritical conditions (SC-CO₂) is able to isolate high-purity bioactive compounds avoiding thermal damage, because the operation temperature in a SCFE process is slightly above T_c of CO₂. Furthermore, there is a decompression stage, at low pressure, where the CO₂ gas releases the extract, remaining it free of contamination. CO₂ is an inert substance. Therefore its use as a solvent prevents undesirable side chemical reactions [4]. Lee et al. [5] used SC-CO₂, pure, and plus a modifier (a solution of aqueous methanol or ethanol), to extract PMFs from Citrus depressa H. The authors studied experimentally the global yields and the concentration of nobiletin in the extract as a function of the modifier composition, extraction temperature and pressure, CO₂ flow rate, and particle size, with the aim to find the optimal extraction conditions.

Appropriate mass transfer models for a SCFE process of PMFs from vegetal substrates (e.g., based on mass balance equations for thin sections of a packed bed) would facilitate the design, as

* Corresponding author. Tel.: +56 (32) 2654221; fax: +56 (32) 2654478.
E-mail address: juan.delafuente@usm.cl (J.C. de la Fuente).
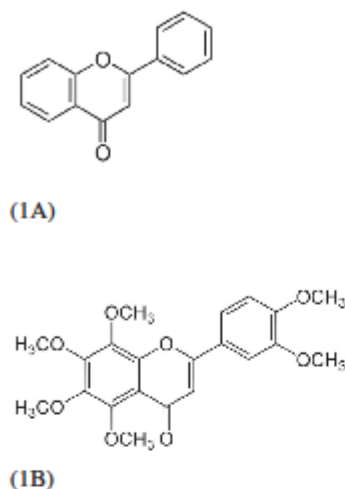
(1A)

(1B)

FIGURE 1. Chemical structure of (1A) Flavone (2-phenyl-4H-chromen-4-one); and (1B) Nobiletin (2-(3,4-Dimethoxyphenyl)-5,6,7,8-tetramethoxychromen-4-one).

well as, the definition and optimization of operational conditions for commercial processes with $SC-CO_2$. The development of models and scale-up of SCFE processes require experimental information of physicochemical and transport properties from laboratory and pilot plant in order to support and adapt a general model to a specific process. Among others, thermodynamic constrains such as, solute solubility and extraction selectivity have to be established for each solute or group of solutes [6]. The reliability and accuracy of physicochemical property data impact on the modelling, design and simulation of chemical processes, taking into account the present capacity and high performance of computational tools to reproduce complex and large chemical processes, and specific physicochemical phenomena [7]. In order to avoid doubt about the validity of experimental physicochemical data measured in laboratory, in particular properties of phase equilibria in chemical thermodynamic, uncertainties should be included regularly as a part of the experimental information in order to assess the accuracy of the data reported.

Accuracy is a qualitative concept defined as the "closeness of agreement between the result of a measurement and the "measurand" [8], therefore, uncertainty is the quantitative parameter used to estimate the dispersion or closeness of the value measured from the true (but unknowable) value [9]. Uncertainties of properties can be estimated using two approaches [10], (A) by a probability distribution from a defined large number of repetitions, or (B) by propagation of uncertainties using the available information, combined with common scientific sense based on previous experience. For thermodynamic properties of phase equilibria (e.g., sets of compositions of phases, temperature and pressure), approach (A) most of the time is inappropriate, considering the dimension of the effort and cost associated, and is limited to verify the repeatability (a type of precision) of a few measures [7]. Approach (B) is preferred. For properties like equilibrium temperature and pressure the standard uncertainty (u) is calculated with one standard deviation (68.27% of level of confidence for a normal distribution). Generally the standard deviation may be estimated from the type of experimental apparatus, methodology and other sources of information from literature, among others. The uncertainty for

each mole fraction can be assessed with the combined uncertainty (u_{Comb}), an arrangement that quantifies the propagation of the individual standard uncertainties of each variable or constraint, appropriately combined and weighted, which defines the mole fraction. The combined expanded uncertainty (U_{Comb}) is defined as the product of the combined uncertainty with a number (coverage factor) greater or equal to one (e.g., 1.645 for 90% of level of confidence for a normal distribution). Note that the definition of all elements for the combined uncertainty in approach (B) is in most of the cases unrealizable, and therefore uncertainties declared for a given set of experimental values are estimations of the real dispersion.

Thermodynamic consistency tests are supplementary tools to evaluate of reliability of a data set (e.g., temperature, pressure and phase compositions at equilibrium), based on the over determination of experimental properties measured, according to the phase rule, along with the use of the Gibbs–Duhem equation to generate values of any one of these properties and to compare them with the laboratory results [11]. Particularly, for experimental solubility of a solid solute dissolved in $SC-CO_2$, i.e., temperature (T), pressure (p) and solute mole fraction in CO_2-rich phase (y_2) at equilibrium, Valderrama and Zavaleta [12] described a simple methodology that combines the Gibbs–Duhem criteria with an appropriate calculation of fugacity coefficients at high pressure equilibria fluid (F) + solid (S) using an equation of state with mixing and combination rules.

Some issues about the consistency test are mainly related to the performance of the equation of state and the lack of information for the solid solute such as, critical parameters, acentric factor, molar volume, and sublimation pressure [13,14]. Semi-empirical models proposed by Mendez-Santiago and Teja [15] and Chrastil [16] are frequently used to correlate the solid solute solubility as a function of temperature, pressure and pure CO_2 density, removing the restriction aforementioned, data of solute properties and performance of equations of state. The three adjustable parameters included in each model are independent of temperature, therefore, an appropriate representation of solute solubility, temperature and pressure versus CO_2 density could result in a collapse of all the experimental data on one straight line for a range approximately from half to twice of the CO_2 critical density, representing a self-consistency test for an experimental solubility data set [13,14,17]. This kind of uncertainty assessment could be referred as precision, because it can be classified as the measure of the deviation from a fitted curve (representing the expected physicochemical relation among properties) for an experimental data set [10].

The objective of this work is to contribute with experimental solubility data of nobiletin in $SC-CO_2$ and drive the study about the dispersion of variables and properties measured from their true (unknowable) values, considering a systematic procedure that includes: (i) estimation of uncertainties; (ii) thermodynamic consistency test; (iii) self-consistency test.

2. Experimental

2.1. Materials

Nobiletin (>0.97 mass fraction purity, CAS: 478-01-3) was from CHEMOS GmbH (Regenstauf, Germany), and low pressure (5.7 MPa) carbon dioxide (0.9999 mass fraction purity) was from AGA-Chile S.A. (Santiago, Chile). For the HPLC analysis [18], the mobile phase used a 40:60 mixture of HPLC-grade acetonitrile Tedia (Fairfield, OH) and HPLC-grade water from Merck KGaA (Darmstadt, Germany), and a reverse-phase, 4.6-mm (inner diameter) wide, 25-cm long, C_{18} column (Waters symmetry column, Waters, Milford, MA) packed with 5-μm (diameter) particles of

TABLE 1
Specification of chemical samples.

Chemical name	Source	Initial mass fraction purity/kg · kg^{-1}	Purification method	Final mass fraction purity/kg · kg^{-1}	Analysis Method
Carbon dioxide	AGA-Chile S.A.	0.9999	None	0.9999	None
Nobiletin	CHEMOS GmbH	0.97	None	0.97	None
Acetonitrile	Tedia	0.999	None	0.999	GC[a]
Water	Merck KGaA	0.99999	None	0.99999	GC[a]

[a] Gas–Liquid Chromatography.

stationary phase. In table 1 were summarized the specifications of the chemical samples used in this work.

2.2. Apparatus and procedure

The solubility of solid nobiletin in SC-CO_2 was measured at 313 K, 323 K, and 333 K and over a pressure range from (17.97 to 31.40) MPa using a dynamic-analytical methodology as described in Araus et al. [19]. The experimental system consists of an stirred, 50 cm^3 (Thar-Tech, Pittsburgh, PA) view-cell placed in a temperature-controlled air bath, a syringe pump (Teledyne ISCO 260D, Lincoln, NE) to load CO_2 into the system and adjust system pressure, and with a gear pump (GAH-T23, Eurotechnica, Bargte-heide, Germany) to recirculate the CO_2-rich phase, aid system equilibration, and to feed samples of the CO_2-rich phase to the HPLC system coupled to the equilibration system. The HPLC system consists of an L-7100 pump, L-7350 oven, and L-7455 photodiode array detector (Hitachi LaChrom, Tokyo, Japan). The methodology defined to assess the solubility of nobiletin in SC-CO_2 initiates with the cell loaded with approximately 0.2 g of solid solute, then the residual air is removed by displacement with CO_2 from a gas cylinder, released with a vacuum pump and (Welch Vacuum, Skokie, IL), after that, CO_2 was loaded into the equilibrium cell using the high-pressure syringe pump. With both components loaded in the equilibrium cell, the stirring system was activated, the magnetic bar and the recirculation of the CO_2-rich phase, up to reaching the equilibrium conditions. Using the two sapphire windows of the view-cell, it was verified for the three isotherms and for the entire pressure range the presence of two phases, fluid and solid. Values of y_2 were calculated using equation (1) [19] based on the chromatographic response (peak area A_2) of $V_N = 20 \mu$L-aliquot (Rheodyne, Rohnert Park, CA), from the loop of the equilibrium cell, as compared to the chromatographic response (peak area A_{S2}) of a $V_S = 20 \mu$L-aliquot (Rheodyne, Rohnert Park, CA), from the loop of the HPLC injector, of a stock solution of known concentration (C_{S2}) of the solute (nobiletin) used for calibration purposes, and properties of CO_2, molar mass (MW_1) and specific volume at test conditions (v_1) calculated as a function of system temperature and pressure using NIST [20] database.

$$y_2 = \left(\frac{A_2/V_N}{A_{S2}/V_S}\right) \cdot C_{S2} \cdot v_1 \cdot MW_1 \tag{1}$$

3. Results and discussion

3.1. Experimental solubility equilibrium data

Isothermal solubility for the system (CO_2 + solid nobiletin) at temperatures of (313, 323 and 333) K as a function of pressure are reported in table 2 and represented graphically in figure 2. Results indicate that solubility started from $y_2 = 107 \cdot 10^{-6}$ mol · mol^{-1} at $T = 333$ K and $p = 18.35$ MPa and increased up to $y_2 = 182 \cdot 10^{-6}$ mol · mol^{-1} at $T = 333$ K and $p = 31.40$ MPa (the highest pressure measured). At constant temperature the solubility showed an increase with the pressure, driven by the increment

TABLE 2
Experimental mole fraction of solid nobiletin (2) (solubility, y_2) in supercritical CO_2 (1)-rich phase as a function of system pressure (p) or density of pure CO_2 (ρ_1) at temperatures (313, 323, and 333) K.

T/K	p/MPa	ρ_1^a/kg · m^{-3}	$y_2 \cdot 10^6$/mol · mol^{-1}	$U_{comb}(y_2) \cdot 10^6$/mol · mol^{-1}
313	17.97	819.0	114	48
	21.93	856.7	126	53
	28.22	899.1	141	60
323	18.09	758.6	109	46
	21.79	804.4	138	58
	27.87	855.7	154	65
	31.03	876.8	164	69
333	18.35	694.1	107	45
	21.95	751.6	152	64
	27.92	813.4	179	76
	32.40	839.6	182	77

$u(T) = 0.1$ K, $u(p) = 0.01$ MPa. Combined expanded uncertainties for mole fraction of nobiletin, $U_{comb}(y_2)$, were estimated with a 0.90 level of confidence.
[a] [20].

in the CO_2 density and its positive effect over the solvent power. An enhancement in the solubility values of nobiletin with the temperature at isobaric condition was observed, indicating that increasing the solute vapour pressure overwhelmed the reduction in CO_2 density. According to figure 2, an inversion in the isothermal response was detected for solubility data at the lowest vale of pressure measured, the behaviour shifted around 18 MPa (temperature crossover), from a negative effect of temperature on solubility (the

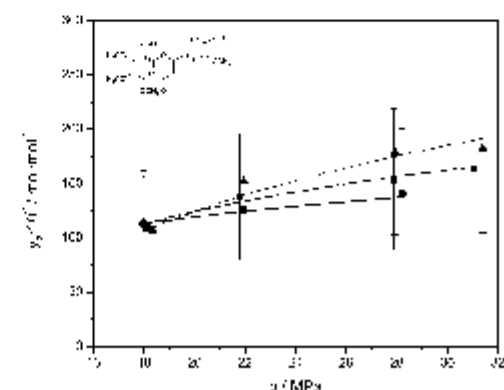
FIGURE 2. Mole fraction of nobiletin (2) (solubility, y_2) in supercritical CO_2 (1)-rich phase as a function of system pressure (p) at temperatures of at 313 K (●, —); 323 K (■, — —) and 333 K (▲, – –). Error bars represent the uncertainties informed in table 2. Symbols represent experimental results measured in this work; lines represent the correlation of Mendez-Santiago and Teja.

TABLE 3
Estimation of the combined expanded uncertainty for mole fraction of nobiletin (2) (solubility, y_2) in supercritical CO_2 (1)-rich phase, $U_{comb}(y_2)$, based on the contributions of properties and variables measured and calculated [19].

Property, Variable	Type of uncertainty (Level of confidence/%)	Uncertainty	Contribution to combined expanded uncertainty of y_2 /%
Temperature ($313 \leqslant T \leqslant 333$) K	Standard	$u(T) = 0.1 K$	–
Pressure ($17.97 \leqslant p \leqslant 31.40$) MPa	Standard	$u(p) = 0.01 MPa$	–
Chromatographic area for sample of nobiletin dissolved in CO_2 ($5778650 \leqslant A_2 \leqslant 11390338$) AU[a]	Standard	$u(A_2) = 3500 AU$	1
Chromatographic area for the stock solution ($344727 \leqslant A_{02} \leqslant 375559$) AU	Standard	$u(A_{02}) = 3500 AU$	4
Volume of sampler loop of the equilibrium cell ($V_N = 20$ μL)	Standard	$u(V_N) = 2$ μL	38
Volume loop of the HPLC injector ($V_S = 20$ μL)	Standard	$u(V_S) = 2$ μL	38
Concentration of stock solution $C_{02} = \frac{m_2}{V_{2F} \cdot MW_2}$ $C_{02} = 0.10935 \cdot 10^{-6}$ mol·cm^{-3}	Combined (68.27)	$\frac{u_{comb}(C_2)}{C_2} = \frac{u(m_2)}{m_2} + \frac{u(V_{2F})}{V_{2F}}$	18
Mass of nobiletin dissolved in acetonitrile $m_2 = 22$ mg	Standard	$u(m_2) = 0.0001 g$	–
Volume of flask to dissolve nobiletin in acetonitrile $V_{2F} = 50$ cm^3	Standard	$u(V_{2F}) = 0.08 cm^3$	–
Specific volume of CO_2 $v_1 = f(T,p)$ ($4.89 \leqslant v_1 \leqslant 6.34$) 10^{-5} m^3·mol^{-1}	Combined (68.27)	$\frac{u_{comb}(v_1)}{v_1} = \mid \frac{1}{v_1} \cdot \frac{\partial v_1}{\partial T} \mid \cdot u(T) + \mid \frac{1}{v_1} \cdot \frac{\partial v_1}{\partial p} \mid \cdot u(p)$	1
Volumetric expansibility of CO_2 $\alpha_1 = \mid \frac{1}{v_1} \cdot \frac{\partial v_1}{\partial T} \mid$ ($0.00446 \leqslant \alpha_1 \leqslant 0.1019$) K^{-1}	–	NIST[b]	–
Isothermal compressibility of CO_2 $\beta_1 = \mid \frac{1}{v_1} \cdot \frac{\partial v_1}{\partial p} \mid$ ($0.00065 \leqslant \beta_1 \leqslant 0.00283$) MPa^{-1}	–	NIST[b]	–
Mole fraction of nobiletin in CO_2-rich phase $y_2 = \left(\frac{A_2/V_N}{A_{02}/V_S}\right) \cdot C_{02} \cdot v_1 \cdot MW_1$ ($107 \leqslant y_2 \leqslant 182$) 10^{-6} mol·mol^{-1}	Combined expanded (90)	$\frac{U_{comb}(y_2)}{U_{comb} y_2} = \frac{\Delta A_2}{A_2} + \frac{\Delta A_{02}}{A_{02}} + \frac{\Delta V_N}{V_N} + \frac{\Delta V_S}{V_S} + \frac{\Delta C_{02}}{C_{02}} + \frac{\Delta v_1}{v_1}$	–

[a] Area units.
[b] [20].

increasing in the solute vapour pressure with the temperature cannot balance the decreasing in the CO_2 density) to a positive effect.

Li et al. [2] isolated flavonoids in peel sweet oranges (*Citrus sinensis* L.) and identified nine hydroxylated polymethoxyflavones (OHPMFs), two polymethoxychalcones (PMCs) and seven PMFs. In addition to solubility data of nobiletin reported in this contribution, there is no information in literature about solubility of others PMFs in SC-CO_2, particularly for sinensetin (2-(3,4-Dimethoxyphenyl)-5,6,7-trimethoxychromen-4-one) and tangeretin (5,6,7,8-tetramethoxy-2-(4-methoxyphenyl)-4H-1-benzopyran-4-one) with a similar positive bioactive effect and industrial interest as those of nobiletin, and with only a methoxy group of difference. As a reference, the solubility of flavone (the backbone of the nobiletin molecule) in SC-CO_2 at T = (308.2 and 318.2) K [21] is approximately 3.7 times higher when is compared with the solubility of nobiletin at T = 313.2 K and pressure range from (17.97 to 28.22) MPa. The lower values in solubility of nobiletin are due to the presence of the six methoxy groups that contribute to increase its Molar mass and polarity relative to flavone, which affect negatively over the solvent power of the SC-CO_2 [4].

3.2. Dispersion of variables and measured properties from their true (unknowable) values

3.2.1. Estimation of uncertainties

Approach (A). From three to five consecutive measures of solubility of nobiletin in SC-CO_2 at similar temperature and pressure were completed. The average value for each temperature and pressure condition is informed in table 2. Results indicated that the

TABLE 4
Pure component properties for carbon dioxide (1) and nobiletin (2) from the literature or estimated in this work.

Property	Value	Source or Estimation Method	Reference
Carbon dioxide (1)			
Molar mass (MW_1)/Da)	44.01	–	–
Critical temperature (T_{c1})/K	304.2	NIST	[20]
Critical pressure ($p_{c,1}$)/MPa	7.38	NIST	
Acentric factor (ω_1)	0.2252	NIST	
Nobiletin (2)			
Molar mass (MW_2)/Da)	402.40	–	–
Critical temperature (T_{c2})/K	1256	Joback	[26,27]
Critical pressure ($p_{c,2}$)/MPa	1.54	Joback	
Acentric factor (ω_2)	1.1884	Definition	
Critical volume ($V_c \cdot 10^6$)/m^3·mol^{-1})	1067.5	Joback	

repeatability is above 95%, adequate to verify the precision of the experimental apparatus and methodology used.

Approach (B). The standard and combined expanded uncertainties were estimated using the available information for the apparatus, experimental methodology and measured values. Results are included in table 2 for temperature, pressure and each individual value of the mole fraction. Table 3 details the methodology used to estimate the uncertainties for all variables and properties measured in this work. Results for the combined expanded uncertainty of the mole fraction of nobiletin ($U_{comb}(y_2) \leqslant 77 \cdot 10^{-6}$ mol·mol^{-1}) are consistent with assessments reported in previous contribution

using the same experimental apparatus and methodology [19]. From table 3 the numerical values indicate as the major contribution to $U_{Comb}(y_2)$, approximately 76%, corresponding to the sum of uncertainties for the volumes of sample loops of 20 µL in equilibrium cell and HPLC injector. The standard uncertainty for volume of each loop was estimated as <2 µL according to the manufacturer (Rheodyne, Rohnert Park, CA). In this work no further measurement of sample loops volumes have been made to evaluate its uncertainty. In order to present in a graphical format the uncertainties estimated in table 2, in figure 2 error bars are included.

3.2.2. Thermodynamic consistency test

The experimental results were analysed using the procedure to evaluate of thermodynamic consistency for the (high-pressure fluid + solid) solubility of binary mixtures proposed by Valderrama and Zavaleta [12] using values previously calculated for the fugacity coefficients of the solute ($\hat{\phi}_2^g$) and CO_2 ($\hat{\phi}_1^g$) in the supercritical fluid-rich phase at constant temperature, in order to assess for an individual data point (j) the area deviation (ΔA_j) evaluating the integrals by using the information for the next data point (j + 1).

$$\Delta A_j = \frac{\int_j^{j+1} (py_2)^{-1} dp - \left\{ \int_j^{j+1} \left[\hat{\phi}_2^g (Z^g - 1) \right]^{-1} d\hat{\phi}_2^g + \int_j^{j+1} (1 - y_2) [y_2(Z^g - 1)\hat{\phi}_1^g]^{-1} d\hat{\phi}_1^g \right\}}{\int_j^{j+1} (py_2)^{-1} dp} \quad (2)$$

where Z^g is the compressibility factor of the fluid mixture. In order to calculate the three parameters needed in equation (2), $\hat{\phi}_1^g$, $\hat{\phi}_2^g$, and Z^g, using the experimental values, the (fluid + solid) equilibria (FSE) at high-pressure was represented using a ϕ–ϕ approach assuming that the solid phase was a pure solute [13], with the solid solubility calculated according equation (3).

$$y_2 = \frac{p_2^{Subl} \exp \left[\frac{V_2^s}{RT}(p - p_2^{Subl}) \right]}{p\hat{\phi}_2^g} \quad (3)$$

where p_2^{Subl} is the sublimation pressure of the pure solid solute at equilibrium temperature, $\bar{V}_2^s$ is the pure solid solute molar volume, and R is the universal gas constant.

According to Valderrama and Zavaleta [12] there are two stages in the test that have to be completed. The first stage is to verify that the equation of state (EoS) with the mixing rules selected to model the FSE for each isotherm properly represent y_2, i.e., with the optimized fitting parameters the square root of the sum of relative differences between calculated (y_2^{Calc}) and measured solubility squared divided by the number (N) of data points (relative root mean square deviation, $RMSD_y$) [10] is within ±20%. To try a different model (TDM) is recommended if this condition is unfulfilled. The second stage is to analyze the values of all ΔA_j calculated with equation (2) and to check that all of them are within ±20% in order to declare the experimental data set -thermodynamically consistent- (TC). In case that only the 75% of the calculated values of ΔA_j verify the condition of ±20%, the data set is defined as -not fully consistent- (NFC). For a fraction lower than 75%, the data set is considered -thermodynamically inconsistent- (TI).

The Peng–Robinson (PR) equation of state [22] with Wong–Sandler (WS) mixing rules [23] with the Non Random Two Liquid model (NRTL) for the calculation of the excess Gibbs energy [24] (PR + (WS + NRTL)) was used in this work to calculate the fugacity coefficients of both components in the fluid phase [25]. Properties of pure components, CO_2 and solid nobiletin, are listed in table 4.

For CO_2 the NIST Standard Database v5.0 [20] was used. For nobiletin the Joback group contribution method was used to estimate the molar volume, critical temperature and pressure, and saturation pressure at the reduced temperature of 0.7 [26]. The acentric factor of nobiletin was calculated from its definition. The sublimation pressure was included as a fifth optimization parameter [13], along with the four binary interaction coefficients (k_{12}, α_{12}, τ_{12}, τ_{21}) included in the combination rules of PR + (WS + NRTL). Table 5 contains results for the first stage, with values for the five selected optimization parameters (k_{12}, α_{12}, τ_{12}, τ_{21} and p_2^{Subl}) and the corresponding $RMSD_y$ calculated for each isotherm. Deviations between modelled and measured data set of nobiletin were $RMSD_y < 12$%, verifying the test condition that it has to be lower than 20%, and therefore was confirmed that the combination PR + (WS + NRTL) was appropriated to represent the FSE.

For the second stage, the PR + (WS + NRTL) was used to calculate the fugacity coefficients of both components in the fluid phase in order to apply of the consistency test. Individual calculations of area deviations were assessed according to equation (3) and are listed as absolute values in table 6. In addition, for each data point in table 6 the absolute value for the relative deviation between nobiletin solubility calculated from PR + (WS + NRTL) and the experimental measured value ($|\Delta y_2|$) is included. Results listed indicate that at T = (313, 323 and 333) K the $|\Delta A_j|$ values are < (18.9, 17.2, and 17.0)%, respectively, therefore all measured isotherms are thermodynamically consistent, according to the criteria established for the test.

3.2.3. Self-consistency test

The correlation of Mendez-Santiago and Teja [15] was selected in order to evaluate the self-consistency of the experimental solubility data of nobiletin, according to equation (4), with three adjustable parameters, A, B and C.

$$T[\ln(p \cdot y_2) - C] = A + B \cdot \rho_1 \quad (4)$$

Using multivariable linear regression of the experimental values shown in table 1, the best-fit parameters A, B and C were assessed. According to Mendez-Santiago and Teja [15] in equation (4) the density of the CO_2-rich phase was replaced by the density of the pure CO_2, because of the low solubility of nobiletin. For the temperature and pressure conditions measured in this work, the range for the density of CO_2 was approximately from 690 kg · m^{-3} (at T = 333 K and 18.35 MPa) to 900 kg · m^{-3} (at T = 313 K and

TABLE 5
Results for the first stage of the consistency test for (fluid + solid) equilibria of {CO_2 (1) + Nobiletin (2)}: Optimal values of parameters for the Peng–Robinson equation of state (p_2^{subl}) with Wong–Sandler mixing rule (k_{12}) and Non Random Two Liquid model (α_{12}, τ_{12}, τ_{21}) for the correlation of the solubility of nobiletin (y_2).

T/K	k_{12}	α_{12}	τ_{12}	τ_{21}	p_2^{subl}/MPa	$RMSD_y{}^a$/%
313	0.876	0.074	22.97	10.19	$2.9 \cdot 10^{-16}$	6.6
323	0.867	0.085	21.12	10.57	$2.7 \cdot 10^{-16}$	7.0
333	0.856	0.075	19.43	11.09	$3.1 \cdot 10^{-16}$	12

^{a} $RMSD_y = \sqrt{\sum_{i=1}^{N} [(y_2 - y_2^{Calc})/y_2]^2 / N}$.

TABLE 6

Results for the second stage of the consistency test for (fluid + solid) equilibria of {CO₂ (1) + Nobiletin (2)} using the Peng–Robinson equation of state with Wong–Sandler mixing rule and Non Random Two Liquid model: Assessed values of the absolute relative deviation ($|\Delta y_2|$) and area deviation (ΔA) for individual nobiletin solubility data points (y_2) according to equation (2).

T/K = 313 K			T/K = 323 K			T/K = 333 K		
p/MPa	$|\Delta y_2|$/%	$|\Delta A|$/%	p/MPa	$|\Delta y_2|$/%	$|\Delta A|$/%	p/MPa	$|\Delta y_2|$/%	$|\Delta A|$/%
17.97	0.3	18.9	18.09	0.3	17.2	18.35	0.3	17.0
21.93	11.5	14.3	21.79	9.0	13.6	21.95	14.8	16.6
28.22	0.1		27.87	0.1	13.5	27.92	0.2	9.2
			31.03	10.7		31.40	18.6	

$\Delta y_2 = (y_2 - y_2^{calc})/y_2$.

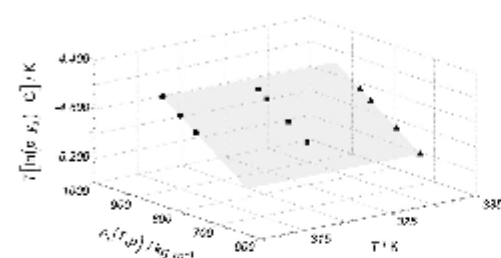**FIGURE 3.** Representation of mole fraction of nobiletin (2) (solubility, y_2) in supercritical CO₂ (1)-rich phase, CO₂ density (ρ_1) and temperature (T) in a three-dimensional arrangement, $T[\ln(p \cdot y_2) - C]$ versus $\rho_1(T, p)$ versus T. Symbols represent experimental results measured in this work, T = 313 K (●); T = 323 K (■) and T = 333 K (▲). The straight plane represents the Mendez-Santiago and Teja correlation with constants, A = −6872 K; B = 2.496 K · m³ · kg⁻¹ and C = 23.03 (RMSD$_y$ ≤ 0.22%).

28.22 MPa), that covers the suggested process conditions for SC-CO₂ extraction of bioactive compounds from vegetal matrices [6]. The three isothermal solubility data sets of nobiletin in SC-CO₂ were used to determine the best-fit values for the parameters in equation (4). The results obtained for the adjustable parameters are A = −6872 K, B = 2.496 K · m³ · kg⁻¹ and C = 23.03, with deviations verified by the corresponding value of RMSD$_y$ ≤ 0.22%, confirming the self-consistency of the solubility data of nobiletin in SC-CO₂. In figure 2, the results from the correlation were included for the three isotherms, where an appropriate agreement between experimental and calculated solubility is observed for the density range considered in this work. Figure 3 illustrates a three-dimensional representation of $T[\ln(p \cdot y_2) - C]$ versus T, defining a single plane where the three data sets of isothermal solubility values measured (cf. Table 2) of nobiletin collapse. From a two-dimensional point of view, the projection $T[\ln(p \cdot y_2) - C]$ versus $\rho_1(T, p)$, confirms that all experimental values are on a single straight line, behaviour observed by Mendez-Santiago and Teja [15], and the graphical verification of the self-consistency for the experimental data set.

4. Conclusions

The isothermal solubility of solid 2-(3,4-Dimethoxyphenyl)-5, 6,7,8-tetramethoxychromen-4-one (nobiletin) dissolved in supercritical carbon dioxide at T = (313, 323 and 333) K and pressures lower than 31.40 MPa was measured by a direct analytic-recirculation methodology. The three solubility data sets were validated using a procedure that allowed the estimation of the combined expanded uncertainty for each value of the experimental nobiletin mole fraction in the CO₂-rich phase value (≤77 · 10⁻⁶

mol · mol⁻¹), to verify for the three isothermal data sets their thermodynamic consistency (reliability of data), and to evaluate the self-consistency (a kind of precision) of the measured solubility.

References

[1] H. Li, H. Wang, L. Guod, H. Zhao, C.-T. Ho, J. Funct. Foods 6 (2014) 2–10.
[2] S. Li, C.-Y. Lo, C.-T. Ho, J. Agric. Food Chem. 54 (2006) 4176–4185.
[3] S. Li, M.-H. Pan, C.-Y. Lo, D. Tan, Y. Wang, F. Shahidi, C.-T. Ho, J. Funct. Foods 1 (2009) 2–12.
[4] G. Brunner, Gas Extraction. An Introduction to Fundamentals of Supercritical Fluids and the Application to Separation Processes, Springer, New York, NY, 1994.
[5] Y.H. Lee, A.L. Charles, H.F. Kung, C.-T. Ho, T.-C. Huang, Ind. Crop. Prod. 31 (2010) 59–64.
[6] J.M. del Valle, J.C. de la Fuente, Crit. Rev. Food Sci. Nutr. 46 (2006) 131–160.
[7] Q. Dong, R.D. Chirico, X. Yan, X. Hong, M. Frenkel, J. Chem. Eng. Data 50 (2005) 546–550.
[8] Guide to the Expression of Uncertainty in Measurement; International Organization for Standardization: Geneva, Switzerland, 1993.
[9] International Vocabulary of Basic and General Terms in Metrology; International Organization for Standardization, Geneva, Switzerland, 1993.
[10] R.D. Chirico, M. Frenkel, V.V. Diky, K.N. Marsh, R.C. Wilhoit, J. Chem. Eng. Data 48 (2003) 1344–1359.
[11] J.D. Raal, A.L. Mühlbauer, Phase Equilibria Measurement and Computation, CRC Press, 1997.
[12] J.O. Valderrama, J. Zavaleta, J. Supercrit. Fluid 39 (2006) 20–29.
[13] J.O. Valderrama, P.A. Robles, J.C. de la Fuente, J. Chem. Eng. Data 51 (2006) 1783–1787.
[14] M. Yurit, M. Crone, T. Kraska, J. Supercrit. Fluids 55 (2010) 462–471.
[15] J. Méndez-Santiago, A.S. Teja, Fluid Phase Equilib. 158–160 (1999) 501–510.
[16] J. Chrastill, J. Phys. Chem. 86 (1982) 3016–3021.
[17] C.-A. Lee, M. Tang, Y.-P. Chen, Fluid Phase Equilib. 367 (2014) 182–187.
[18] S.V. Ting, R.L. Rouseff, M.H. Dougherty, J.A. Attaway, J. Food Sci. 44 (1979) 69–71.
[19] K. Araus, R. Canales, J.M. del Valle, J.C. de la Fuente, J. Chem. Thermodyn. 43 (2011) 1991–2001.
[20] NIST, Fluid Thermodynamic and Transport Properties, Version 5.0. (<http://www.nist.gov/srd/nist23.htm>).
[21] H. Uchiyama, K. Mishima, S. Oka, M. Ezawa, M. Ide, T. Takai, P.W. Park, J. Chem. Eng. Data 42 (1997) 570–573.
[22] S.M. Walas, Phase Equilibria in Chemical Engineering, Butterworth Publisher, Boston, MA, 1985.
[23] H. Orbey, S.I. Sandler, Modelling Vapour–Liquid Equilibria, Cubic Equations of State and Their Mixing Rules, Cambridge University Press, Cambridge, U.K., 1998.
[24] H. Renon, J.M. Prausnitz, AIChE J. 14 (1968) 135–144.
[25] J.C. de la Fuente, J.O. Valderrama, S.B. Bottini, J.M. del Valle, J. Supercrit. Fluid. 34 (2005) 195–201.
[26] B.E. Poling, J.M. Prausnitz, J.P. O'Connell, The Properties of Gases and Liquids, fifth ed., Mc Graw Hill, New York, NY, 2001.
[27] K.G. Joback, R.C. Reid, Chem. Eng. Commun. 57 (1987) 233–243.

JCT 15-405

Appendix B. Published data of menadione solubility in SC-CO₂.

Solubility of menadione and dichlone in supercritical carbon dioxide

Andrea G. Reveco-Chilla [a], Adolfo L. Cabrera [b], Juan C. de la Fuente [b, *], Flavia C. Zacconi [c], José M. del Valle [a], Loreto M. Valenzuela [a]

[a] Departamento de Ingeniería Química y Bioprocesos, Facultad de Ingeniería, Pontificia Universidad Católica de Chile, Santiago, Chile
[b] Laboratorio de Termodinámica de Procesos, Departamento de Ingeniería Química y Ambiental, Universidad Técnica Federico Santa María, Valparaíso, Chile
[c] Departamento de Química Orgánica, Facultad de Química, Pontificia Universidad Católica de Chile, Santiago, Chile

ABSTRACT

This work reports the solubility of menadione (2-methyl-1,4-naphthoquinone) and dichlone (2,3-dichloro-1,4-naphthoquinone) in SuperCritical (SC) carbon dioxide (CO_2) at 313, 323, and 333 K and (7.1–33) MPa. A Gibbs-Duhem test was applied to assess the thermodynamic consistency of experimental data using the Peng-Robinson equation of state with Wong-Sandler mixing rule to represent the solubility, and the non-random two-liquid model to compute Gibbs' excess free energy. In addition, the solubility of menadione and dichlone in SC-CO_2 at 313 K and 9.5 MPa, a solubility correction by a change in the density of SC-CO_2 as compared to this reference condition (580 kg/m³), and a solubility correction by a change in absolute temperature compared to 313 K were estimated using Chrastil's equation. The solubility of menadione at the reference conditions was 8.3 times higher than that of dichlone (3095 versus 375 mg kg⁻¹ solute/CO_2). However, both CO_2 density and system absolute temperature had anomalously smaller effects on the solubility of menadione than dichlone, so that menadione was only 4.2 time more soluble in SC-CO_2 than dichlone at the extreme conditions of 333 K and 33 MPa (3460 versus 831 mg kg⁻¹ solute/CO_2) for which $\rho = 851.1$ kg/m³. The anomalous behavior of the solubility of menadione in SC-CO_2 was imputed to experimental difficulties (solute precipitation resulting in tube blocking, saturation of HPLC detector signal) associated with high solubility values ($\geq 0.5 \times 10^{-3}$ M fraction) that may have been also responsible for thermodynamically inconsistent results reported by others in literature. We compared the solubilities in SC-CO_2 of menadione and dichlone with those for several solutes sharing the same molecule core (1,4-naphthoquinone) and concluded they are negatively impacted by polar and non-polar substituents, but that these negative steric and polarity effects could be partially compensated by a non-polar olefin substituent, or ameliorated by distancing substitutions from the carbonyl groups.

1. Introduction

There exist a wide range of quinone derivatives [1] that have demonstrated biological activity, mainly as antioxidants [2–4]. The positive effect on human health of menadione (2-methyl-1,4-naphthoquinone or vitamin K₃, Fig. 1) has prompted its study by the pharmaceutical industry. Menadione is a fat-soluble vitamin that is used as an antihemorrhagic factor [5], a precursor of vitamin K that is transformed to menaquinone-4 and deposited in brain tissue [6], and a promising oncogenic agent against mammalian cancer [7,8]. Menadione can be synthetized by the oxidation of 2-methylnaphthalene or 2-methyl-1-naphthol using conventional organic solvents, and supercritical carbon dioxide [9–12].

SuperCritical (SC) carbon dioxide (CO_2) is commonly used as solvent in biological (e.g., extraction of antioxidants from natural matrices) and pharmaceutical (e.g., chromatographic purification) processes at near-critical temperature ($T_c = 304.85$ K, in the case of CO_2 [13]), due to its interesting liquid-like density and solvent power, and gas-like transport properties (low viscosity and high diffusivity). Prevention of thermal damage to compounds dissolved in the gaseous phase at near-environmental temperature, ease precipitation of dissolved solutes by simple depressurization, and convenient chemical properties (e.g. nontoxicity, nonflammability) make SC-CO_2 an excellent alternative to conventional organic

* Corresponding author. Avenida España 1680, Valparaíso, Chile.
E-mail address: juan.delafuente@usm.cl (J.C. de la Fuente).

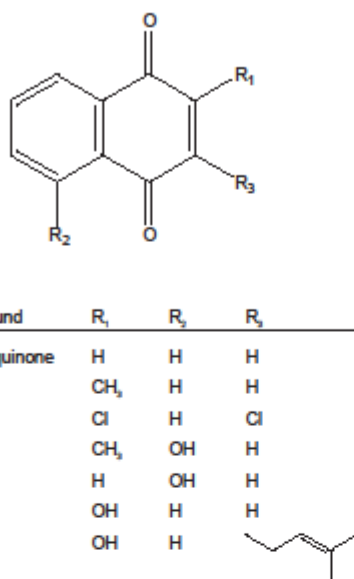| Compound	R_1	R_2	R_3
1,4-Naphtoquinone	H	H	H
Menadione	CH_3	H	H
Dichlone	Cl	H	Cl
Plumbagin	CH_3	OH	H
Juglone	H	OH	H
Lawsone	OH	H	H
Lapachol	OH	H	

Fig. 1. Chemical structure of 1,4-naphthoquinone and derivatives analyzed in this manuscript.

solvents [13]. There are two previous studies on the solubility of menadione in SC-CO_2. Johannsen and Brunner [14] measured its solubility at 313 K and 22–32 MPa as part of a study on the solubility of fat-soluble vitamins in SC-CO_2. Knez and Skerget [15] reported solubility isotherms at 313, 333, and 353 K and 8–30 MPa as part of a comparative study on the solubility of vitamins D_2, D_3, and K_3 in supercritical CO2 and propane. As discussed later, results of these two studies are contradictory. Valderrama and Zavaleta [16] proposed a methodology to discern good from questionable experimental data on solute solubility in SC-CO_2 that will be applied in this study. Their thermodynamic consistency test uses the Gibbs-Duhem equation for solid-gas phase equilibria [17], and requires the fugacity coefficient of the solid solute in the gaseous phase as a function of system pressure, system temperature, and the solubility of the solute in the CO_2-rich phase. The method was previously applied to analyze the consistency of experimental data for the solubility of another fat-soluble vitamin (β-carotene) in SC-CO_2 [18].

We are embarked in a long-term project to study the effect of small structural changes in chemicals on the solubility in SC-CO_2 that will demand chemical synthesis, solubility measurements, and molecular simulations. In its first stages, the project will use menadione and dichlone (2,3-dichloro-1,4-naphthoquinone, Fig. 1) as base structures to which different substituents will be attached. These chemical changes will alter the size, polarity, and halogen content of the molecules. To establish a baseline for solubilities, this work will measure and model the solubility of menadione and dichlone in SC-CO_2 at 313, 323, and 333 K, and 7–33 MPa.

2. Material and methods

2.1. Materials

Table 1 summarizes the source and purity of the solutes and solvent used in solubility measurements, and of solvents used in chromatographic analysis. Menadione, dichlone, and CO_2 were used in tests without further purification.

2.2. Measuring the solubility of menadione and dichlone in CO_2

The solubility of menadione or dichlone in SC-CO_2 was measured using the experimental equipment and dynamic-analytical method of Araus et al. [19]. The experimental system consists of a 50-cm^3, stirred, high-pressure view-cell (Thar-Tech, Pittsburgh, PA) placed in a temperature-controlled air bath, a syringe pump (Teledyne ISCO 260D, Lincoln, NE) to load CO_2 into the system and adjust system pressure, and a gear pump (GAH-T23, Eurotechnica, Bargteheide, Germany) to recirculate the CO_2-rich phase, aid system equilibration, and feed samples of the CO_2-rich phase to the HPLC system coupled to the equilibration system. The HPLC system consists of a L-7100 pump, L-7350 oven, and L-7455 photodiode array detector from Hitachi LaChrom (Tokyo, Japan). To determine solute solubility in SC-CO_2, the equilibrium cell is loaded with approximately 2 g of menadione or dichlone, residual air is evacuated with a vacuum pump (Welch Vacuum, Skokie, IL), CO_2 is loaded using the high-pressure syringe pump, and temperature and pressure are adjusted to the required initial values. With the solute and CO_2 loaded in the equilibrium cell, the magnetic stirring (bar) and recirculation of the CO_2-rich phase were activated up to reaching equilibrium. After reaching equilibrium, a two-way, six-port injection valve Rheodyne 7010 (Rohnert Park, CA) equipped with a sampling loop of $V_i = 20$ μL that interfaced the equilibration system with the HPLC apparatus, was used to sample the CO_2-rich phase. The molar fraction of solute (component 2) in the CO_2 (component 1) phase was estimated using Eq. (1):

$$y_2 = \left(\frac{A_i}{A_S}\right) \cdot \left(\frac{V_C}{V_i}\right) \cdot \left(\frac{MW_1}{\rho_1}\right) \cdot C_S, \tag{1}$$

where A_i is the chromatographic area for the tested sample, V_C and V_i are the volumes of sampling loops of the injection valves of the HPLC and high-pressure view-cell, respectively, MW_1 is the molecular weight of CO_2 (44.01 g/mol), ρ_1 is the density of CO_2 at equilibration temperature and pressure (calculated using NIST [20] database), and C_S is the concentration of the standard solution used to calibrate the HPLC (chromatographic area A_S). The solubility isotherm was completed by adding CO_2 to the cell to increase the pressure and attaining new equilibrium conditions up to reaching the required final pressure. Additional isotherms were obtained repeating this procedure using another initial temperature.

The isocratic HPLC method of by Hu et al. [21] with small modifications was used to determine the solute content in SC-CO_2. Separation was carried out 30 °C in a reverse-phase 2-mm (inner diameter) wide, 25-cm long, RP-18 HPLC column from Merck KGaA (Darmstadt, Germany) packed with 5-μm (diameter) adsorbent beads, using 1 cm^3/min of a 70/30 (v/v) mixture of methanol and water as the mobile phase. Solute was detected at a wavelength of 300 nm. Solutions containing $C_S = 0.1$ mg/cm^3 of menadione or dichlone in methanol were prepared and injected for calibration.

Five measurements of solubility data in SC-CO_2 were made at 313, 323, or 333 K and 7.1–32.6 MPa. Combined standard uncertainties were calculated using the methodology of Araus et al. [19], which included the relative inherent error associated to independent variables such as pressure, temperature, and others. In

Table 1
Specification of solvent, solute, and mobile phase solvents for HPLC analysis.

Chemical name	Source	Initial mass fraction purity (kg·kg^{-1})	Purification method	Final mass fraction purity (kg·kg^{-1})	Analysis method
Carbon dioxide	AGA-Chile S.A.	0.9999	None	0.9999	None
Menadione	Sigma-Aldrich	0.98	None	0.98	None
Dichlone	Sigma-Aldrich	0.98	None	0.98	None
Methanol	Merck KGaA	0.999	None	0.999	GC[a]
Water	Merck KGaA	0.99999	None	0.99999	GC[a]

[a] Gas-Liquid Chromatography.

this work, solubility data are presented with a 95% level of confidence as proposed by Chirico et al. [22] with a coverage factor of 1.96 to obtain the combined expanded uncertainty (U_{comb}).

2.3. Testing thermodynamic consistency of experimental data

The thermodynamic consistency test used in this work requires i) solubility data as a function of temperature and pressure, ii) an Equation of State (EoS) with a mixing rule to represent solubility data and estimate the fugacities of the solute in the two phases, and iii) a relationship defining thermodynamic consistency based on the fundamental Gibbs-Duhem equation.

The Gibbs-Duhem equation for two consecutive experimental data points (i and i+1) can be written as follows [17]:

$$A_p^i = A_\phi^i,\qquad(2)$$

where the two terms can be computed using experimental information, Eq. (2a), or from estimated fugacities that represent the phase equilibrium, Eq. (2b):

$$A_p^i = \int_i^{i+1} \frac{dp}{p\, y_2},\ and\qquad(2a)$$

$$A_\phi^i = \int_i^{i+1} \frac{1-y_2}{y_2\,(Z^V-1)\phi_1^V}d\phi_1^V + \int_i^{i+1} \frac{1}{(Z^V-1)\phi_2^V}d\phi_2^V.\qquad(2b)$$

In these equation, p is the system pressure, y_2 is the mole fraction of the solute (component 2) in the CO_2 (component 1) phase, ϕ_j^V is the fugacity coefficient of component "j" in the same phase, and Z^V is the compressibility factor of the gas mixture calculated using an EoS with proper mixing and combining rules.

Term A_ϕ^i can be computed following representation of the phase equilibrium using a $\phi-\phi$ approach, and assuming that the solid phase is pure solute. In this work, the Peng-Robinson (PR) [23] EoS with the Wong-Sandler (WS) [24] mixing rule, with the excess Gibbs free energy being computed using the Non-Random Two-Liquid (NRTL) model [25] (PR + (WS + NRTL)) was used to compute ϕ_1^V and ϕ_2^V using the procedure outlined by Cabrera et al. [26]. Four binary interaction parameters (k_{12}, α_{12}, τ_{12}, τ_{21}) were best-fitted to the solid-gas equilibrium data. In cases of solid-gas equilibrium, where the solid phase is assumed to be pure solute, the solubility (y_2), is calculated as a function of the fugacity coefficient of the solute (component 2) for both phases, as follows:

$$y_2 = \frac{\phi_2^S}{\phi_2^V}.\qquad(3)$$

In Eq. (3), ϕ_2^S can be computed as follows [27]:

$$\ln\phi_2^S = \ln\phi_2^{SCL} + \frac{\Delta H_{tp}}{R}\left(\frac{1}{T_{tp}} - \frac{1}{T}\right),\qquad(4)$$

that relates it to the fugacity coefficient of the Sub-Cooled Liquid (SCL) at absolute temperature T. The only data required for calculating the fugacity coefficient of the pure solid phase, are the heat of fusion (ΔH_{tp}) and absolute temperature (T_{tp}) at the triple point, and the fugacity coefficient of the pure solute in the sub-cooled liquid phase (ϕ_2^{SCL}) at T and p, which can be also calculated using PR-EoS.

The best-fitting method was the one of Brent [28] that minimizes the Root Mean Square Deviation (RMSDy) of experimental as compared to predicted values:

$$RMSD_y = \sqrt{\frac{1}{N}\sum_{i=1}^{N}\left(1 - \frac{y_2^{i,Calc}}{y_2^i}\right)^2},\qquad(5)$$

where N is the number of experimental data points, y_2^i is an experimental value, and $y_2^{i,Calc}$ is its corresponding calculated value.

Pure component properties needed for calculations such as the critical temperature and critical pressure (T_c, P_c) and acentric factor (ω) of CO_2 and menadione were those published by Knez et al. [15]. On the other hand, the critical properties of dichlone were estimated using Joback's method [29], and its ω was estimated using Pitzer's vapor pressure correlation [29]. Results are reported in Table 2.

This consistency analysis was applied author-by-author and isotherm-by-isotherm. For each individual point, it is possible to estimate a prediction error, Eq. (6a). In addition, for each pair of neighbors i and i+1 (consecutive pressures tested), it is possible to estimate a percent difference between A_p^i and A_ϕ^i as shown in Eq. (6b). To identify the thermodynamically inconsistent value when this difference exceeded a threshold, the comparison between A_p^i and A_ϕ^i was repeated deleting one of the two at a time; the thermodynamically inconsistent term was the one that, if deleted, allowed this difference to remain within an acceptable interval in a percent basis. Percent errors for each experimental point and each pair of neighbor data points were respectively estimated as follows:

$$\%\Delta y_2^i = 100\left(1 - \frac{y_2^{i,Calc}}{y_2^i}\right),\ and\qquad(6a)$$

$$\%\Delta A^i = 100\left(1 - \frac{A_\phi^i}{A_p^i}\right).\qquad(6b)$$

2.4. Modeling of solubility data

The methodology to estimate the best-fit the parameters of the equation of Chrastil [30] to experimental solubility data detailed by Valenzuela et al. [31] was applied. Chrastil's equation, Eq. (7),

Table 2
Pure component properties for carbon dioxide (1), menadione, and dichlone (2) from literature or estimated in this work.

Property	Value	Source (estimation method)	Reference
Carbon dioxide (1)			
Molecular weight (MW_1, Da)	44.01	–	–
Critical temperature ($T_{c,1}$, K)	304.2	NIST standard reference database	[20]
Critical pressure ($p_{c,1}$, MPa)	7.38	NIST standard reference database	[20]
Acentric factor (ω_1)	0.2252	NIST standard reference database	[20]
Menadione (2)			
Molecular weight (MW_2, Da)	172.18	–	–
Critical temperature ($T_{c,2}$, K)	639.58	Literature	[15]
Critical pressure ($p_{c,2}$, MPa)	46.53	Optimization from data	–
Acentric factor (ω_2)	0.6226	Literature	[15]
Triple point temperature (T_{tp}, K)	379.3	Joback, assumed equal to fusion temperature	[29]
Heat of fusion at triple point (ΔH_{tp}, J mol^{-1})	21,488	Joback, assumed equal to enthalpy of fusion	[29]
Dichlone (2)			
Molecular weight (MW_2, Da)	227.04	–	–
Critical temperature ($T_{c,2}$, K)	731.96	Joback	[29]
Critical pressure ($p_{c,2}$, MPa)	6.41	Joback	[29]
Acentric factor (ω_2)	0.6385	Definition	[29]
Triple point temperature (T_{tp}, K)	466	Joback, assumed equal to fusion temperature	[29]
Heat of fusion at triple point (ΔH_{tp}, J mol^{-1})	18,130	Joback, assumed equal to enthalpy of fusion	[29]

predicts the solubility of a solute in SC-CO_2 (w_2, mg kg^{-1} solute/CO_2) as a function of three parameters: i) the solubility at a reference condition (w_2^0, mg kg^{-1} solute/CO_2), ii) a correction factor depending on the density of SC-CO_2 (ρ_1, kg/m^3), and, iii) a correction factor depending on absolute temperature (T, K) of the system [31]:

$$\log(w_2) = \log\left(w_2^0\right) + (k-1)\log\left(\frac{\rho_1}{\rho_1^0}\right) - \frac{\Delta H}{2.303 R}\left(\frac{1}{T} - \frac{1}{T^0}\right),$$

(7)

where w_2^0 is the solubility of the solute at pressure P^0 and temperature T^0, ρ_1^0 is the density of CO_2 at the reference conditions (P^0 and T^0), k is an association number describing the number of CO_2 molecules forming a solvate complex with a single solute molecule, ΔH is the total heat (vaporization and dissolution) required to form the solvate complex, and R is the universal gas constant (0.0008314 kJ mol^{-1} K^{-1}). Prior to modeling, solubility data (y_2, mol/mol $\times$ 10^3) were expressed as weight fractions (w_2, mg kg^{-1} solute/CO_2) using Eq. (8):

$$w_2 = \frac{10^3\, y_2}{10^3 - y_2}\left(\frac{MW_2}{44.01}\right),$$

(8)

where $MW_1 = 44.01$ is the molecular weight of CO_2, and MW_2 is the molecular weight of the solute ($MW_2 = 172.11$ g/mol for menadione, and $MW_2 = 227.04$ g/mol for dichlone).

The parameters of the Eq. (7) were estimated using $T^0 = 313.15$ K and $P^0 = 9.5$ MPa as reference conditions, where the density of pure CO_2 is $\rho_1^0 = 580.01$ kg/m^3. For best-fitting of Eq. (7), we considered that the dissolved solute did not affect the density of its mixture with CO_2, that was obtained using NIST standard reference database for pure CO_2 [20]. High solubility data ($0.001 w_2 \rho_1 > 100$ g/m^3 solute/CO_2) were discarded because this condition does not apply for a solute solubility above 100 g/m^3 [30]. Best-fit parameters of Eq. (7) were selected by minimizing the sum of average mean error for the three isotherms (considering valid data points only) using Solver function of Excel®.

Finally, the percent Absolute Average Relative Deviation (% AARD) was computed using Eq. (9) to evaluate the fitting of the Chrastil's model to each solubility isotherm measured in this work:

$$\%AARD = \frac{100}{N}\sum_{i=1}^{N}\left|1 - \frac{y_2^{i,Calc}}{y_2^i}\right|.$$

(9)

3. Results

All experimental data point on solubility of menadione in SC-CO_2 measure in this work for each isotherm was analyzed in order to remove those values far of the overall trend (outsiders). Table 3 reports selected solubility data measured for menadione at 313, 323, and 333 K and 9.7–30.7 MPa. The Coefficients of Variation (CV, percent ratio of standard deviation to average) for quintuplets ranged from 37.2 to 52.9%. Fig. 2 shows that the solubility of menadione in SC-CO_2 measured in this work does not coincide with previous results of Johannsen and Brunner [14] at 40 °C, nor those of Knez and Skerget [15] at 40 or 60 °C. With the only exception of the solubility isotherm of Knez and Skerget [15] at 40 °C, there was a moderate effect of system pressure on the solubility of menadione in SC-CO_2 at either 40 or 60 °C. The largest effect was due to the experimental method, with Johannsen and Brunner [14] reporting the highest solubilities and this work the lowest. Data of Johannsen and Brunner [14] showed limited trends (large scattering) because the authors selected a very narrow range of experimental conditions.

Thermodynamic consistency tests were performed to the solubility data for each isotherm and each reference. Table 4 reports values for the optimization parameters and the corresponding RMSDy estimated for each data set. The maximal allowable error in predictions of solubilities using the PR + (WS + NRTL) framework, for this work, was 50%, with predictions exhibiting larger discrepancies being discarded from analysis. If the PR + (WS + NRTL) model fits ($|\%\Delta y_2^i| < 50\%$) less than 85% of the experimental points in any given isotherm, one should Try a Different Model (TDM) to represent it. Furthermore, the maximal allowable discrepancy between A_ϕ^i and A_ϕ^i for two consecutive data points i and (i+1) was 20%. Solubility isotherms for which $|\%\Delta y_2^i| \leq 50\%$ for each data point and $|\%\Delta A^i| \leq 20\%$ for each pair of consecutive points are considered to be Thermodynamically Consistent (TC). If less than 15% of the experimental data points in an isotherm need to be discarded, the isotherm is considered to be Not Fully Consistent (NFC). Finally, if the 15% threshold for discarded data points is

Table 3
Experimental molar fraction of menadione (2) (solubility, y_2) in supercritical CO_2 (1)-rich phase as a function of system absolute temperature (T) and pressure (p).

T^a (K)	p^b (MPa)	$\rho_1{}^c$ (kg·m^{-3})	y_2 ($\times 10^3$ mol mol^{-1})	$U_{comb}(y_2)$ ($\times 10^3$ mol mol^{-1})^d
313	10.32	650.0	0.800	0.373
	14.13	765.7	0.843	0.392
	17.61	815.1	0.864	0.386
	19.58	835.8	0.873	0.408
	22.41	860.5	0.884	0.394
	25.72	884.3	0.893	0.389
	30.67	913.5	0.905	0.391
323	9.87	368.7	0.794	0.359
	15.36	785.8	0.923	0.411
	20.38	788.9	0.954	0.401
	21.89	805.5	0.961	0.479
	26.41	845.4	0.976	0.401
333	9.72	273.5	0.750	0.280
	13.15	514.9	0.864	0.440
	13.43	531.2	0.880	0.468
	17.17	668.8	0.948	0.431
	20.53	732.0	0.983	0.426
	24.24	778.6	1.006	0.410

^{a} $u(T)$ = 0.1 K.
^{b} $u(p)$ = 0.01 MPa.
^{c} The density of the CO_2 (ρ_1) was estimated using NIST standard reference database for pure CO_2 [20] at T and p.
^{d} Combined expanded uncertainties for molar fraction of menadione, $U_{comb}(y_2)$, were estimated with a 0.95 level of confidence.

exceeded, the isotherm is considered to be Thermodynamically Inconsistent (TI).

Thermodynamic consistency for measured solubility of menadione in SC-CO_2 is higher in this than previously reported works (Supplementary Material contains details on this thermodynamic consistency analysis.). Table 5 shows that the data of Johannsen and Brunner [14] is thermodynamically inconsistent because 33% of the data points need to be discarded to comply with our criteria. In the case of Knez and Skerget [15], the 313 K isotherm is thermodynamically consistent but the one that at 333 K is thermodynamically inconsistent (17% of the data points need to be discarded). Our three isotherms are thermodynamically consistent. Because of trends in Fig. 2 and results in Table 5 we did not attempt to model our data together with literature data for the solubility of menadione in SC-CO_2.

The best-fit parameters of Chrastil's model applied to the solubility data of menadione in SC-CO_2 in Table 3 are reported in Table 6, where the estimated %AARD for solubility isotherms were 0.79% for 313 K, 2.84% for 323 K, and 0.96% for 333 K. Fig. 3 displays the data points together with the model predictions, where a slight increment in solubility is observed when system temperature or CO_2 density increase.

An equivalent work to that for menadione was carried for the solubility data of dichlone in SC-CO_2. Table 7 presents solubility data selected at 313, 323, and 333 K and 7.1–32.6 MPa. CV values for quintuplet measurements of the solubility of dichlone in SC-CO_2 ranged from 42.9 to 46.6% depending on system conditions. Table 5 shows also the results of the thermodynamic consistency test performed to real solubility data of dichlone in SC-CO_2, where 96% of those are thermodynamically consistent (Supplementary Material contains details on this thermodynamic consistency analysis.). A single thermodynamically inconsistent data point was identified at 40 °C that represented 14.3% of all measurements at that temperature. This data was modeled using Chrastil's equation and the best-fitting values of model parameters are reported also in Table 6. The model fitted the solubility of dichlone in SC-CO_2 well, with %AARD values being 5.51% for 313 K, 7.25% for 323 K, and 13.60% for 333 K. Fig. 3 (below) compares data and model predictions for the solubility of dichlone in SC-CO_2, which increased as either system temperature or CO_2 density increased. These results, compared with those to menadione under equivalent temperature

and pressure conditions (Fig. 3, above), show that the presence of two chloride groups had a negative effect on the solvent power of SC-CO2, as expected.

Table 6 also includes Chrastil's parameters for the solubility in SC-CO_2 of a series of compounds closely related to menadione and dichlone (derivatives of 1,4-naphthoquinone) that are presented in Fig. 1. Valenzuela et al. [31] best-fitted solubility data for 1,4-naphthoquinone from several sources. We re-fitted this data using the procedure outlined by Valenzuela et al. [31] because we identified two other data sources in literature [30,31] that were relevant to our study. Our analysis indicated that Marceneiro et al. [33], Schmitt and Reid [34], and Zhang et al. [35] reported mutually consistent data (average mean error of log(w) for all solubility isotherms below 0.2, unbiased predictions) that was modeled using Chrastil's equation (values of best-fitting parameters informed in Table 6), whereas data of Rodrigues et al. [32] and Ngo et al. [36] was inconsistent. Indeed experimental measurements of Rodrigues et al. [32] were consistently above predictions made using model parameters in Table 6, whereas experimental measurements of Ngo et al. [36] were consistently below predictions made using these same parameters. It is relevant noting that Valenzuela et al. [31] also noted that Ngo et al. [36] underestimated the solubility of 1,4-naphthoquinone in SC-CO_2.

Rodrigues et al. [32] measured a solubility isotherm of plumbagin in SC-CO_2 at 313 K and 7.3–13.5 MPa, whereas Marceneiro et al. [33] measured also its solubility at 308, 318, and 328 K and 9.1–24.3 MPa. Table 6 informs the best-fit values of Chrastil's parameters to these data. The same as in the case of 1,4-naphthoquinone, experimental data of Rodrigues et al. [32] at 313 K was above values predicted using the parameters in Table 6 for T = 313 K, confirming that the method of these authors may slightly overpredict the solubility of 1,4-naphthoquinone derivatives in SC-CO_2. It is relevant to point out that parameters in Table 6 for plumbagin do not coincide with those informed by Marceneiro et al. [33]. We realized that there were mistakes in the estimation of concentrations in SC-CO_2 (in g/L, as required by Chrastil's model) from the equilibrium molar fractions at 318 and 328 K, which was possibly responsible for errors in the best-fitting procedure.

Rodrigues et al. [32] measured also a solubility isotherm for juglone at 313 K and 8.3–13.6 MPa, whereas the group of de Sousa
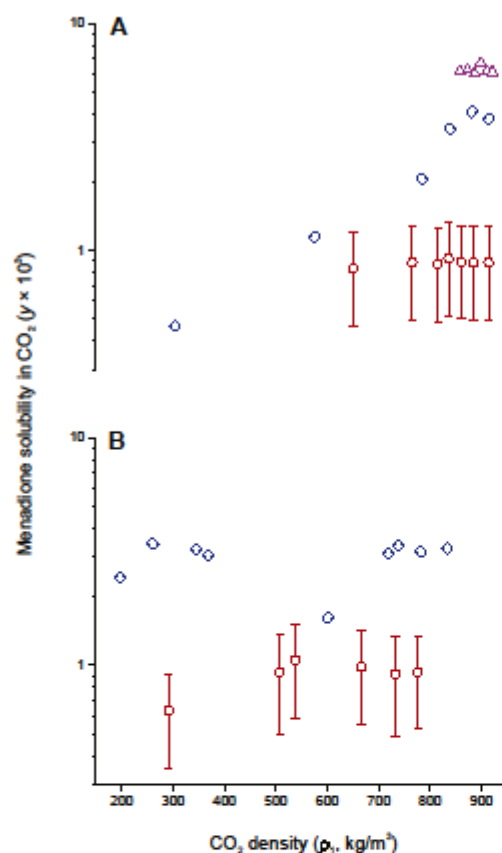
Fig. 2. Changes in the solubility of menadione in supercritical CO_2 as a function of CO_2 density at (A) 313 K and (B) 333 K reported by (Δ) Johannsen and Brunner [14], (◊) Knez et al. [15], and (○) this work. Bars signal the uncertainty of our experimental measurements.

parameters best-fitted to these data. The same as in the cases of 1,4-naphthoquinone and plumbagin, experimental data of Rodrigues et al. [32] at 313 K was above values predicted using the parameters in Table 7 for $T = 313$ K, as expected if their method slightly over-predicts the solubility of 1,4-naphthoquinone derivatives in SC-CO_2. It is relevant to point out that parameters in Table 6 for juglone do not coincide with those informed by Marceneiro et al. [37] because these authors made mistakes also in estimating concentrations in SC-CO_2 (in g/L, as required by Chrastil's model) from the equilibrium molar fractions at 318 and 328 K.

Rodrigues et al. [32] also measured solubility isotherms in SC-CO_2 at 313 K of lawsone (8.4–15.2 MPa) and lapachol (9.0–21.0 MPa) and Table 6 informs the best-fit values of their solubility at 313 K and 9.5 MPa and parameter $(k - 1)$ of Chrastil's model. It is important pointing out that a high-pressure (17.4 MPa) outlier was identified in the case of lawsone that was not considered in the best-fitting procedure, and that values of w_2^0 for lawsone and lapachol may slightly overpredict the true solubilities of these compounds in SC-CO_2 at 313 K and 9.5 MPa as observed in the cases of 1,4-naphthoquinone, plumbagin, and juglone.

Table 6 suggests that the solubility of 1,4-naphthoquinone and derivatives at the selected reference conditions (313 K and 9.5 MPa) is high for 1,4-naphthoquinone, menadione, and juglone, intermediate-high for plumbagin, intermediate-low for dichlone and lapachol, and low for lawsone. Table 6 suggests also that the effect of CO_2 density (and system pressure) is comparable for all solutes but menadione. Given values of $(k - 1)$ between about 2.0 and 4.5, an increase in pressure from 9.5 to 30 MPa ($\rho = 912.6$ kg/m^3 at 313 K and 30 MPa) would result in an increase in solubility of 211–769% (the solubility of menadione increases only 14% under equivalent conditions). Finally, Table 6 suggests also that the effect of system absolute temperature is comparable for all solutes but menadione. Indeed, given a value of 0.434 $\Delta H/R$ between about 1000 and 2500 K, an increase in temperature from 313 to 333 K keeping CO_2 density constant (increasing the pressure from 9.5 MPa at 313 K to 14.4 MPa at 333 K) would result in an increase in solubility of 55–200% (the solubility of menadione increases only 16% under equivalent conditions).

4. Discussion

The experimental methodology used in this work reports data which are thermodynamic consistent for the system of menadione and dichlone in SC-CO_2 (Table 5). However, solubilities of mena-

Table 4
Results for the first stage of the consistency test for solid + fluid equilibria of the (CO_2 + menadione and CO_2 + dichlone) binary systems. Optimal values of parameters for the PR + (WS + NRTL) equation of state (k_{12}, α_{12}, τ_{12}, τ_{12}) for the correlation of the solubility (y_2) for the three tested isotherms.

Solute	Model parameter	313 K			323 K	333 K	
		Johannsen and Brunner [14]	Knez and Skerget [15]	This work	This work	Knez and Skerget [15]	This work
Menadione	k_{12}	0.5363	−0.5008	−0.5155	−0.4763	−0.9935	0.0226
	α_{12}	−0.0050	0.0026	0.0924	0.0001	−0.0011	0.1412
	τ_{12}	0.0012	2.3249	5.9078	5.1459	2.8896	5.6111
	τ_{21}	−0.0047	1.6423	1.5356	3.0027	5.1987	3.5151
	$10^2 \cdot RMSD_y$ [Eq. (5)]	32.6	10.7	2.9	9.1	47.0	12.8
Dichlone	k_{12}			0.5437	0.5569		0.5534
	α_{12}			0.2425	0.2232		0.2023
	τ_{12}			4.9181	5.0656		5.4774
	τ_{21}			3.1836	2.8812		3.1805
	$10^2 \cdot RMSD_y$ [Eq. (5)]			8.4	13.3		5.4

also measured its solubility in SC-CO_2 at 308, 318, and 328 K and 9.2–24.4 MPa [37]. Table 6 informs also the values of Chrastil's

dione in SC-CO_2 are confined to a small experimental region that suggests minimal effect of system conditions on it (Table 3, Fig. 3).

Table 5
Results of the thermodynamic consistency test performed to the solubility data of menadione and 2,3-dichloro-1,4-naphthoquinone in SC-CO_2 measured in this work.

Solute	Isotherm (T, °C)	Data points	Consistency test*	Percent valid data	Reference
Menadione	40	6	TI	67	Johannsen and Brunner [14]
	40	6	TC	100	Knez and Skerget [15]
	60	9	TI	78	Knez and Skerget [15]
	80	6	TDM	17	Knez and Skerget [15]
	40	7	TC	100	This work
	50	5	TC	100	This work
	60	6	TC	100	This work
Dichlone	40	7	NFC	86	This work
	50	8	TC	100	This work
	60	8	TC	100	This work

* The results of the consistency test are as follows: TC = thermodynamically consistent data set, NFC = not fully consistent data set; TDM = try a different EoS model; and, TI = thermodynamically inconsistent data set.

Table 6
Parameters of Chrastil's model for the solubility of 1,4-naphthoquinone and derivatives in supercritical CO_2 at a reference condition of 40 °C and 9.5 MPa ($\rho = 580.0$ kg/m³).

Compound	$w_2 0$ (mg/kg)	$\kappa - 1$ (–)	$0.434\ \Delta H/T$ (K)
1,4-Naphthoquinone	3126	3.685	2064
Menadione	3095	0.292	346
Dichlone	375	2.077	1391
Plumbagin	1080	4.132	1129
Juglone	3765	4.622	2512
Lawsone	194	2.354	–
Lapachol	361	3.798	–

This relates to small values of $(k - 1)$ (below 2) and $0.434\ \Delta H/R$ (below 1000 K) that make menadione very different from 1,4-naphthoquinone and other derivatives presented in Table 6. We believe these abnormalities relate to experimental restrictions of the systems we used to measure solubility in SC-CO_2 (e.g., blocking of tubing with precipitated solute, saturation of the signal of the HPLC detector) that make it unreliable for solute solubilities above 0.5×10^{-3} mol/mol. Typically, we complete a whole solubility isotherm with a single load of the equilibrium cell, but when measuring the isotherms for menadione we were forced to do several, partly because of malfunctions caused by the blocking of lines. For these reasons, we do not feel fully confident of experimental values for the solubility of menadione in SC-CO_2 informed in Table 3, beyond the order of magnitude. It is apparent, however, that there are intrinsic difficulties in measuring the solubility of menadione in SC-CO_2 as attested by thermodynamic inconsistency of experimental results informed by Johannsen and Brunner [14] and Knez and Skerget [15] (Table 5). Indeed, Trupej et al. [38] recently measured the solubility of menadione in SC-CO_2 and found that it was lower than reported by both Johannsen and Brunner [14], and Knez and Skerget [15]. They claimed that there was some methodological problems with these prior measurements, and in the specific case on Knez and Skerget [15] the experimental system was modified to get this improved measurements that are closer to the values reported in Table 3. It is important, however, stating that experimental data of Trupej et al. [38] exhibited considerable scattering, the same as in prior measurements (Fig. 1), and that the solubility declined for large pressures above 20 MPa, confirming the trend of limited effect of CO_2 density on solubility that can be concluded from Fig. 3, and the small value of $(k - 1)$ for menadione in Table 6. For future measurements, it is recommended selecting compounds whose solubilities are below the upper limit mentioned above ($<0.5 \times 10^{-3}$ mol/mol).

It is a well-known fact that the size and polarity of a solute determine its solubility in SC-CO_2, which can be analyzed at an
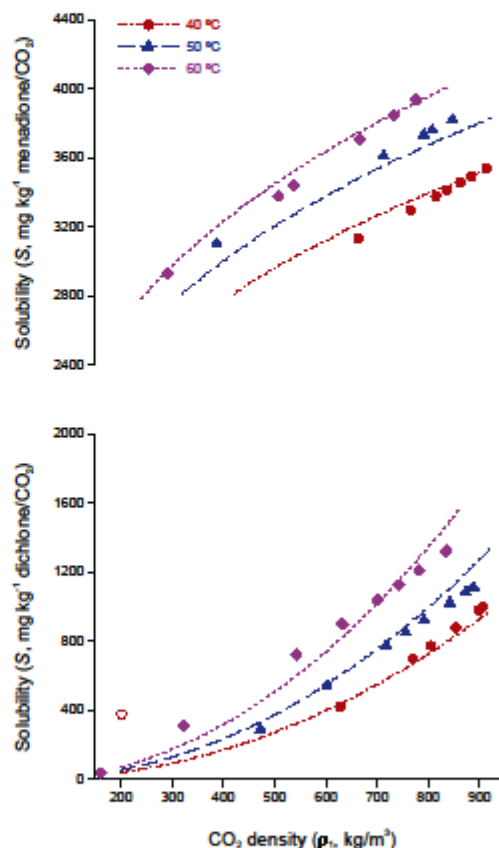

Fig. 3. Solubility isotherms of menadione and dichlone in supercritical CO_2 as a function of CO_2 density. Closed symbols represent experimental data points and lines predictions of Chrastil's model using best-fitted parameter values. The open symbol signals a data point that was thermodynamically inconsistent.

arbitrary reference condition (e.g., 313 K and 9.5 MPa), in our particular case by analyzing differences between values of w_2^0 in Table 6. In addition, values of parameter $(k - 1)$ relate to differences

Table 7
Experimental molar fraction of dichlone (2) (solubility, y_2) in supercritical CO_2 (1)-rich phase as a function of system absolute temperature (T) and pressure (p).

T^a (K)	p^b (MPa)	ρ_1^c (kg·m^{-3})	y_2 ($\times 10^3$ mol mol^{-1})	$U_{comb}(y_2)$ ($\times 10^3$ mol mol^{-1})^d
313	7.07	202.8	0.073	0.033
	9.95	628.0	0.091	0.041
	14.30	769.8	0.150	0.066
	16.75	805.7	0.166	0.073
	21.49	853.7	0.189	0.083
	27.90	898.6	0.210	0.092
	29.15	905.8	0.214	0.094
323	10.17	407.5	0.057	0.026
	12.26	602.4	0.107	0.047
	15.76	718.3	0.152	0.067
	18.10	759.6	0.167	0.073
	20.54	791.6	0.181	0.079
	25.90	842.1	0.201	0.088
	29.32	866.6	0.213	0.093
	32.58	886.6	0.219	0.096
333	7.15	160.8	0.007	0.003
	10.49	322.6	0.060	0.027
	13.61	543.1	0.138	0.061
	15.86	634.6	0.172	0.076
	18.61	700.5	0.198	0.087
	21.23	742.9	0.214	0.094
	24.54	782.6	0.230	0.101
	30.62	834.9	0.251	0.110

^{a} $u(T) = 0.1$ K.
^{b} $u(p) = 0.01$ MPa.
^{c} The density of the CO_2 (ρ_1) was estimated using NIST standard reference database for pure CO_2 [20] at T and p.
^{d} Combined expanded uncertainties for molar fraction of menadione, $U_{comb}(y_2)$, were estimated with a 0.95 level of confidence.

in solvation of a given solute by CO_2 molecules in that a decreasing number suggests increased impediments for CO_2 molecules to approach and solvate it. Dandge et al. [39] wrote a seminal contribution stating the effect of structural features of hydrocarbons, alcohols, phenols, aldehydes, ethers, esters, amines, and nitro compounds on limitations to or enhancements in their solubility in SC-CO_2, that were summarized by Luque de Castro et al. [40] as a list of conditions warranting miscibility in CO_2 of organic compounds as a function of the number of carbon atoms, branching, and type and number of functional groups. In general, the solubility in SC-CO_2 of a solute in a homologous series of compounds decreases as the molecular weight or the polarity of the compound increases. The effect of the chemical structure of 1,4-naphthoquinone derivatives (Fig. 1) on their solubility in SC-CO_2 was analyzed in this work, and from Table 6, the effect of different substituent groups such as methyl, hydroxyl, chloride, and olefin on the solubility in SC-CO_2 at 313 K and 9.5 MPa of a single molecule core (1,4 naphthoquinone) can be ascertained. The differences in solubility between 1,4-naphtoquinone and menadione (Table 6) suggest that a methyl group (in position R_5, Fig. 1) diminishes solubility due to steric and mass effect. Furthermore, a similar effect was observed in dichlone as compared to 1,4-naphthoquinone where the two chlorine atoms decrease solubility due to these steric and mass effects, and an additional polar effect. The negative effect of polarity in solubility can be concluded by the replacement of a methyl group in position R_1 of menadione by a hydroxyl group in lawsone that decreases w_2^0 by approximately 16 times (Table 6). Hydroxyl groups influence negatively the solubility in SC-CO_2 even when they are not next to carbonyl groups in, e.g., position R_2 in the case of plumbagin and juglone. In this particular case, the negative steric effect produced by an additional methyl group at R_1 in plumbagin has a relatively minor effect on the solubility in SC-CO_2 (w_2^0 diminishes about 3.5 times) and solvation (k decreases only about 9%) as compared to juglone. The relative position of the hydroxyl and carbonyl groups is also important as can be ascertained by comparing lawsone (hydroxyl in position R_1 next to a carbonyl, Fig. 1) and juglone (hydroxyl in position R_2 away from the

carbonyls, Fig. 1) in Table 6; w_2^0 decreases about 19 times and k decreases about 67% when this polar and bulky hydroxyl group approaches the carbonyls possibly interfering with their eventual solvation by CO_2 molecules. The negative impact on the solubility in SC-CO_2 and solvation of a hydroxyl near a carbonyl group in, e.g., position R_1 in the case of lawsone and lapachol, can be partially compensated by a non-polar olefin group in the position R_3 (lapachol) despite the increase in molecular weight, because this hydrocarbon substituent may bind CO_2 molecules with the end result of an increase of 86% in w_2^0 and an increase of 43% in k for lapachol as compared to lawsone.

It is also a well-known fact that solute solubility in SC-CO_2 is highly dependent on system conditions, which can be analyzed using a model such as the one of Chrastil [30]. In this particular model, the magnitude of the effect of system pressure (CO_2 density) on solubility is given by parameter ($k - 1$) which in the case of 1,4-naphthoquinene and derivatives ($3.0 < k < 5.5$) predicts an increase in solubility of 3-to-8 times when increasing system pressure from 9.5 to 30 MPa at 313 K (that causes an increase in CO_2 density of about 50% from 580 to 912 kg/m^3). In Chrastil's model, the magnitude of the effect of system absolute temperature on solubility is given by parameter $0.434\,\Delta H/R$, which in the case of 1,4-nathoquinone and derivatives ($1.9 < \Delta H < 4.8$ kJ/mol) predicts an increase in solubility of 1.5-to-3 times when increasing temperature from 313 to 333 K while keeping CO_2 density constant at 580 kg/m^3 (that requires an increase in system pressure from 9.5 MPa at 313 K to 14.4 MPa at 333 K).

In conclusion, this work exemplified the use of experimental and data analysis protocols to measure and model solute (menadione, dichlone) solubility in SC-CO_2. Data analysis protocols included testing thermodynamic consistency and best-fitting Chrastil model to non-fully consistent experimental data collected by us and reported in literature. This work also concluded that small differences in substituent groups (methyl, olefin, hydroxyl, halogen) and their position when attached to a single molecule core (1,4-naphthoquinone) may have large effects on the solubility in SC-CO_2 by changing the polarity and molecular weight

of the compound. Because the experimental device and procedure used in this work proved to be adequate only to measure solubilities below those of 1,4-naphthoquinone and menadione at 313–333 K and 7.1–33 MPa ($y_2 \leq 0.5 \times 10^{-3}$), modifications introduced by chemical synthesis to menadione and dichlone should be aimed to increasing molecular weight and/or polarity. This can be done adding bulky (olefin, phenyl) and/or polar (hydroxyl, amine, halogen) substituents to the 1,4-naphthoquinone molecular core analyzed in this work. This chemical synthesis effort will provide candidate solutes to our program aimed at relating solubility in SC-CO_2 and chemical structure.

Acknowledgments

Appendix A. Supplementary data

Supplementary data related to this article can be found at http://dx.doi.org/10.1016/j.fluid.2016.04.001.

References

[1] K.T. Finley, The addition and substitution chemistry of quinones, in: S. Patai (Ed.), Quinonoid Compounds, vol. 2, John Wiley & Sons, Chichester, UK, 1974.
[2] B.A. Bouchard, B. Furie, B.C. Furie, Glutamyl substrate-induced exposure of a free cysteine residue in the vitamin K-dependent γ-glutamyl carboxylase is critical for vitamin K epoxidation, Biochemistry 38 (1999) 9517–9523.
[3] J. McCall, C. Alexander, M.M. Richter, Quenching of electrogenerated chemiluminescence by phenols, hydroquinones, catechols, and benzoquinones, Anal. Chem. 71 (1999) 2523–2527.
[4] S.Y. Reddy, T.C. Bruice, Mechanism of glucose oxidation by quinoprotein soluble glucose dehydrogenase: insights from molecular dynamics studies, J. Am. Chem. Soc. 126 (2004) 2431–2438.
[5] A.J. Quick, G.E. Collentine, Role of vitamin K in the synthesis of prothrombin, Am. J. Physiol. 164 (1951) 716–721.
[6] D.J. Card, R. Gorska, J. Cutler, D.J. Harrington, Vitamin K metabolism: current knowledge and future research, Mol. Nutr. Food Res. 58 (2013) 1590–1600.
[7] S.W. Ham, H.J. Park, D.H. Lim, Studies on menadione as an inhibitor of the cdc25 phosphatase, Bioorg. Chem. 25 (1997) 33–36.
[8] S.W. Ham, J. Park, S.J. Lee, W. Kim, K. Kang, K.H. Choi, Naphthoquinone analogs as inactivators of cdc25 phosphatase, Bioorg. Med. Chem. Lett. 8 (1998) 2507–2510.
[9] W. Adam, J. Lin, C.R. Saha-Möller, W.A. Herrmann, R.W. Fischer, J.D.G. Correia, Homogeneous catalytic oxidation of arenes and a new synthesis of vitamin K3, Angew. Chem. Int. Ed. Engl. 33 (1995) 2475–2477.
[10] S. Narayanan, K. Murthy, K.M. Reddy, N. Premchander, A novel and environmentally benign selective route for vitamin K3 synthesis, Appl. Catal. A Gen. 228 (2002) 161–165.
[11] G. Strukul, F. Somma, N. Ballarini, F. Cavani, A. Frattini, S. Guidetti, D. Morselli, The oxidation of 2-methyl-1-naphthol to menadione with H_2O_2 catalyzed by Nb-based heterogeneous systems, Appl. Catal. A Gen. 356 (2009) 162–166.
[12] E. Shimanskaya, V. Doluda, M. Sulman, V. Matveeva, E. Sulman, Catalytic syntheses of 2-methyl-1,4-naphthoquinone in conventional solvents and supercritical carbon dioxide, Chem. Eng. J. 238 (2014) 206–209.
[13] J.M. del Valle, J.M. Aguilera, High pressure CO_2 extraction. Fundamentals and applications in the food industry, Food Sci. Technol. Int. 5 (1999) 1–34.
[14] M. Johannsen, G. Brunner, Solubilities of the fat-soluble vitamins A, D, E, and K in supercritical carbon dioxide, J. Chem. Eng. Data 42 (1997) 106–111.
[15] Z. Knez, M. Škerget, Phase equilibria of the vitamins D_2, D_3 and K_3 in binary systems with CO_2 and propane, J. Supercrit. Fluids 20 (2001) 131–144.
[16] J.O. Valderrama, J. Zavaleta, Thermodynamic consistency test for high pressure gas–solid solubility data of binary mixtures using genetic algorithms, J. Supercrit. Fluids 39 (2006) 20–29.
[17] A. Bertucco, M. Barolo, N. Elvassore, Thermodynamic consistency of vapor-liquid equilibrium data at high pressure, AIChE J. 43 (1997) 547–554.
[18] J.O. Valderrama, P.A. Robles, A. Reátegui, Data analysis, modeling and thermodynamic consistency of CO_2 + β-carotene high pressure mixtures, J. Supercrit. Fluids 55 (2010) 609–615.
[19] K.A. Araus, R.I. Canales, J.M. del Valle, J.C. de la Fuente, Solubility of β-carotene in ethanol- and triolein-modified CO_2, J. Chem. Thermodyn. 43 (2011) 1991–2001.
[20] E.W. Lemmon, M.L. Huber, M.O. McLinden, NIST Standard Reference Database 23: Mini-reference Fluid Thermodynamic and Transport Properties (REFPROP), Version 9.0, National Institute of Standards and Technology, Standard Reference Data Program, Gaithersburg, MI, 2007.
[21] Q.Y.P. Hu, C.Y. Wu, W.K. Chan, F.Y.H. Wu, Determination of anticancer drug vitamin K 3 in plasma by high-performance liquid chromatography, J. Chromatogr. B Biomed. Sci. Appl. 666 (1995) 299–305.
[22] R.D. Chirico, M. Frenkel, V.V. Diky, K.N. Marsh, R.C. Wilhoit, ThermoML—An XML-based approach for storage and exchange of experimental and critically evaluated thermophysical and thermochemical property data. 2. Uncertainties, J. Chem. Eng. Data 48 (2003) 1344–1359.
[23] D.Y. Peng, D.B. Robinson, A new two-constant equation of state, Ind. Eng. Chem. Fundam. 15 (1976) 59–64.
[24] D.S.H. Wong, S.I. Sandler, A theoretically correct mixing rule for cubic equations of state, AIChE J. 38 (1992) 671–680.
[25] H. Renon, J. Prausnitz, Local compositions in thermodynamic excess functions for liquid mixtures, AIChE J. 14 (1968) 135–144.
[26] A.L. Cabrera, A.R. Toledo, J.M. del Valle, J.C. de la Fuente, Measuring and validation for isothermal solubility data of solid 2-(3,4-dimethoxyphenyl)-5,6,7,8-tetramethoxychromen-4-one (nobiletin) in supercritical carbon dioxide, J. Chem. Thermodyn. 91 (2015) 378–383.
[27] J.M. Prausnitz, R.N. Lichtenthaler, E.G. de Azevedo, Molecular Thermodynamics of Fluid Phase Equilibria, 3rd. ed., Prentice Hall, New Jersey, NJ, 1998.
[28] R.P. Brent, Algorithms for Minimization without Derivatives, Courier Corporation, Chelmsford, MA, 2013.
[29] B.E. Poling, J.M. Prausnitz, J.P. O'Connell, The Properties of Gases and Liquids, 5th. ed., McGraw-Hill, , New York, NY, 2000.
[30] J. Chrastil, Solubility of solids and liquids in supercritical gases, J. Phys. Chem. 5 (1984) 3016–3021.
[31] L.M. Valenzuela, A.G. Reveco-Chilla, J.M. del Valle, Modeling solubility in supercritical carbon dioxide using quantitative structure–property relationships, J. Supercrit. Fluids 94 (Oct. 2014) 113–120.
[32] S.V. Rodrigues, L.M. Viana, W. Baumann, UV/Vis spectra and solubility of some naphthoquinones, and the extraction behavior of plumbagin from Plumbago scandens roots in supercritical CO_2, Anal. Bioanal. Chem. 385 (2006) 895–900.
[33] S. Marceneiro, M.E.M. Braga, A.M.A. Dias, H.C. de Sousa, Measurement and correlation of 1,4-naphthoquinone and of plumbagin solubilities in supercritical carbon dioxide, J. Chem. Eng. Data 56 (2011) 4173–4182.
[34] W.J. Schmitt, R.C. Reid, Solubility of monofunctional organic solids in chemically diverse supercritical fluids, J. Chem. Eng. Data 31 (1986) 204–212.
[35] X. Zhang, B. Han, Z. Hou, J. Zhang, Z. Liu, T. Jiang, J. He, H. Li, Why do cosolvents enhance the solubility of solutes in supercritical fluids? New evidence and opinion, Chem. Eur. J. 8 (2002) 5107–5111.
[36] T.T. Ngo, D. Bush, C.A. Eckert, C.L. Liotta, Spectroscopic measurement of solid solubility in supercritical fluids, AIChE J. 47 (2001) 2566–2572.
[37] S. Marceneiro, P. Coimbra, M.E.M. Braga, A.M.A. Dias, H.C. de Sousa, Measurement and correlation of the solubility of juglone in supercritical carbon dioxide, Fluid Phase Equilib. 311 (2011) 1–8.
[38] N. Trupej, M. Knez Hrncic, M. Skerget, Z. Knez, Investigation of the thermodynamic properties of the binary system vitamin K3/carbon dioxide, Food Chem. (2015) personal communication.
[39] D. Dandge, J. Heller, K. Wilson, Structure solubility correlations: organic compounds and dense carbon dioxide binary systems, Ind. Eng. Chem. Prod. Res. Dev. 24 (1985) 162–165.
[40] M.D. Luque de Castro, M. Valcarcel, M.T. Tena, Analytical Supercritical Fluid Extraction, Springer-Verlag, Berlin, Germany, 1994.